Charged Scalar fields and Superconductivity in AdS_4/CFT_3

Andrew J Fox (B.Sc, M.Sc)

Submitted in fulfillment of the requirements for the degree of
Master of Science at the Dept. of Mathematical Physics,
National University of Ireland, Maynooth, Ireland

27th October 2010

Head of Department: Professor Daniel M. Heffernan

Supervisor: Dr. Brian P. Dolan

Contents

Abstract

In this thesis I shall examine the energy behaviour of a massive charged scalar field in an Anti de-Sitter-Reissner-Nordström space-time background using the AdS/CFT correspondence. After obtaining the equations of motion for the system I numerically solve for the vacuum expectation values of the energy momentum tensor of the field on an AdS_4 background. It will be shown that the vev condenses as the temperature of the black hole is lowered, suggesting superconductivity.

I then add a time dependent part to the scalar field and examine how it behaves on the AdS_4 boundary with respect to a varying frequency and momentum. The boundary field shows evidence of the emergence of quasiparticle pairs at large momentum. The relevant Greens functions are then calculated numerically and presented as a sequence of surface and contour plots. From these we are able to determine the dispersion relations for the field. I shall also find pseudo-particle masses at zero momentum, and consequently see the lowest energy bound which a particle in this field can adopt.

Chapter 1

Introduction

For over the last decade or so, it has been conjectured that there exists an equivalence between a class of quantum field theories, and theories possessing gravity, living in a certain space-time background. This idea was put forth in 1997 by Juan Maldacena, and is thus often refered to as "The Maldacena duality". Much of the mathematics of the theory was further developed in works by Witten, Gubser, Klebanov, Hartnoll, Herzog and Polyakov to name but a few. It was initially born from a conjectured equivalence between Type IIB string theory (which is a theory of gravity in a particular low energy limit) living in an $AdS_5 \times S_5$ space-time background, and a super-symmetric $\mathcal{N}$=4 Yang-Mills gauge field (which is a conformal field theory without gravity) living on the boundary of this space. $AdS_5 \times S_5$ represents a five dimensional Anti de-Sitter space (AdS_5), times a 5-sphere (S_5), and so the conjecture is more commonly deemed the AdS/CFT correspondence [1, 2, 3, 4, 5, 6, 7, 8]. All spaces conforming to this correspondence are strictly Einstein spaces, as Anti de-Sitter space is itself a solution to the vacuum Einstein equations with constant negative curvature.

The correspondence is conjectured to generalise to other dimensions. The conformal field theory (CFT) on the boundary naturally lives in one less dimension than the bulk gravity theory. For this reason it makes sense to label the correspondence as 'AdS_{d+1}/CFT_d'. It is known that the isometry group of a (d+1) dimensional Anti de-Sitter space is equivalent to the conformal group ($SO(d,2)$) in d dimensions. The AdS/CFT correspondence provides a dictionary between operators O in the conformal field theory on the AdS boundary, and the fields living in the bulk gravity theory. The bulk fields effectively act as a source for the boundary operators. It is thus a working example of the holographic principle, first conceived by Gerard 't Hooft, which suggests gravity is related to a lower dimensional theory, and provides a real means of solving complicated, quantum systems at strong coupling in d dimensions, from the dynamics of simple gravity theories at weak coupling in d +1 dimensions.

AdS/CFT Dictionary

Field theory		Bulk Theory
Vev of operator $\langle O \rangle$	$\leftrightarrow$	field φ
energy-momentum tensor $T_{\mu\nu}$	$\leftrightarrow$	metric tensor $g_{\mu\nu}$
dimension of operator	$\leftrightarrow$	mass of field
global symmetry	$\leftrightarrow$	gauge symmetry
conserved current	$\leftrightarrow$	gauge field

It has been applied, with striking success to many strong coupling problems within condensed matter physics, such as holographic superconductor's and quantum critical phenomena, see for example [9-14]. Within the grounds of the AdS/CFT correspondence, superconductivity emerges from an instability in an electrically charged black hole living in an Anti de-Sitter background, against perturbations from a charged scalar field. The instability occurs in the black hole when its Hawking temperature T reaches some critical point T_c. For temperature's $T < T_c$, the charged operators on the conformal boundary condense, while their dual fields in the bulk geometry take on non-vanishing profiles within the black hole background. It is shown in [10] that such condensates can form even for a very weakly charged scalar field when the black hole is close enough to being extremal. That is to say, extremal in the sense of having zero temperature.

Perhaps the most fundamental quantity in the bulk gravity theory is the metric tensor $g_{\mu\nu}$. Considering the classical matter action

$$S_M = \int d^4x \sqrt{-g}\,\mathcal{L}_M \tag{1.1}$$

Where $\mathcal{L}_M$ is the matter Lagrangian and g is the determinant of the metric tensor. Varying the metric such that $g_{\mu\nu} \rightarrow g_{\mu\nu} + \delta g_{\mu\nu}$, then the variation in the matter action can be written in terms of the energy momentum tensor as

$$dS_M = \frac{1}{2}\int d^4x\sqrt{-g}T_{\mu\nu}\delta g_{\mu\nu} \tag{1.2}$$

In conformally invariant theories the energy momentum tensor is traceless,

$$T = g^{\mu\nu}T_{\mu\nu} = 0 \tag{1.3}$$

and as stated in the dictionary above, for Anti de-Sitter space the metric tensor in the bulk space gives rise to the energy momentum operator on the boundary. The metric can be regarded as the being a source whose endpoints correspond to the boundary operators. There is a general correspondence between fields in the bulk and operators on the boundary of AdS.

A precise prescription of the conjecture can be written as

$$\left\langle e^{i\int d^d x\varphi_0(x)O(x)}\right\rangle_{CFT} = Z\left[\varphi_{|_{boundary}} = \varphi_0(x)\right] \tag{1.4}$$

for some field φ in the bulk geometry, and operators O on the boundary. Here Z is the partition function for the field, and φ_0 is the boundary value of the bulk field, coupled to operator O on the boundary. Equation (1.4) allows one to compute correlation functions for strongly coupled quantum fields on a d dimensional boundary from the partition functions of a $d+1$ dimensional Anti de-Sitter space.

We will use this conjecture in chapter 2 to show that the operator corresponding to the energy momentum tensor of a massive charged scalar field on the boundary of an Anti de-Sitter space-time background, containing an electrically charged black hole, does indeed condense as the temperature of the black hole is lowered. This would suggest that the current associated with the charged operator will superconduct.

I shall first provide a brief description of Conformal theory followed by a review of some of the elementary properties of Anti de-Sitter space. From that point we will be in a position to proceed with obtaining independent results.

1.1 Conformal Field Theory

Conformal field theories have played a pivotal role in the development of several areas of theoretical physics for over the last decade. They have provided a model for describing interacting quantum systems, and also naturally describe critical phenomenon in two dimensions. An important first point to note is that all conformal field theories are scale invariant. Moreover, when studying critical phenomena, this scale invariance is also obeyed at the critical point itself. A conformal field theory not only enjoys the Euclidean symmetries but also a number of special conformal transformations which also preserve angle, but not length. If one looks at a conformal field theory in two dimensions, there exists an infinite dimensional group of local conformal transformations which are described by holomorphic functions (see for example [17]).

A good starting point now would be to look at familiar critical system such as the liquid-gas phase transition, whose critical point is described by the Van der Waals equation of state.

$$\left(P+\frac{aN^2}{V^2}\right)\left(V-bN\right)=NRT \tag{1.5}$$

Here N is the number of moles of the liquid, and the rest of the parameters are defined as usual. It should be recalled that in general the coefficient's a and b differ for every liquid considered. The critical temperature for water is approximately 374K, and the phase transition is shown graphically in figure 1 below. Examining one mole of water we can write

$$\left(PV^2+a\right)\left(V-b\right)-V^2RT=0 \tag{1.6}$$

Multiplying this out we get the cubic expression

$$V^3-\left(b+\frac{RT}{P}\right)^2V^2+\frac{a}{P}V-\frac{ab}{P}=0 \tag{1.7}$$

which can be generalised as

$$(V-V_1)(V-V_2)(V-V_3)=0 \tag{1.8}$$

The critical point V_c of the transition is where $V_1 = V_2 = V_3$. One can solve for the

critical Volume, Pressure and Temperature from the above to obtain the following

$$P_c = \frac{a}{27b^2}, \qquad V_c = 3b, \qquad T_c = \frac{8a}{27Rb} = \frac{8bP_c}{R} \tag{1.9}$$

If one defines the dimensionless variables

$$\tilde{P} = \frac{P}{P_c}, \qquad \tilde{V} = \frac{V}{V_c}, \qquad \tilde{T} = \frac{T}{T_c} \tag{1.10}$$

then the Van der Waals equation can be recast in the following dimensionless form

$$\left(\tilde{P} + \frac{3}{\tilde{V}^2}\right)\left(3\tilde{V} - 1\right) = 8\tilde{T} \tag{1.11}$$

This result is known as the law of corresponding states, and it provides an example of universality. That is to say that near the critical point, there is no intrinsic length scale in the physics; all length scales are important. The critical point in equation (1.11) corresponds to where

$$\tilde{P} = \tilde{V} = \tilde{T} = 1$$

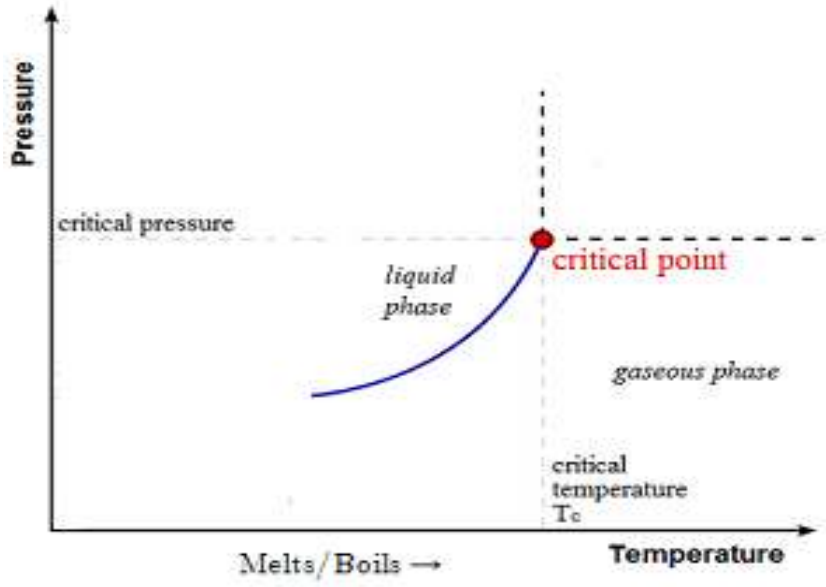

Figure 1. The critical point of a liquid. Image obtained from Wikipedia. File:Phase-diag2.svg

and at this critical point the physics is also invariant under scale transformations. The critical point in Equation (1.11) is the same for all fluids near the critical point, no matter what the value of the parameters *a* and *b*. This example provides a trivial and classical example of a scale invariant theory.

For the case of relativistic quantum field theories, massless theories are conformal, see for example [15], [16]. In Minkowski space, a theory is conformal only if $m = 0$. This point can be made clear if one considers a quantum scalar field in a flat Minkowski space. Throughout this paper I shall use units for which the speed of light and Planck's constant are set to unity. Consider a neutral scalar field obeying the Klein Gordon equation

$$(\Box - m^2)\varphi = 0 \tag{1.12}$$

where the wave operator has a mostly plus signature. The energy momentum tensor of the field is

$$T_{\mu\nu} = \partial_\mu\varphi\partial_\nu\varphi - \frac{1}{2}g_{\mu\nu}\left(\partial^\rho\varphi\partial_\rho\varphi + m^2\varphi^2\right) \tag{1.13}$$

In a conformal field theory, the energy momentum tensor of a scalar field is traceless. Considering a plane wave solution for the field, one finds the trace of the energy momentum tensor to be

$$T^\mu{}_\mu = -m^2|\varphi|^2 \tag{1.14}$$

and so, for a neutral quantum scalar field obeying the Klein Gordon equation to be conformal, one can clearly see from (1.14) that we require $m^2 = 0$.

I now describe briefly some aspects of the conformal symmetry group. Conformal symmetry is a symmetry under scale invariance, and under the special conformal transformations. Along side the Poncairé group, they generate the full conformal symmetry group. If we first consider a *d*-dimensional Euclidean flat space $\mathbb{R}^d$

$$\mathbb{R}^d : (x^1,...,x^d) \quad : \quad x^2 = \underline{x}\cdot\underline{x} \quad \Rightarrow \text{ Invariant under rotations} \tag{1.15}$$

where the rotation generators are given as

$$L_{ab} = x_a\partial_b - x_b\partial_a = -L_{ba} \tag{1.16}$$

where the indices $a,b = 1,...,d$. There are $d(d\text{-}1)/2$ generators here, and they generate the algebra

$$[L_{ab}, L_{cd}] = \delta_{bc} L_{ad} - \delta_{bd} L_{ac} - \delta_{ac} L_{bd} + \delta_{ad} L_{bc} \tag{1.17}$$

Equation (1.16) defines infinitesimal generators acting on an infinite dimensional space of functions, and it generates the SO(d) symmetry group. We also have translational invariance

$$x_a \to x_a + \delta x_a \tag{1.18}$$

The generators of the group being given as

$$P_a = \partial_a \tag{1.19}$$

with algebra

$$[P_a, P_b] = 0 \tag{1.20}$$

and

$$[L_{ab}, P_c] = \delta_{bc} P_a - \delta_{ac} P_b \tag{1.21}$$

The set $\{L_{ab}, P_a\}$ generate's the $d(d+1)/2$ dimensional Euclidean group.

We also have dilations, whose generators are given by

$$D = x^a \partial_a \qquad \text{(scaling: } x^2 \to e^{\lambda} x^2\text{)} \tag{1.22}$$

with algebra

$$[D, L_{ab}] = 0, \qquad [D, P_a] = -P_a \tag{1.23}$$

and finally inversions.

$$x^a \to \frac{x^a}{x^2} = \frac{1}{x^2}\left(\delta^{ab} - \frac{2x^a x^b}{x^2} \right) dx^a \tag{1.24}$$

The eigenvalues of D in the algebra (1.23) represents the canonical dimensions of the generators L and P. Inversions preserve angles but not straight lines; they are conformal transformations. We also have the special conformal transformations whose generators are given by

$$K_a = x^2 \partial_a - 2x^a x^b \partial_b \tag{1.25}$$

We thus have a closed algebra

$$\begin{aligned} &[K_a, K_b] = 0 \\ &[P_a, K_b] = 2(L_{ab} - \delta_{ab} D) \\ &[D, K_a] = K_a \\ &[L_{ab}, K_c] = \delta_{bc} K_a - \delta_{ac} K_b \end{aligned} \tag{1.26}$$

One can count the number of generators to find the dimension of this algebra. There are $(d+2)(d+1)/2$ generators and they generate the conformal group $SO(d+1,1)$. Looking briefly now at the Lorentz group in a $d+1$ dimensional space-time, we have

$$\mathbb{R}^{d,1}: \quad x^2 = -(x^0)^2 + \underline{x} \cdot \underline{x} = \eta_{ab} x^a x^b \tag{1.27}$$

where the metric has a mostly plus signature and the indices $a,b = 0,1,...,d$. In $d+1$ dimensions the boost generators are given as

$$L_{ab} = \eta_{ac} x^c \partial_b - \eta_{bc} x^c \partial_a \tag{1.28}$$

with algebra

$$[L_{ab}, L_{cd}] = \eta_{bc} L_{ad} - \eta_{bd} L_{ac} - \eta_{ac} L_{bd} + \eta_{ad} L_{bc} \tag{1.29}$$

The dimension of this algebra is now $d(d+1)/2$, and and it generates the symmetry group $SO(d,1)$. For $a,b = 0,1,...,d$, (1.28) above would be a rotation and not a boost. For a light cone in Minkowski space (mostly plus signature again)

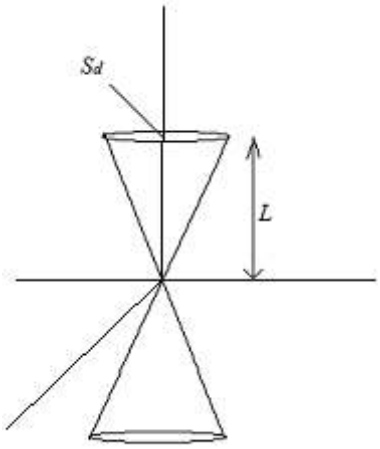

Figure 2: Light cone

one would have the coordinate system

$$\mathbb{R}^{d,1}: \ (x^0, x^1, ..., x^d) \ : \quad (x^0)^2 = \underline{r} \cdot \underline{r} = L^2 \tag{1.30}$$

In general, one can say that the conformal group acting on $\mathbb{R}^d$, is equivalent to the Lorentz group acting on $\mathbb{R}^{d+1,1}$. Similarly the conformal group acting on Minkowski $\mathbb{R}^{d,1}$ is equivalent to the Lorentz group acting on $\mathbb{R}^{d+1,2}$. A more general result in $\mathbb{R}^{d,1}$ is given as

$$\rightarrow \qquad SO(d,1) \ \subset \ SO(d+1,2) \tag{1.31}$$

where the l.h.s is the Lorentz group of $\mathbb{R}^{d,1}$, and the r.h.s is the conformal group of $\mathbb{R}^{d,1}$.

This concludes the section on conformal field theory, and for a more comprehensive review, see for example [3,7].

1.2 Basics of Anti de-Sitter Space

As stated in the introduction, Anti de-Sitter space is a maximally symmetric solution to the vacuum Einstein equations plus a negative cosmological constant Λ. I will discuss some of the basic ideas here but for a thorough review of this space and its features, see for example [2-4], [18-21].

Now consider the gravitational action

$$S_G = \frac{1}{16\pi G} \int d^d x \sqrt{-g} (R - 2\Lambda) \tag{1.32}$$

Where from here on, I shall use the same convention as that of [25] and set Newton's constant G to $1/16\pi$. The vacuum Einstein equations read

$$R_{\mu\nu} - \frac{1}{2} g_{\mu\nu} R = -\Lambda g_{\mu\nu} \tag{1.33}$$

$$\Rightarrow \qquad R = -\frac{2\Lambda}{2-d} d \tag{1.34}$$

where R is the Ricci curvature and d is the dimension of the space-time. For such Einstein spaces, one sees that the Ricci tensor is directly proportional to the metric tensor and dependent only on the dimension of the space in question. The difference between de-Sitter space and Anti de-Sitter space is in the sign of the cosmological constant. A positive value corresponding to de-Sitter space and a negative value to Anti de-Sitter space. For all such Einstein spaces the Ricci tensor can be written in terms of the de-Sitter/Anti de-Sitter radius L as

$$R_{\mu\nu} = \pm\frac{(d-1)}{L^2} g_{\mu\nu} \tag{1.35}$$

$$\Rightarrow \qquad R = \pm\frac{d(d-1)}{L^2} \tag{1.36}$$

The Einstein tensor would then be given as

$$G_{\mu\nu} = R_{\mu\nu} - \frac{1}{2} g_{\mu\nu} R \tag{1.37}$$

$$\Rightarrow \qquad G_{\mu\nu} = \mp\frac{(d-1)(d-2)}{2L^2} g_{\mu\nu} \tag{1.38}$$

The positive choice of (1.36) corresponds to de-Sitter Space while the negative corresponds to Anti de-Sitter space. One can then equate (1.34) and (1.36) to obtain expressions for the cosmological constant in both de-Sitter and Anti de-Sitter space as follows

$$dS: \qquad \Lambda = \frac{(d-1)(d-2)}{2L^2} \tag{1.39}$$

and

$$AdS: \qquad \Lambda = \frac{-(d-1)(d-2)}{2L^2} \tag{1.40}$$

Changing from a mostly plus to a mostly minus metric merely swaps the sign of the cosmological constant.

Focusing first on de-Sitter space

$$dS^{d-1,1}: \quad x_1^2+\cdots+x_d^2-x_0^2=L^2 \ , \quad dS^{d-1,1}\subset\mathbb{R}^{d,1} \tag{1.41}$$

$$\Rightarrow \qquad ds^2=dx_1^2+\cdots+dx_d^2-dx_0^2 \tag{1.42}$$

with

$$dS^{d-1,1}\cong\frac{SO(d,1)}{SO(d-1,1)} \tag{1.43}$$

We make the following parametrisations

$$\begin{aligned}\rho^2&=x_1^2+\cdots+x_d^2\\ \rho&=L\cosh\upsilon\\ x_0&=L\sinh\upsilon\end{aligned} \tag{1.44}$$

and obtain the metric

$$ds^2=L^2\left(-d\upsilon^2+\cosh^2\upsilon d^{d-1}\Omega\right) \tag{1.45}$$

where $d^{d-1}\Omega$ is the transverse line element in $d-1$ dimensions. If we let $d=4$ for example, we find from (1.39) and (1.36) respectfully

$$\Lambda=\frac{3}{L^2}>0 \tag{1.46}$$

$$\Rightarrow \qquad R=4\Lambda \tag{1.47}$$

which corresponds to an expanding de-Sitter universe. We can also see that (1.43) becomes

$$dS^{3,1}\cong\frac{SO(4,1)}{SO(3,1)} \tag{1.48}$$

where on the r.h.s of (1.48) above we see the Lorentz group for the $\mathbb{R}^{3,1}$ tangent plane in the denominator, while the isometry group of de-Sitter space is in the numerator.

We now examine the hyperbolic plane

$$H^d: \quad x_1^2+\cdots+x_d^2-x_0^2=-L^2 \ , \quad H^d\subset\mathbb{R}^{d,1} \tag{1.49}$$

letting

$$\rho = L\sinh u$$
$$x_0 = L\cosh u \tag{1.50}$$

to obtain

$$ds^2 = L^2\left(du^2 + \sinh^2 u d^{d-1}\Omega\right) \tag{1.51}$$

with

$$H^d \cong \frac{SO(d,1)}{SO(d)} \tag{1.52}$$

A useful parametrisation now is to let

$$r = L\sinh u \quad \rightarrow \quad dr^2 = \left(L^2 + r^2\right)du^2 \tag{1.53}$$

and the metric (1.51) becomes

$$ds^2 = \frac{dr^2}{\left(1 + r^2/L^2\right)} + r^2 d^{d-1}\Omega \tag{1.54}$$

Finally we turn to the Anti de-Sitter space with coordinate system

$$AdS^{d-1,1}: \quad x_1^2 + \cdots + x_{d-1}^2 - x_0^2 - \tilde{x}_0^2 = -L^2 \ , \quad AdS^{d-1,1} \subset \mathbb{R}^{d-1,2} \tag{1.55}$$

where the quotient of symmetry groups is now

$$AdS^{d-1,1} \cong \frac{SO(d-1,2)}{SO(d-1,1)} \ \approx \ S^1 \times \mathbb{R}^{d-1} \ \approx \ time \ \times \ H^{d-1} \tag{1.56}$$

The numerator in (1.56) is now evidently the conformal group in Minkowski space $\mathbb{R}^{d-2,1}$, living in one less dimension than the Anti de-Sitter space. For the case of $AdS^{2,1}$ we can making the following parametrisations

$$\left.\begin{aligned} x_1 &= L\cos\phi\sinh w \\ x_2 &= L\sin\phi\sinh w \end{aligned}\right\} \ dx_1^2 + dx_2^2 = L^2\left(\cosh^2 w dw^2 + \sinh^2 w d\phi^2\right) \tag{1.57}$$

and

$$\left.\begin{aligned} x_0 &= L\cos\tau\cosh w \\ \tilde{x}_0 &= L\sin\tau\cosh w \end{aligned}\right\} \; dx_0^2 + d\tilde{x}_0^2 = L^2\left(\sinh^2 w dw^2 + \cosh^2 w d\tau^2\right) \tag{1.58}$$

we can write the metric for Anti de-Sitter space in *d*-dimensions as

$$ds^2 = L^2\left(-\cosh^2 w d\tau^2 + dw^2 + \sinh^2 w d\phi^2\right) \tag{1.59}$$

This generalises to

$$ds^2 = L^2\left(-\cosh^2 w d\tau^2 + dw^2 + \sinh^2 w d^{(d-2)}\Omega\right) \tag{1.60}$$

Now making the following substitution

$$(w,\tau)\to(r,t): \qquad t = L\tau, \qquad r = L\sinh w, \qquad \cosh^2 w = 1+\frac{r^2}{L^2} \tag{1.61}$$

we find the general expression for the metric in AdS_d

$$ds^2 = -\left(1+\frac{r^2}{L^2}\right)dt^2 + \frac{dr^2}{\left(1+r^2/L^2\right)} + r^2 d^{(d-2)}\Omega \tag{1.62}$$

where it is seen that the last two terms on the r.h.s of (1.62) comprise the *d*-1 dimensional hyperbolic plane of Anti de-Sitter space, and the coordinate *r* runs from -∞ to +∞. In the case of AdS_4, we have group quotient

$$AdS_4 \cong \frac{SO(3,2)}{SO(3,1)} \;\approx\; S^1\times\mathbb{R}^3 \;\approx\; time \;\times\; H^3 \tag{1.63}$$

and the cosmological constant is found from (1.40) to be

$$\Lambda = -\frac{3}{L^2} \tag{1.64}$$

with

$$R = 4\Lambda \tag{1.65}$$

The Ricci scalar (1.65) is just as in the de-Sitter case. More generally we have

$$AdS_{d+1} = AdS^{d,1} \cong \frac{SO(d,2)}{SO(d,1)} \tag{1.66}$$

Below is a graphical representation of a maximally symmetric Anti de-Sitter space with two time axes

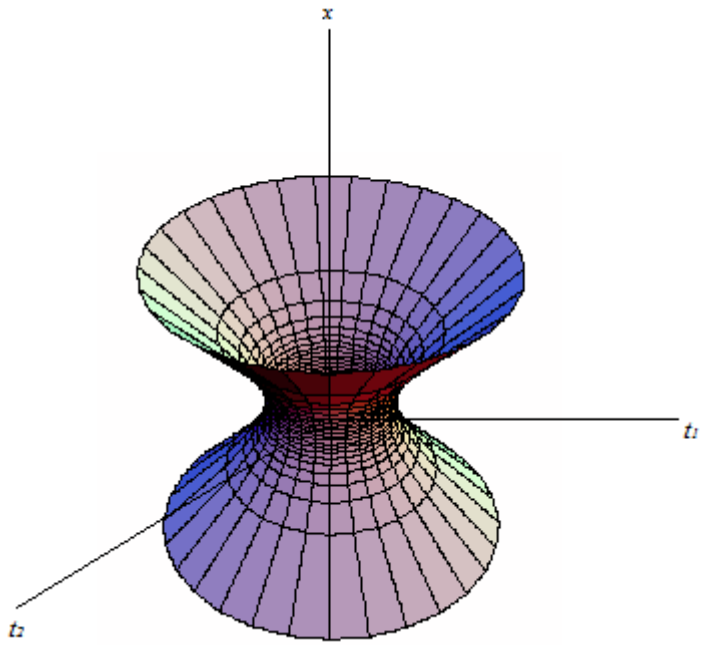

Figure 3: Graphical representation of Maximally symmetric Anti de-Sitter space

where

$$x^2 - {t_1}^2 - {t_2}^2 = -L^2 \tag{1.67}$$

and time is cyclic in an Anti-clockwise direction in the t_1 -t_2 plane. This concludes the brief discussion on Anti de-Sitter space. For a more detailed account of this space see for example [2,4,7,18].

1.3 Black holes

Before proceeding to the next section I will give a very brief account of electrically charged (Reissner-Nordström) black holes and some appropriate results that apply to the work herein.

The Reissner-Nordström solution of the Einstein field equations describes the space surrounding a spherical, non rotating, charged black hole. The metric is found by solving the coupled Einstein-Maxwell equations, got from considering the action

$$S = \int d^d x\sqrt{-g}R - \frac{1}{4}\int d^d x\sqrt{-g}F^2 \tag{1.68}$$

with

$$\begin{aligned} g^{\mu\nu}\ \nabla_\mu F_{\nu\sigma} &= 0 \\ \nabla_{[\mu}F_{\nu\rho]} &= 0 \end{aligned} \tag{1.69}$$

Where for now I am working with zero cosmological constant. The energy momentum tensor for electromagnetism is given by

$$T_{\mu\nu} = F_{\mu\rho}F_\nu^\rho - \frac{1}{4}g_{\mu\nu}F_{\rho\sigma}F^{\rho\sigma} \tag{1.70}$$

and in terms of a differential form, the electromagnetic field strength is taken to be

$$F = dA = \frac{\boldsymbol{Q}}{4\pi r^2}dt \wedge dr \tag{1.71}$$

with potential

$$A_0 = \frac{\boldsymbol{Q}}{4\pi r} \tag{1.72}$$

A complete derivation of the Reissner-Nordström metric is given in [22], where they also consider the black hole to possess a magnetic charge. Throughout this work I shall focus on an electric potential only, and furthermore this electric potential will only have a non vanishing 0-component as in (1.63). The metric can be written in 3+1 dimensions as

$$ds^2 = -\Delta(r)\,dt^2 + \frac{dr^2}{\Delta(r)} + r^2 d^2\Omega \tag{1.73}$$

where the horizon function $\Delta(r)$ is derived to be

$$\Delta(r) = 1 - \frac{M}{8\pi r} + \frac{\boldsymbol{Q}^2}{4r^2} \tag{1.74}$$

Where here and throughout this paper I shall work in relativistic units where $c = \hbar = 1$. The Reissner Nordström black hole has an inner and an outer event horizon, both these horizons are an example of coordinate singularities [23] due to the fact that they can be resolved by choosing an appropriate coordinate system. The only intrinsic singularity lies at $r = 0$. The inner and outer horizon can be found readily from (1.74). A regular black hole horizon occurs at the largest root of the horizon function.

$$r_{\pm} = \frac{M}{16\pi} \pm \frac{1}{2}\sqrt{(8\pi)^{-2}M^2 - \boldsymbol{Q}^2}, \qquad r_{outer} = r_{+} \tag{1.75}$$

We are interested in the black hole's outer horizon and can readily see from (1.75) that there are three distinct possible scenario's for an outer horizon. For the case where $\boldsymbol{Q}^2 > (M/8\pi)^2$ it is clear that there are no real solutions, and moreover, the metric will be nonsingular everywhere except at the intrinsic singularity where $r = 0$. Consequently this region will not be covered by an event horizon and as a result will disobey Penrose's *cosmic censorship* against naked singularities. We could also have the case where $\boldsymbol{Q}^2 = (M/8\pi)^2$. In this case the black hole becomes extremal, due to the fact that one would have $r_+ = r_- = (M/8\pi)$. As a result the t-coordinate is everywhere time-like except at the horizon $r = (M/8\pi)$ where it becomes null [24]. For $\boldsymbol{Q}^2 < (M/8\pi)^2$ (1.66) becomes singular at $r = 0$ and $r = r_+$ becomes the event horizon. Thus outside the region $r > r_+$ the r-coordinate is space-like and the t-coordinate is time-like, so the weak cosmic censorship criteria is satisfied.

As a last introductory topic, we take a brief look at a black hole solution with a non-zero cosmological constant. The horizon function (1.74) then takes on an extra term as

$$\Delta(r) = 1 - \frac{M}{8\pi r} + \frac{\boldsymbol{Q}^2}{4r^2} + \frac{r^2}{L^2} \tag{1.76}$$

The temperature of the black hole is calculated from the function (1.76) at the horizon, and is given as

$$\mathrm{T} = \frac{\Delta'(r_+)}{4\pi} \tag{1.77}$$

where the prime denotes differentiation with respect to r. The numerator of the r.h.s of (1.77) represents the surface gravity of the black hole. I shall calculate an exact analytic form for the temperature in the next chapter. Now choosing a gauge for the field such that the potential vanishes at the outer horizon, we have.

$$A = A_0 dt = \boldsymbol{Q}\left(\frac{1}{r} - \frac{1}{r_+}\right)dt \tag{1.78}$$

I shall stick to this choice of gauge for the rest of the paper. As mentioned above, in asymptotically AdS regions, ie, at large r, a scalar field obeys the Klein Gordon wave equation

$$(\Box - m^2)\varphi(r) = 0$$

where here, the scalar only depends on the radial coordinate r. For a charged field the equations of motion read

$$\Rightarrow \qquad \frac{1}{\sqrt{-g}} D_\mu \left(\sqrt{-g}\, g^{\mu\nu} D_\nu \varphi\right) - m^2 \varphi = 0 \tag{1.79}$$

where the gauge covariant derivative is given as

$$D_\mu = \partial_\mu - iqA_\mu$$

The determinant of the metric tensor is

$$\sqrt{-g} = r^2 \tag{1.80}$$

For large r the horizon function can be approximated as

$$\Delta(r) \to \left(\frac{r^2}{L^2}\right) \tag{1.81}$$

then for a scalar field $\varphi=\varphi(r)$, (1.79) becomes

$$\frac{1}{r^2}\partial_r\left(\frac{r^4}{L^2}\partial_r\varphi\right)-m^2\varphi=0 \tag{1.82}$$

$$\Rightarrow \quad r^2\varphi''+4r\varphi'-m^2L^2\varphi=0 \tag{1.83}$$

$$\Rightarrow \quad -\delta(-\delta-1)-4\delta-m^2L^2=0$$

$$\Rightarrow \quad \delta^2-3\delta-m^2L^2=0$$

$$\Rightarrow \quad \delta_\pm=\frac{3\pm\sqrt{9+4m^2L^2}}{2} \tag{1.84}$$

which has solutions

$$\delta_+=3-\delta_- \tag{1.85}$$

These are thus the choices of dimension for a scalar operator on the AdS boundary, relating to a field in the bulk geometry with mass m. At the boundary, the leading order terms of the field behave like

$$\varphi\approx\frac{A}{r^{3-\delta}}+\frac{B}{r^\delta}+\cdots \tag{1.86}$$

for some relevant operators A and B describing the conformal field. The only criteria which must be obeyed here, is that the mass of the field operators must be above the Breitenlohner-Freedman (BF) bound. That is that $m^2L^2 > -9/4$. Outside this range, the field becomes unstable. In the next chapter we shall look closely at the case of a conformally coupled scalar field. This takes on a negative mass with a value $m^2L^2=-2$ which is well inside the BF bound. For more information regarding the conformal dimension of operators on the boundary of Anti de-Sitter space, see for example [2].

Chapter 2

It has been argued [25] that black hole horizons can exhibit spontaneous symmetry breaking of an Abelian gauge field for theories with gravity coupled to a matter Lagrangian as simple as the following.

$$\mathcal{L} = R + \frac{6}{L^2} - \frac{1}{4}F_{\mu\nu}^2 - \left|\partial_\mu\varphi - iqA_\mu\varphi\right|^2 - m^2\left|\varphi\right|^2, \qquad \varphi = \varphi(r) \tag{2.1}$$

Where φ is a charged scalar field, and is a function only of its position variable r. The first two terms in (2.1) are just the Einstein-Hilbert Lagrangian plus a negative cosmological constant term. The remaining terms are the Abelian Higgs Lagrangian minus the usual $|\varphi^4|$ term in the potential. It has been stated [25] that this term can be added or discarded without altering the story much.

As explained in the introduction, Anti de-Sitter space is a maximally symmetric vacuum solution to Einsteins field equations with a negative cosmological constant and thus to the equations of motion above. From here on in I shall use a "mostly plus" signature, and take this opportunity to point out once more that Newton's constant G has been set to a value of $1/16\pi$. I shall also always assume that the scalar field $\varphi(r)$ is too small to significantly back-react on the surrounding geometry, thus simplifying our calculations. This yields marginally stable modes in the scalar field. A marginally stable mode being one for which the scalar is infinitesimally small and only position dependent. More importantly, a marginally stable mode is one for which either A or B in (1.86) vanish. The interesting physics lies in the first observed marginally stable mode as the temperature of the black hole is lowered. This first mode occurs at a critical temperature for which the field operator on the boundary space begins to condense.

The initial work presented here shall mirror [25] quite closely, and I shall start out by making plots of the scalar field running from the outer horizon of the black hole out to asymptotic infinity as the black hole gets colder and colder. By examining the boundary values of the field, it will allow us to find marginally stable modes around black hole solutions that do not break the $U(1)$ symmetry. It should be noted that in section 2.2 below, no new results are proven, however the equations of motion along

with their boundary conditions as given in [25] are recast into a dimensionless form. Comparisons are made to plots in [25] as a consistency check. I shall also provide the matlab code which generates both my own graphs, and those in [25] for the interested reader.

2.1 The Reissner-Nordstrom black hole in AdS_4

We begin our analysis by considering a spherically symmetric, time independent, charged scalar field $\varphi(r)$ with charge q and mass m in an Anti de-Sitter-Reissner-Nordström space-time containing a black hole with electric charge $\boldsymbol{Q}$. Such a space-time describes charged black holes in a theory governed by the coupled Einstein-Maxwell equations, and is a solution to the equations of motion following from the Lagrangian (2.1). The metric for the space-time is given as

$$ds^2 = -\Delta(r)dt^2 + \frac{dr^2}{\Delta(r)} + r^2 d^2\Omega_k \tag{2.2}$$

where the horizon function $\Delta(r)$ is given by

$$\Delta(r) = \left(k - \frac{M}{8\pi r} + \frac{\boldsymbol{Z}^2}{r^2} + \frac{r^2}{\boldsymbol{L}^2} \right), \qquad \Delta(r_+) = 0 \tag{2.3}$$

The transverse metric $d^2\Omega_k$ is defined through the curvature constant k as

$$d^2\Omega_k = \begin{cases} \sin^2\theta \, d\theta d\phi, & k = 1, \quad 0 \le \theta < \pi \\ d\theta d\phi, & k = 0, \quad 0 \le \theta < 2\pi \\ \sinh^2\theta \, d\theta d\phi, & k = -1, \quad -\infty < \theta < \infty \end{cases}$$

For the case where $k = 1$, the metric corresponds to that of a unit 2-sphere, while for $k = 0$ it corresponds to the flat space metric on $\mathbf{R}^2$. The $k = -1$ case corresponds to the metric of a hyperbolic plane $\mathbf{H}^2$. Throughout this work I shall focus only on the $k = 0$ case, and only use the $k = 1$ case as a comparison of this work to that of [25]. The parameter $\boldsymbol{Z}$ in (2.3) is related to the charge of the black hole by

$$\boldsymbol{Z}^2 = \frac{1}{4}\boldsymbol{Q}^2 \tag{2.4}$$

and i am now using a bold face type for the Anti de-Sitter radius $\boldsymbol{L}$ as it will be convenient shortly when making these parameters dimensionless. As in (1.77) we work in a gauge where the electric potential only possesses a 0-component and vanishes at the outer horizon r_+ of the black hole. It is define it to be

$$A_0 = \boldsymbol{Q}\left(\frac{1}{r} - \frac{1}{r_+}\right) \tag{2.5}$$

The parameter M in (2.3) represents the mass of the black hole, while as we saw in §1.2, the Anti de-Sitter radius $\boldsymbol{L}$ is related to the cosmological constant via (1.40). We shall see below, the mass term in (2.3) can be got rid of quite easily, and the horizon function (2.3) reduces to a 3 parameter family labelled by k, $\boldsymbol{L}$ and $\boldsymbol{Q}$. One can for example study the Poincaré patch of AdS by fixing the charge of the black hole, whilst keeping $\boldsymbol{L}$ finite and letting k go to zero. The value of the black hole charge $\boldsymbol{Q}$ will also have a finite range, and this range will be determined by finding an exact analytic form of the Hawking temperature at the horizon of the black hole. This will be done below.

We turn our attention now to the horizon function and show that the mass M is completely determined by the outer horizon radius r_+ and the other parameters in (2.3). To that end we note that a regular horizon form's for a positive root of (2.3), and write

$$\Delta(r) = \frac{1}{r^2\boldsymbol{L}^2}\left(r^4 + k\boldsymbol{L}^2r^2 - \frac{M\boldsymbol{L}^2 r}{8\pi} + \boldsymbol{Z}^2\boldsymbol{L}^2\right) \tag{2.6}$$

Pulling a factor of $(r - r_+)$ out of this gives

$$\Delta(r) = \frac{1}{r^2\boldsymbol{L}^2}(r - r_+)\left(r^3 + r_+r^2 + (k\boldsymbol{L}^2 + r_+^2)r + [-\frac{M\boldsymbol{L}^2}{8\pi} + r_+(k\boldsymbol{L}^2 + r_+^2)]\right) \tag{2.7}$$

The last term in square brackets can be easily checked

$$-r_+\left\{-\frac{M\boldsymbol{L}^2}{8\pi}+r_+(k\boldsymbol{L}^2+r_+^2)\right\}=\boldsymbol{Z}^2\boldsymbol{L}^2 \tag{2.8}$$

$$\Rightarrow \quad -r_+^4-k\boldsymbol{L}^2r_+^2+\frac{M\boldsymbol{L}^2}{8\pi}r_+-\boldsymbol{Z}^2\boldsymbol{L}^2=0 \tag{2.9}$$

$$\Rightarrow \quad -\frac{M\boldsymbol{L}^2}{8\pi}+r_+(k\boldsymbol{L}^2+r_+^2)=-\frac{\boldsymbol{Z}^2\boldsymbol{L}^2}{r_+} \tag{2.10}$$

Taking a factor of r_+^4 out of (2.7) and inserting (2.10) we find

$$\Delta(r)=\frac{r_+^4}{r^2\boldsymbol{L}^2}\left(\frac{r}{r_+}-1\right)\left[\left(r/r_+\right)^3+\left(r/r_+\right)^2+\left(\frac{k\boldsymbol{L}^2}{r_+^2}+1\right)\left(r/r_+\right)-\frac{\boldsymbol{Z}^2\boldsymbol{L}^2}{r_+^4}\right] \tag{2.11}$$

At this point it is convenient to define a new set of dimensionless parameters necessary for numerical analysis later. We define them as

$$Z=\frac{\boldsymbol{Z}}{r_+}, \qquad L=\frac{\boldsymbol{L}}{r_+} \tag{2.12}$$

With these definitions in place it is easy to see from (2.10) that the parameter M is determined by the following simple relation

$$M=8\pi r_+(k+Z^2+L^{-2}) \tag{2.13}$$

We now move on to find the equations of motion for the field.

2.2 Equations of Motion

The wave equation for a scalar field in the presence of both gravity and an electric field is

$$\frac{1}{\sqrt{-g}} D_\mu \left(\sqrt{-g} g^{\mu\nu} D_\nu \varphi \right) - \mathrm{m}^2 \varphi = 0 \tag{2.14}$$

Where m is the mass of the scalar field and and g is the determinant of the metric tensor. Again a slightly different type set has been used for the mass of the scalar from the previous chapter as it will shortly be non-dimensionalized, The gauge-covariant derivative is given as

$$D_\mu = \partial_\mu - iqA_\mu \tag{2.15}$$

where, as specified above, the electric potential $A_\mu = \{A_0, 0\}$ is defined such that it vanishes on the outer horizon of the black hole. It is explained in [25] that this is a preferred gauge choice if we are to examine a scalar which doesn't vanish at the outer horizon. This is due to the fact that if the field does not have a time dependent part, the energy in its Lagrangian will diverge to infinity if we choose a non vanishing potential at the horizon.

The first step now is to make a change of position variable for the scalar field and introduce the new dimensionless quAntity

$$u = \frac{r_+}{r} \tag{2.16}$$

This change of variables is for computational reasons later on, and u naturally runs from 1 to 0 as r runs from the outer horizon to infinity. With this in place we may re write the horizon function (2.11) as

$$\Delta(u) = \frac{u^2}{L^2}\left(u^{-1} - 1\right)\left[u^{-3} + u^{-2} + \left(1 + kL^2\right)u^{-1} - Z^2L^2\right] \tag{2.17}$$

$$\Rightarrow \qquad \Delta(u) = \frac{1}{L^2u^2}\left(1 - u\right)\left[1 + u + \left(1 + kL^2\right)u^2 - Z^2L^2u^3\right] \tag{2.18}$$

Now returning back to (2.14) and noting the following

$$g_{\mu\nu} = \begin{pmatrix} -\Delta & & & \\ & 1/\Delta & & \\ & & r^2 & \\ & & & r^2 \end{pmatrix} \qquad g^{\mu\nu} = \begin{pmatrix} -1/\Delta & & & \\ & \Delta & & \\ & & 1/r^2 & \\ & & & 1/r^2 \end{pmatrix} \tag{2.19}$$

and

$$g = \det(g_{\mu\nu}) \quad \Rightarrow \quad \sqrt{-g} = r^2 \tag{2.20}$$

Expanding (2.14) and recalling that gauge covariant derivatives are replaced by partial derivatives when acting on a scalar, we have

$$\frac{1}{r^2}\left\{\partial_0(r^2 g^{00}\partial_0\varphi) + \partial_r(r^2 g^{rr}\partial_r\varphi)\right\} - \mathrm{m}^2\varphi = 0$$

$$\Rightarrow \qquad \frac{1}{r^2}\partial_r(r^2\Delta\partial_r\varphi) + \frac{(q\boldsymbol{Q})^2}{\Delta}\left(\frac{1}{r} - \frac{1}{r_+}\right)^2\varphi - \mathrm{m}^2\varphi = 0 \tag{2.21}$$

Now using the definition (2.16), and rewriting our scalar field as follows so as to make it dimensionless

$$\varphi = \frac{r_+}{r}y = y\cdot u \tag{2.22}$$

Eq (2.21) becomes

$$\frac{u^2}{r_+^2}\left[-\frac{u^2}{r_+}\frac{d}{du}\left(-r_+\cdot\Delta\frac{d}{du}(u\cdot y)\right)\right] + \frac{(q\boldsymbol{Q})^2}{r_+^2}\frac{(u-1)^2}{\Delta}\varphi - \mathrm{m}^2\varphi = 0 \tag{2.23}$$

$$\Rightarrow \qquad u^5\Delta\cdot y'' + u^4(2\Delta + u\Delta')y' + \left\{u^4\Delta' + \frac{Q^2u(1-u)^2}{\Delta} - m^2u\right\}y = 0 \tag{2.24}$$

Where in the last line we multiplied across by r_+^2 and made the following definitions

$$Q = q\boldsymbol{Q}\ , \qquad m = \mathrm{m}r_+ \tag{2.25}$$

to make them dimensionless. The primes in (2.24) indicate differentiation with respect to the variable u. The horizon function $\Delta(u)$ in (2.18) can be rewritten as

$$\Delta(u) = \frac{1}{L^2}\left(4Z^2L^2u^2 - \left(1 + kL^2 + Z^2L^2\right)u + kL^2 + u^{-2}\right) \tag{2.26}$$

Similarly we find

$$\Delta'(u) = \frac{1}{L^2}\left(2Z^2L^2u - \left(1 + kL^2 + Z^2L^2\right) - 2u^{-3}\right)$$

$$\Rightarrow \qquad u^4\Delta'(u) = \frac{u}{L^2}\left(2Z^2L^2u^4 - \left(1 + kL^2 + Z^2L^2\right)u^3 - 2\right) \tag{2.27}$$

and

$$(2\Delta + u\Delta') = \frac{1}{L^2}\left(4Z^2L^2u^2 - 3\left(1 + kL^2 + Z^2L^2\right)u + 2kL^2\right) \tag{2.28}$$

Now dividing (2.24) by u and inserting (2.26)→ (2.28) we find

$$u^4\Delta \cdot y'' + u^3(2\Delta + u\Delta')y' + \left\{u^3\Delta' + \frac{Q^2(1-u)^2}{\Delta} - m^2\right\}y = 0 \tag{2.29}$$

and our equation of motion reads

$$\begin{aligned}&(1-u)(1+u+u^2(1+kL^2)-u^3Z^2L^2)\frac{d^2}{du^2}y(u) \ + \ u\left\{2kL^2 - 3(1+kL^2+Z^2L^2)u + 4Z^2L^2u^2\right\}\frac{d}{du}y(u)\\ &+\left\{\frac{Q^2L^4(1-u)}{(1+u+u^2(1+kL^2)-u^3Z^2L^2)} + 2Z^2L^2u^2 - u(1+kL^2+Z^2L^2) - \frac{1}{u^2}(m^2L^2+2)\right\}y(u) = 0\end{aligned} \tag{2.30}$$

We can now work out the appropriate boundary conditions. Making use of the linearity of this equation, we can choose our first boundary to be $y(1) = 1$ at the horizon without loss of generality. Equation (2.30) is singular at $u = 1$, since the coefficient of y'' vanishes there. At $u = 1$, we have

$$(Z^2L^2 - kL^2 - 3)y'(1) - (1 + kL^2 - Z^2L^2 - m^2L^2 - 2)y(1) = 0 \tag{2.31}$$

and our boundary conditions are

$$y(1) = 1, \qquad y'(1) = \frac{(1 + kL^2 - Z^2L^2 - m^2L^2 - 2)}{(Z^2L^2 - kL^2 - 3)} \tag{2.32}$$

Where the above parameters are subject to only one constraint; namely that the Hawking radiation at the outer horizon of the black hole be positive. The temperature as defined in the previous chapter is

$$\mathrm{T} = \frac{\Delta'(r_+)}{4\pi} \tag{2.33}$$

The prime here represents differentiation with respect to *r*. As mentioned in the previous section, the term in the numerator of the r.h.s of (2.33) represents the surface gravity of the black hole. Working this quAntity out we find

$$\Delta'(r_+) = \frac{M}{8\pi r_+^2} - \frac{2\boldsymbol{Z}^2}{r_+^3} + \frac{2r_+}{\boldsymbol{L}^2}$$

We can use the result obtained in (2.13) to eliminate the *M* term altogether.

$$\Rightarrow \qquad \Delta'(r_+) = \frac{1}{r_+}\left(k + \frac{\boldsymbol{Z}^2}{r_+^2} + \frac{r_+^2}{\boldsymbol{L}^2}\right) - \frac{2\boldsymbol{Z}^2}{r_+^3} + \frac{2r_+}{\boldsymbol{L}^2}$$

$$\Rightarrow \qquad \Delta'(r_+) = \frac{1}{r_+}\left(k - \frac{\boldsymbol{Z}^2}{r_+^2} + \frac{3r_+^2}{\boldsymbol{L}^2}\right)$$

Thus the temperature of the black hole at the outer horizon is expressed in terms of the above parameters as

$$\mathrm{T} = \frac{(kL^2 - Z^2L^2 + 3)}{4\pi r_+} \tag{2.34}$$

Demanding that this be positive at the outer horizon of the black hole places the following constraint on the parameters

$$kL^2 - Z^2L^2 + 3 > 0 \tag{2.35}$$

For the case where k=0, the above constraint reduces to

$$Z^2L^2 < 3 \tag{2.36}$$

Thus the product of Z and L cannot be too large. We may assign the black hole an intrinsic charge, thus fixing the value of the parameter Z . In [25] Gubser fixes the charge of the black hole to unity. If we assign it the same value, then our parameter Z takes on a value of 1/2. This naturally places an upper limit on the parameter L. To 4 decimal places we must have that $L < 3.4641$, and when this condition is saturated the black hole becomes extremal; in the sense that it has zero temperature. One could also equate (2.34) to (2.13) and write the Hawking temperature in terms of the mass parameter M as

$$\mathrm{T} = \frac{1}{4\pi r_+}\left(\frac{ML^2}{8\pi r_+} + 2(1 - Z^2L^2)\right) \tag{2.37}$$

leaving it independent of the curvature constant k. Now, for the special case of a conformally coupled scalar field, $m^2L^2 = -2$, and k=0, so (2.30) simplifies to

$$\begin{aligned}(1-u)(1+u+u^2-u^3Z^2L^2)\frac{d^2}{du^2}y(u) \;+\; u\left\{4Z^2L^2u^2 - 3(1+Z^2L^2)u\right\}\frac{d}{du}y(u) \\ +\left\{\frac{Q^2L^4(1-u)}{(1+u+u^2-u^3Z^2L^2)} + 2Z^2L^2u^2 - u(1+Z^2L^2)\right\}y(u) = 0\end{aligned} \tag{2.38}$$

with boundary conditions

$$y(1) = 1, \qquad y'(1) = \frac{(1 - Z^2L^2)}{(Z^2L^2 - 3)} \tag{2.39}$$

Unfortunately there is no method of finding an analytic solution to (2.38), so we solve it numerically for different values of the two parameters L and Q.

The boundary conditions however are slightly subtle at u=1 due to the singularity there. Thus for computational reasons we must reset the boundary conditions so that

they are close to, but not exactly at u=1. To that end we may re-write (2.38) shorthand as

$$f(u)y''(u)+g(u)y'(u)+h(u)y(u)=0 \tag{2.40}$$

Where

$$f(u)=u^2\Delta(u)L^2=(1-u)(1+u+u^2-u^3Z^2L^2)$$

$$g(u)=4Z^2L^2u^3-3(1+Z^2L^2)u^2$$

$$h(u)=\frac{Q^2L^4(1-u)}{(1+u+u^2-u^3Z^2L^2)}+2Z^2L^2u^2-u(1+Z^2L^2) \tag{2.41}$$

We can now Taylor expand $y(u)$, $f(u)$, $g(u)$ and $h(u)$ about u=1. Letting u=1–ε, with ε small and positive we can write,

$$y(1-\varepsilon)=y_0-\varepsilon y_1+\frac{1}{2}\varepsilon^2 y_2+o(\varepsilon^3)+... \tag{2.42}$$

and

$$f(1-\varepsilon)=-\varepsilon f_1+o(\varepsilon^2)+...$$

$$g(1-\varepsilon)=g_0-\varepsilon g_1+o(\varepsilon^2)+...$$

$$h(1-\varepsilon)=h_0-\varepsilon h_1+o(\varepsilon^2)+... \tag{2.43}$$

Here the subscript "$_0$" represents each function evaluated at u=1, while the subscript "$_1$" represents its derivative evaluated at u=1. From (2.38) one can see that f_0 =0, while the rest of the coefficients are given as

$$g_0=Z^2L^2-3$$

$$h_0=Z^2L^2-1$$

$$f_1=g_0=Z^2L^2-3$$

$$g_1=6(Z^2L^2-1)$$

$$h_1 = -\frac{Q^2 L^4}{(3 - Z^2 L^2)} + 3Z^2 L^2 - 1 \tag{2.44}$$

We now proceed to work out the values of y_i. Expanding (2.40) to first order in ε, we have

$$-\varepsilon f_1 y_2 + (g_0 - \varepsilon g_1)(y_1 - \varepsilon y_2) + (h_0 - \varepsilon h_1)(y_0 - \varepsilon y_1) + o(\varepsilon^2) = 0 \tag{2.45}$$

Equating the coefficients of zeroth order power in ε yields

$$\begin{aligned} & g_0 y_1 + h_0 y_0 = 0 \\ \Rightarrow \qquad & y_1 = -\frac{h_0}{g_0} y_0 \end{aligned} \tag{2.46}$$

Setting $y(1) = y_0 = 1$, we can see from (2.44) that

$$y_1 = -\frac{(1 - Z^2 L^2)}{(3 - Z^2 L^2)} \tag{2.47}$$

Solving for y_2 in the remainder of (2.45), one finds

$$y_2 = \frac{\left(\frac{h_0}{g_0}(g_1 + h_0) - h_1 \right)}{(f_1 + g_0)} \tag{2.48}$$

This demands that $f_1 + g_0 \neq 0$. In fact one can readily see that $f_1 + g_0 = 2g_0$, and so (2.48) can be written more compactly as

$$\Rightarrow \qquad y_2 = \frac{{h_0}^2 + g_1 h_0 - h_1 g_0}{2{g_0}^2} \tag{2.49}$$

Subbing eq's (2.44) into this we find

$$y_2 = \frac{Q^2L^4 - 4(Z^4L^4 - Z^2L^2 + 1)}{2(3 - Z^2L^2)^2} \tag{2.50}$$

Inserting (2.47) and (2.50) into (2.42) we obtain the leading order terms in the series solution about u=1–ε

$$y(1-\varepsilon) = 1 + \left(\frac{1 - Z^2L^2}{3 - Z^2L^2}\right)\varepsilon + \left(\frac{Q^2L^4 - 4(Z^4L^4 - Z^2L^2 + 1)}{4(3 - Z^2L^2)^2}\right)\varepsilon^2 + o(\varepsilon^3) + \ldots \tag{2.51}$$

Thus, to order ε, we can consistently set our boundary conditions as

$$y(1-\varepsilon) = 1 + \left(\frac{1 - Z^2L^2}{3 - Z^2L^2}\right)\varepsilon \tag{2.52}$$

and

$$y'(1-\varepsilon) = -\left(\frac{1 - Z^2L^2}{3 - Z^2L^2}\right) - \left(\frac{Q^2L^4 - 4(Z^4L^4 - Z^2L^2 + 1)}{2(3 - Z^2L^2)^2}\right)\varepsilon \tag{2.53}$$

After fixing the value of ε to be sufficiently small, we may integrate the scalar from directly outside the black hole horizon out to asymptotic infinity. We're now in a position to write a matlab routine (See Appendix) that examines the behaviour of the scalar field. It is a trivial matter if one wishes to examine the scalar for different masses and different values of the curvature constant k. Including the mass and curvature terms, equations (2.44) become

$$\begin{aligned} g_0 &= Z^2L^2 - kL^2 - 3 \\ h_0 &= g_0 - m^2L^2 \\ f_1 &= g_0 \\ g_1 &= 6(Z^2L^2 - 1) - 4kL^2 \\ h_1 &= -\frac{Q^2L^4}{(3 + kL^2 - Z^2L^2)} + 3(Z^2L^2 + 1) - kL^2 + 2m^2L^2 \end{aligned} \tag{2.54}$$

Although the rest of this work will focus only on the case of a scalar with negative

mass, I have added for completeness, plots for the case of positive mass and curvature constant k=1. For figures 4 and 5 below, I have used L values coinciding with those taken in [25].

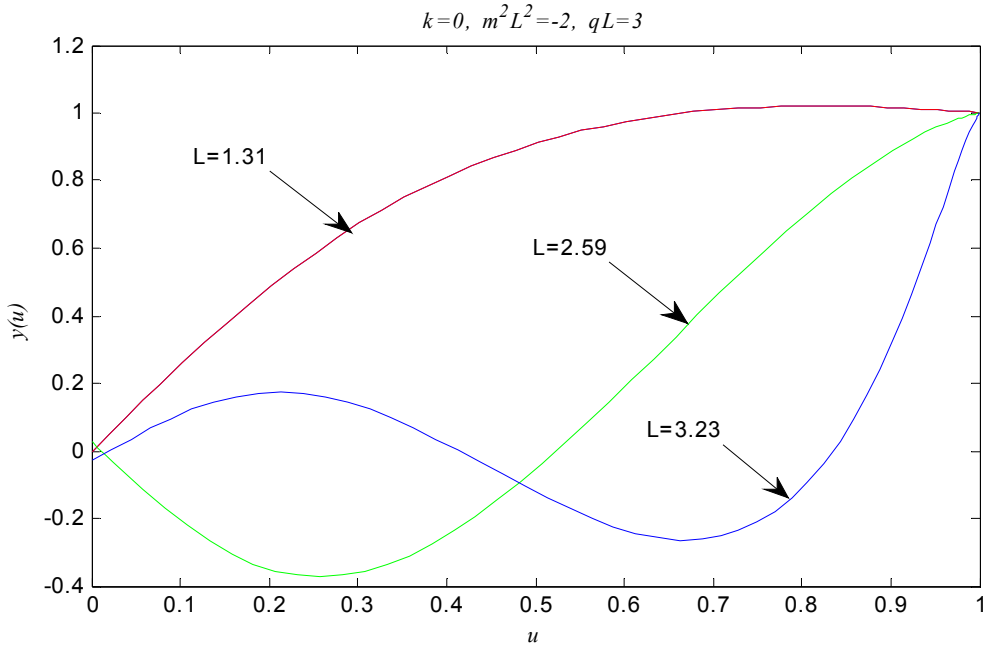

Figure 4: Examples of marginally stable modes in an AdS4 geometry.

As a consistency check, eq(2.30) and its boundary conditions where rewritten in terms of the position variable r instead of u. Writing the equation of motion out shorthand as

$$f(r)\varphi''(r)+g(r)\varphi'(r)+h(r)\varphi(r)=0 \tag{2.55}$$

where

$$f(r)=\frac{1}{r^2L^2}(r-1)(r^3+r^2+r(1+kL^2)-Z^2L^2)$$

$$g(r)=\left(\frac{2f}{r}+f'\right)$$

$$h(u)=\frac{(qQ)^2}{f}(r^{-1}-1)^2-m^2 \tag{2.56}$$

and

$$f'(r)=\frac{1}{r^2L^2}\left\{2r^3+Z^2L^2+kL^2+1-\frac{2Z^2L^2}{r}\right\} \tag{2.57}$$

with boundary conditions

$$\varphi(1)=1, \qquad \varphi'(1)=\frac{m^2L^2}{3+kL^2-Z^2L^2} \tag{2.58}$$

In the conformal limit with k=0 and $m^2L^2=-2$, the latter bound reduces simply to

$$\varphi'(1)=\frac{2}{Z^2L^2-3} \tag{2.59}$$

Which naturally also requires the condition (2.36) to hold true. These results produced the following plots, which should be compared to [25].

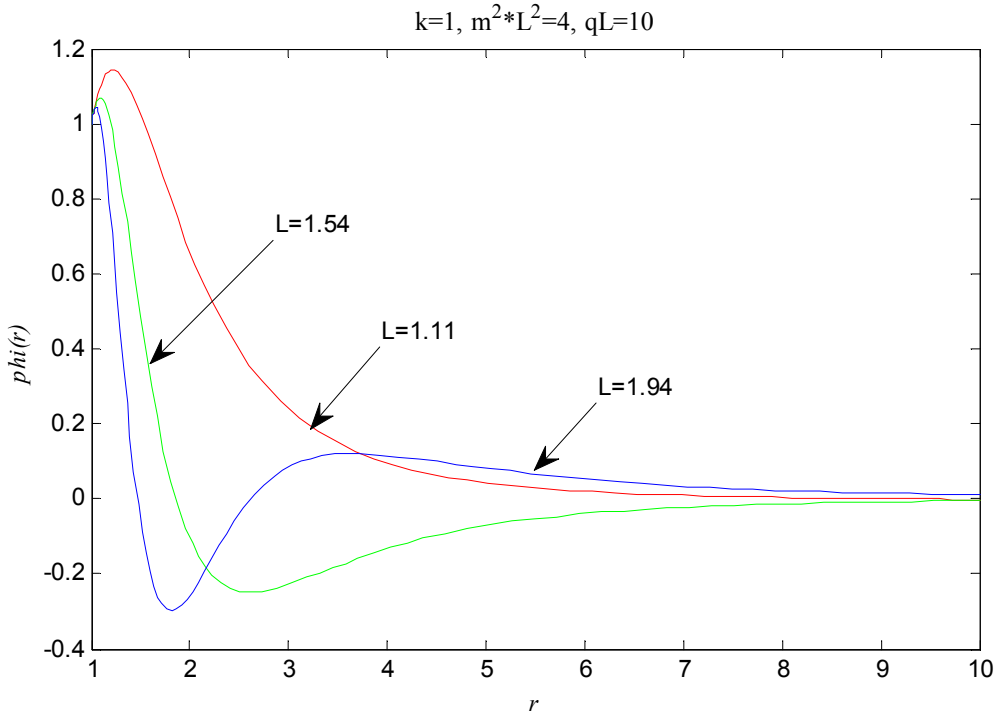

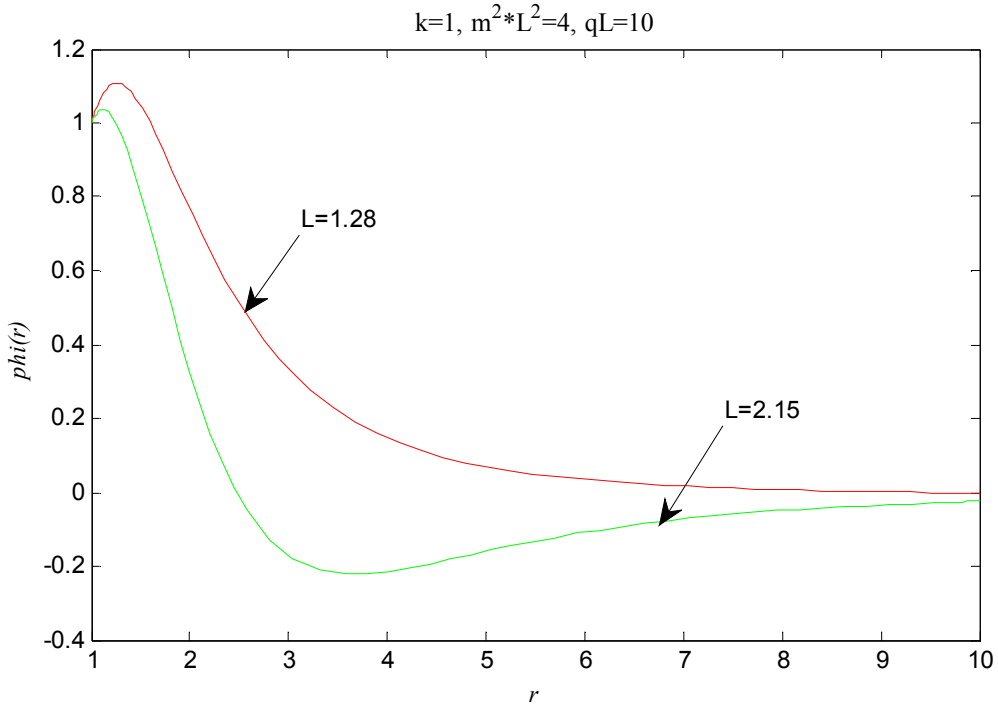

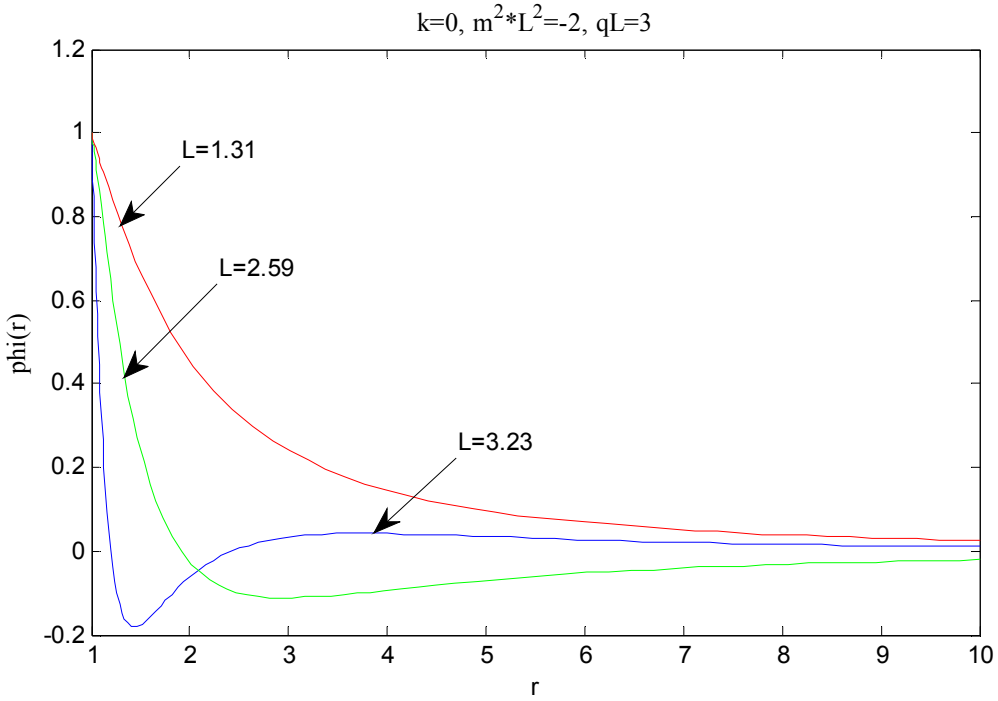

Figure 5(a),(b),(c): Example of Marginally stable modes in φ(*r*)

In Figures 4 and 5, the product's m^2L^2 and qL are held fixed while L is varied. These values of the parameters essentially hold the theory fixed as the temperature of the black hole is varied. For the values of the parameters chosen in Figure 4b, $m^2 > 0$, and the field is only integrated out to a value of u=0.1. When taken closer to infinity the field begins to diverge, compounding the fact that a scalar with a positive mass can never reach the conformal boundary. This point is also made in [25]. We can also clearly see the field become more and more unstable as the temperature of the black hole is lowered; that is, as the parameter L is raised.

We are interested in finding the vacuum expectation value of the operators in the conformal quantum field at the AdS_4 boundary. They correspond to the field points at $u = 0$ in figure 4. They will be dual to the scalar field in the bulk gravity theory. We will show in the next section that there are certain values of the vev and its coupling in the conformal field theory that leave the action of the boundary theory unperturbed and consequently give rise to an intermittent vanishing of the energy momentum tensor for the field at the boundary. As mentioned, it will be the very first instance that the vev or its coupling strength vanishes that will be the critical temperature T_c for the system, and it is from this point that the scalar begins to condense as the black hole gets colder and colder, giving rise to superconductivity.

Writing (1.86) in terms of the dimensionless variable u we see the behaviour of the solutions of (2.38) at the AdS boundary go like

$$y = A_y u^{2-\delta} + B_y u^{\delta-1} \tag{2.60}$$

For some operators A_y and B_y in the conformal boundary. These operators can be considered to be the 'endpoints' of the scalar field in the bulk gravity theory. As explained in the previous chapter, δ is the mass dimension of the field and its value is determined by the quadratic expression

$$m^2L^2 = \delta(\delta - 3) \tag{2.61}$$

where the product m^2L^2 needs only to obey the BF bound. For the case of a conformally coupled scalar field where $m^2L^2 = -2$, (2.61) has roots $\delta_+ = 2$ and $\delta_- = 1$. Using the positive root, (2.60) become

$$y = A_y + uB_y \tag{2.62}$$

If one instead takes the negative root, it becomes

$$y = B_y + uA_y \tag{2.63}$$

Switching from δ_+ to δ_- merely swaps operators [2]. We examine these operators in the section below.

2.3 The VEV of the trace Energy Momentum Tensor

The vacuum expectation value of the trace energy momentum tensor sets the local scale for the theory. The energy momentum tensor itself can be generally written in terms of a matter action and a dynamical metric as

$$T_{\mu\nu} = -\frac{2}{\sqrt{-g}}\frac{\delta S_M}{\delta g_{\mu\nu}} \tag{2.64}$$

where

$$S_M = \int d^4x\sqrt{-g}L_M$$

and L_M is the matter part of the Lagrangian. When working in a quantum field theory (as we are on the conformal boundary of Anti de-Sitter space), one deals with the local operators to set the scale, and to that end we call upon the associated trace identity, which takes the form

$$g^{\mu\nu}\langle T_{\mu\nu}\rangle = \langle\Theta\rangle \tag{2.65}$$

where

$$\Theta = \beta^i O_i \tag{2.66}$$

for operators O_i on the boundary space. Equation (2.65) assumes that the operators O_i form a basis for the trace of the energy momentum tensor with coefficients, the β-functions. The β-functions arise from the renormalisation group, and encode the energy dependence of the operator and its coupling for a given process. As stated in chapter 1,

the energy scale and the length scale are viewed on the same footing in Anti de-Sitter space-time. The parameter L will set this scale for us. The β-functions are then expressed as

$$\beta(g_i) = L\frac{d}{dL}g_i \tag{2.67}$$

This dependence on the energy/length scale is known as the 'running' of the coupling parameter. Our beta functions will thus find the logarithmic derivatives of the vev and its coupling for a varying temperature of the black hole.

We turn our attention now to (2.62). We are interested in computing the vacuum expectation values of the operators A_y and B_y at the conformal boundary of Anti de-Sitter space. This corresponds to where u=0, and we accordingly define our operator to be

$$A_y = \langle O_y \rangle = y_L(0) \tag{2.68}$$

with coupling strength

$$B_y = g_y = y'_L(0) \tag{2.69}$$

The prime in (2.69) indicates the derivative of the scalar with respect to u, while the subscript "$_L$" indicates that both the operator and the coupling parameter are evaluated on the boundary as the temperature of the black hole is varied. It is evident from §2.2 that in general $\langle O_y \rangle \neq 0$, thus the system exhibits a spontaneous breaking of the global $U(1)$ symmetry on the boundary.

Now, the effective action for the boundary theory can be written as

$$S_{eff}[g_y] = S_0 + g_y \langle O_y \rangle \tag{2.70}$$

Where S_0 is a fixed point in the action of the conformal field theory. The second term on the r.h.s of (2.70) represents perturbations away from this fixed point. In what follows we shall see that there exists value's of the vev, and its coupling for which the action (2.70) remains unperturbed at the boundary, and consequently leads to a vanishing of the energy momentum tensor.

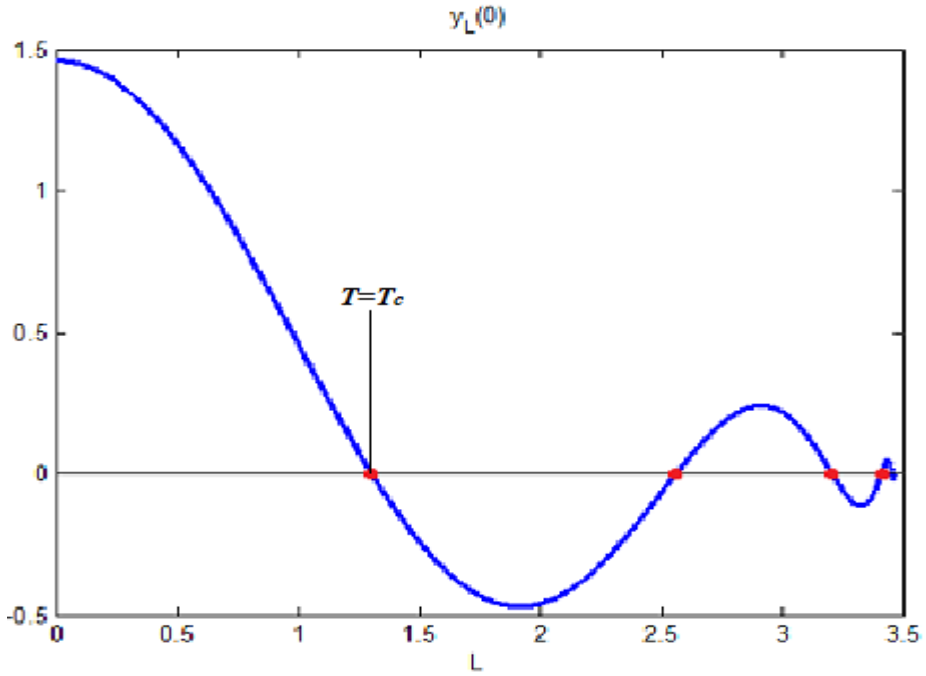

Figure 6: (a) Operator O_y on the AdS_4 boundary, $qL=3$, $\boldsymbol{Q}=1$, $Z=1/2$

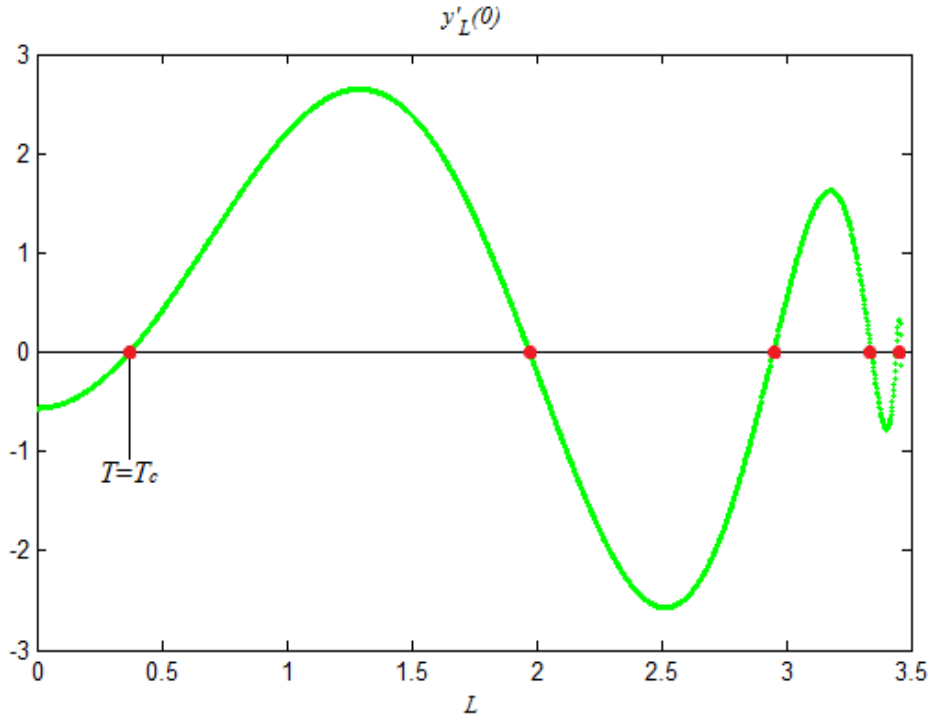

Figure 6: (b) coupling constant g_y on the boundary, $qL=3$, $\boldsymbol{Q}=1$, $Z=1/2$

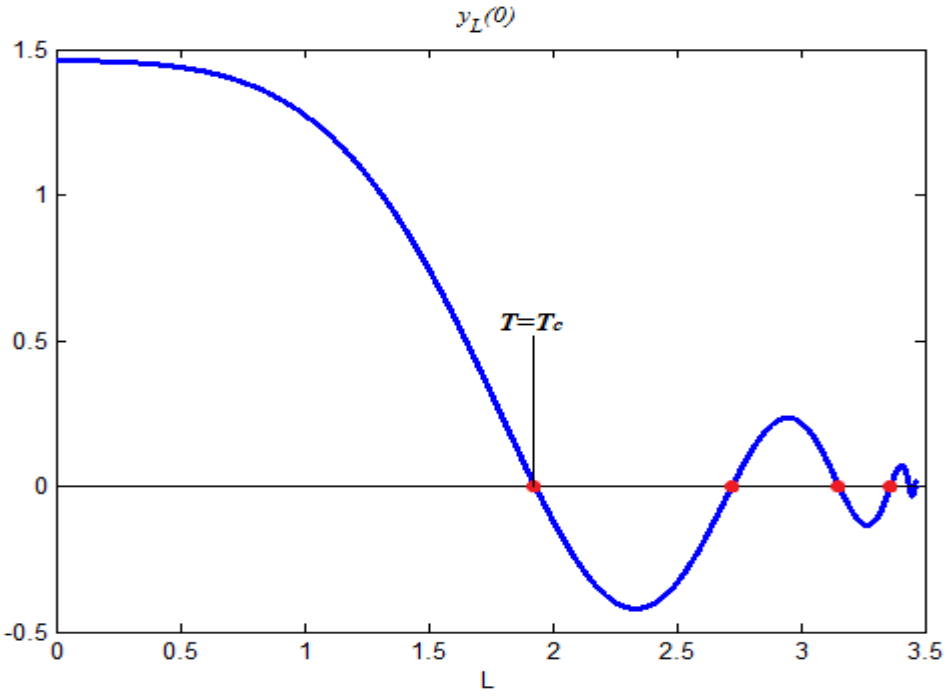

Figure 6: (c) Operator O_y on the AdS_4 boundary, q=1, $\boldsymbol{Q}$=1, Z=1/2

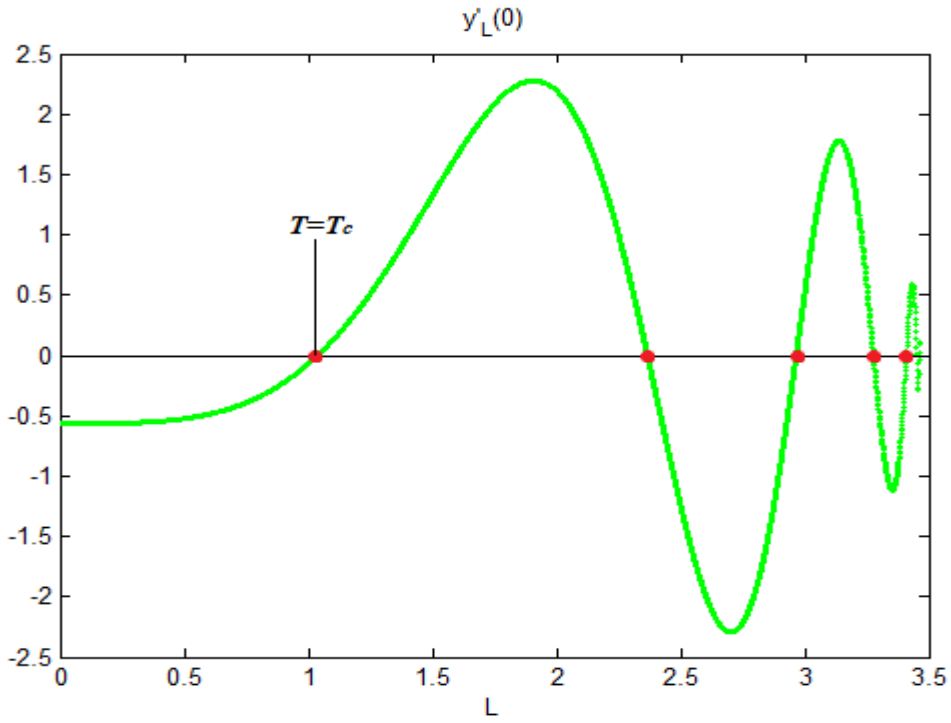

Figure 6: (d) coupling constant g_y on the boundary, q=1, $\boldsymbol{Q}$=1, Z=1/2

Above are plots of both the operator and its coupling at the conformal boundary. It is important to note that for all the below plots in this section I work in the case of a conformally coupled scalar field and so take k=0 and $m^2L^2 = -2$. The charge q of the scalar was absorbed into the total system charge Q in the previous section, and I set the value of Q to be unity, thus assigning the parameter Z a value of 1/2. These values of the parameters apply to all the plots in this section unless specified under the graph. It can be seen from figures 6(a) and (c) that the operator A_y takes on a positive value of 1.46 at zero L. The points of interest are where either the vev, or its coupling vanish (the points marked with a red dot above), and more importantly the first instance at which one of them vanishes. This point represents the critical temperature of the system and can be seen in figure 6(b) to occur at L=0.371. Here we have set qL=3 as in [25], and one see's from figure 6(c) and (d) that if one instead sets the scalar charge to unity, that the L value at which the critical temperature is reached increases by quite a bit, with T_c occuring at L=1.93 for 6(c) and L=1.037 for 6(d). In figure 6(a) the critical temperature for the vev is clearly marked, and the L value at which this critical temperature occurs coincides with the lowest L value chosen by Gubser in [25] for the parameters chosen above. As in [25], I have let the product qL=3 in figures 6 (a) and 6(b), and the critical temperature in 6(a) occurs at L=1.31. This marginally stable mode can be seen plotted in figure 5(a) above. Plugging the L value of the critical temperature in figure 6(a) into (2.34) and recalling that we're working with k= 0, we find $T_c = 0.205/r_+$, and for figure 6(b) we find $T_c = 0.236/r_+$. This is the critical temperature for the system if one holds qL=3, while varying L. When the scalar charge is set at unity as in figures 6(c) and (d), we find the critical temperature for 6(c) corresponding to the vev $y(0)$ to be $T_c = 0.165/r_+$. and for 6(d), which corresponds to the coupling $y'(0)$ to be $T_c = 0.217/r_+$. We can set r_+ to unity without a loss in generality. At the critical temperature in each instance the scalar begins to condense and for temperatures $T < T_c$ it can be seen that the scalar tends towards a zero value. This point can perhaps be made slightly clearer if one performs a parametric plot of the operator versus its coupling. The resultant plot displays a rather striking spiral-like behaviour near the origin. In figure 7 below we are seeing the temperature of the black hole decrease as the curve spirals in on itself, and just as in the previous plots of the operator and its coupling, the curve naturally tends towards zero the colder the black hole gets. This kind of spiral behaviour near the origin has been observed in

other works such as [26] and [27]. Albeit for very different theories, in which they work with a system of fermions, the motivation and resultant plots are indeed quite similar.

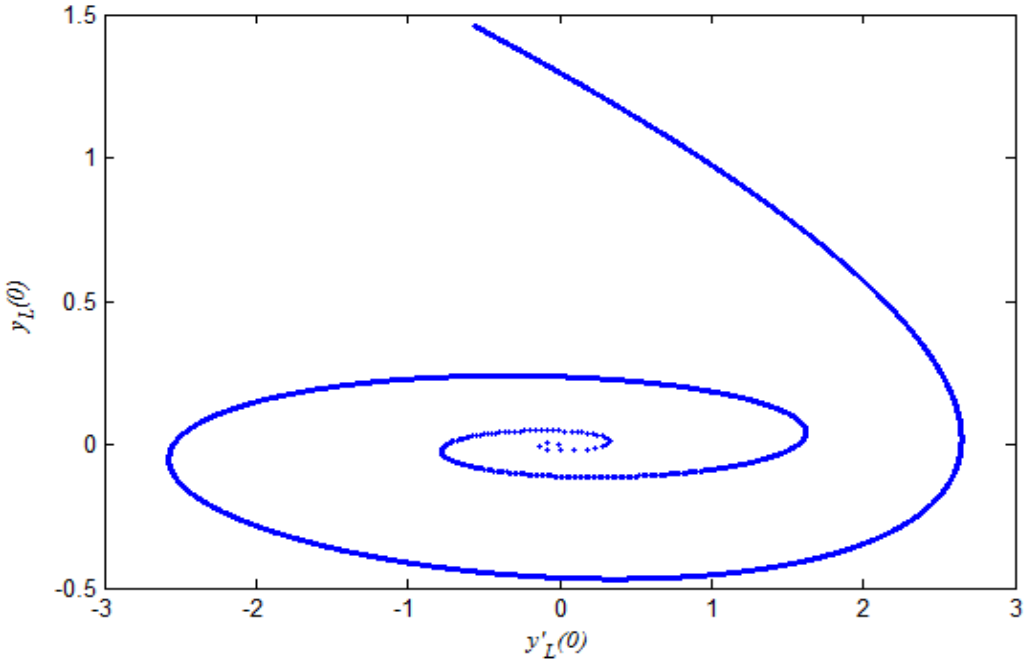

Figure 7(a): Parametric plot of the vev $<A_y>$ verses its coupling g_y, qL=3, $\boldsymbol{Q}$=1, Z=1/2

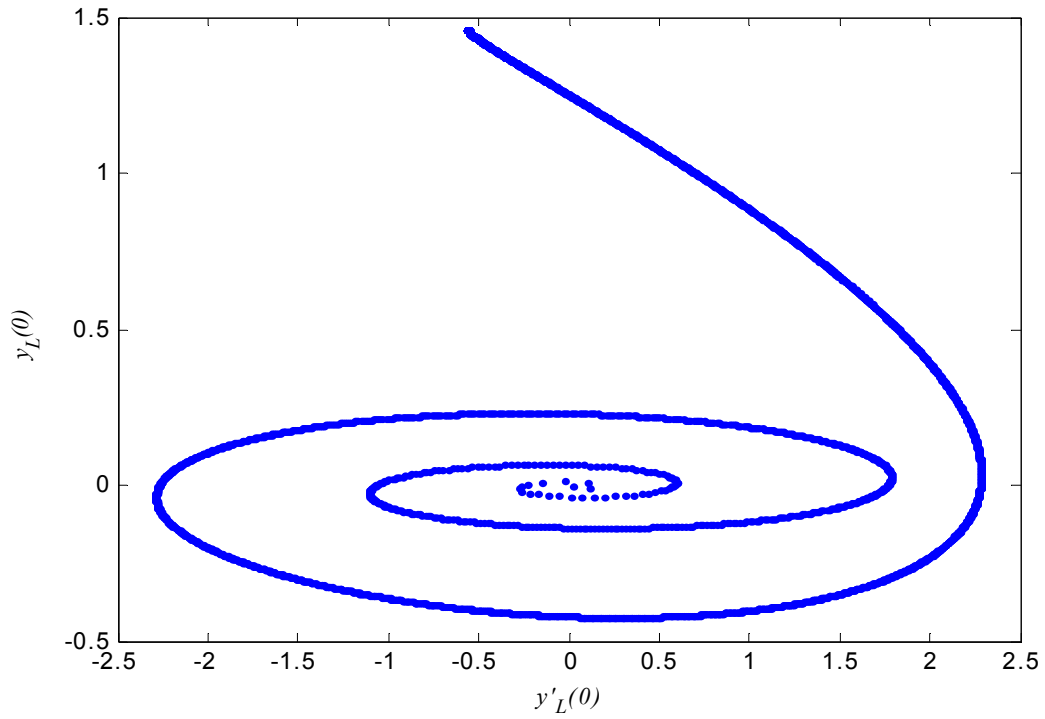

Figure 7(b): Parametric plot of the vev $<A_y>$ verses its coupling g_y, q=1, $\boldsymbol{Q}$=1, Z=1/2

The dotted red points in figures 6 represent a fixed action in the boundary theory, ie, at these points the action for the field at the boundary remains unperturbed because the second term on the r.h.s of (2.70) vanishes giving

$$S_{eff}[g_y] = S_0$$

Now, essentially what we are looking for, from (2.65 - 2.67) is the following

$$\langle \Theta \rangle = \beta(g_y)\langle O_y \rangle \tag{2.71}$$

$$\Rightarrow \qquad \langle \Theta \rangle = \left[L\frac{d}{dL} g_y \right] A_y \;=\; \left[L\frac{d}{dL} y'_L(0) \right] y_L(0) \tag{2.72}$$

One could also work in terms of the negative root of (2.61) with a mass dimension $\delta_- = 1$. In this case the vev of the energy momentum tensor would read

$$\langle \Theta \rangle = \left[L\frac{d}{dL} y_L(0) \right] y'_L(0) \tag{2.73}$$

If we set the fixed action S_0=0, then the total effective action becomes the product of the operator and its coupling strength,

$$S_{eff}[g_y] = y(0)\cdot y'(0) \tag{2.74}$$

The reader will notice that taking the logarithmic derivative of this action will result in the sum of the vev's for both roots of (2.61).

$$L\frac{d}{dL} S_{eff}[g_y] = \left[L\frac{d}{dL} y'(0) \right] y(0) + \left[L\frac{d}{dL} y(0) \right] y'(0) \tag{2.75}$$

$$\Rightarrow \qquad S'_{eff}[g_y] = \langle \Theta_1 \rangle \;+\; \langle \Theta_2 \rangle \tag{2.76}$$

Where the prime and subscripts in (2.76) are clarified in (2.75). We make separate

plots of the effective action and vevs of the energy momentum tensor on the AdS boundary.

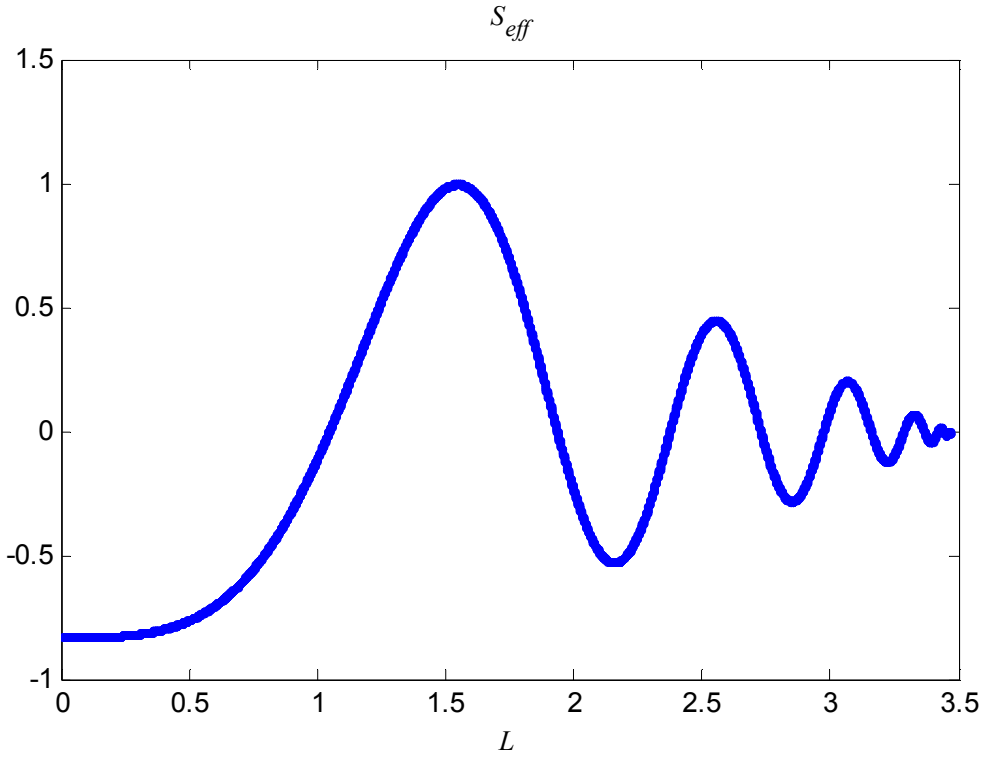

Figure 8: The effective action of the theory at the boundary, q=1, $\boldsymbol{Q}$=1, Z=1/2

This is reminiscent of Fig.7(b) and naturally possesses precisely the same amount of zero nodes, as L is increased from 0 to its cut off point. We thus expect the energy momentum tensor to vanish accordingly at these points. As the temperature of the black hole is reduced, the amplitude of each crest in the effective action decreases periodically until it oscillates around zero near extremality.

To obtain the vevs of the energy tensor numerically, a central difference technique was used in accordance with (2.72) and (2.73). The results are as follows

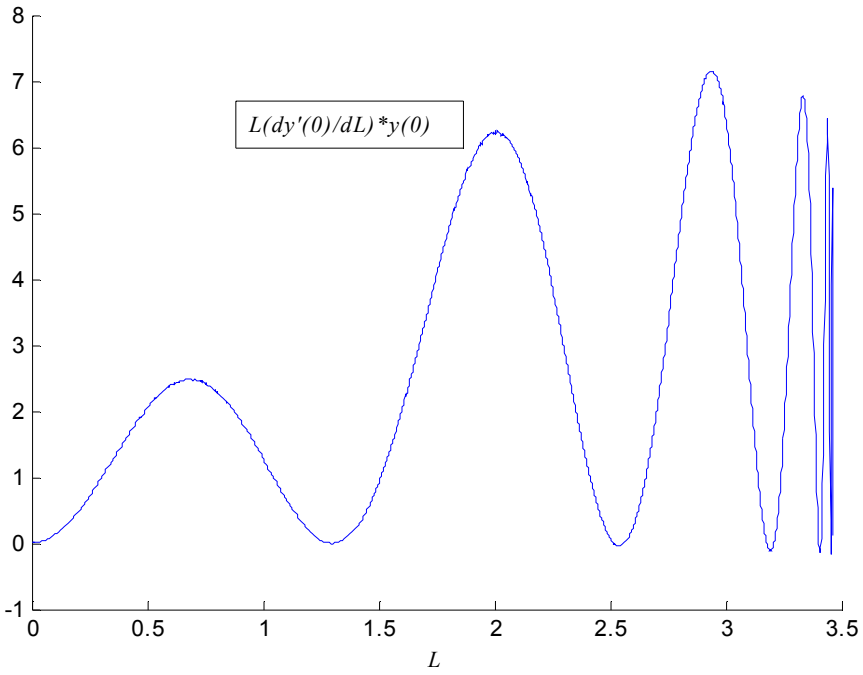

Figure 9(a): The VEV of the trace energy momentum tensor for mass dimension $\delta_+ = 2$, qL=3, $\boldsymbol{Q}$=1

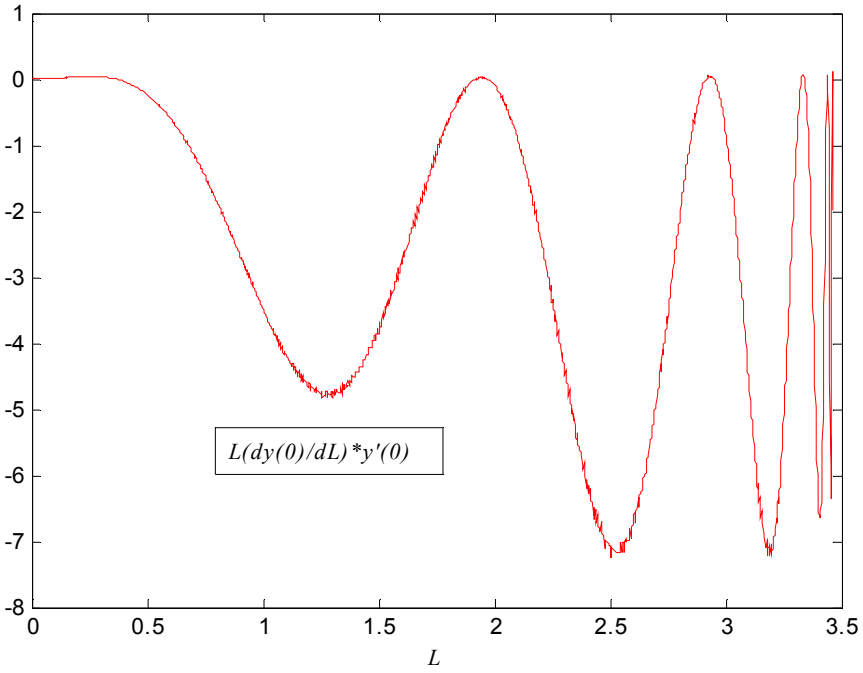

Figure 9(b): The VEV of the trace energy momentum tensor for mass dimension $\delta_- = 1$, qL=3, $\boldsymbol{Q}$=1

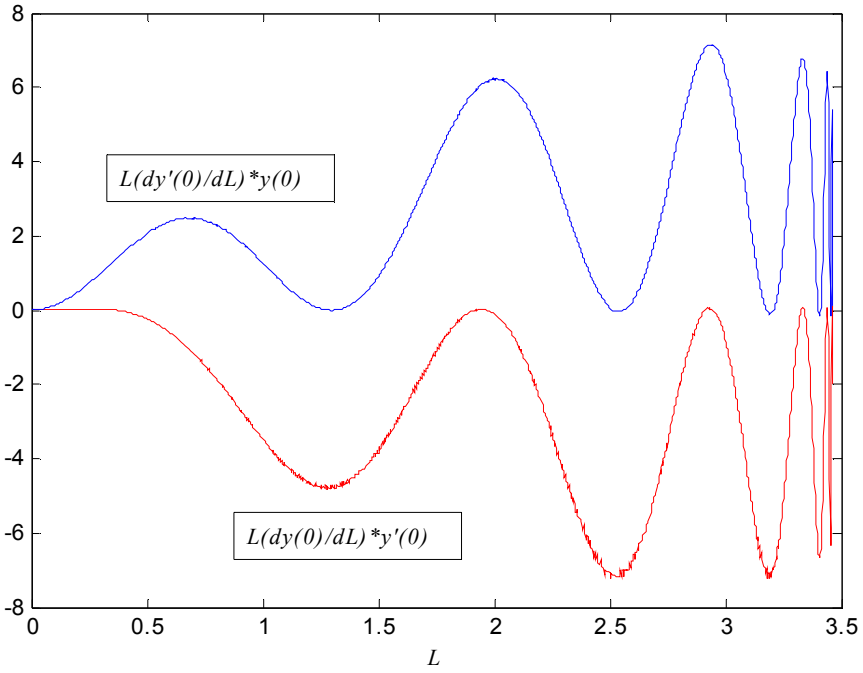

Figure 9(c): Plot of 9(a) and 9(b) back to back

Setting the scalar charge to unity doesn't alter the plots a whole lot.

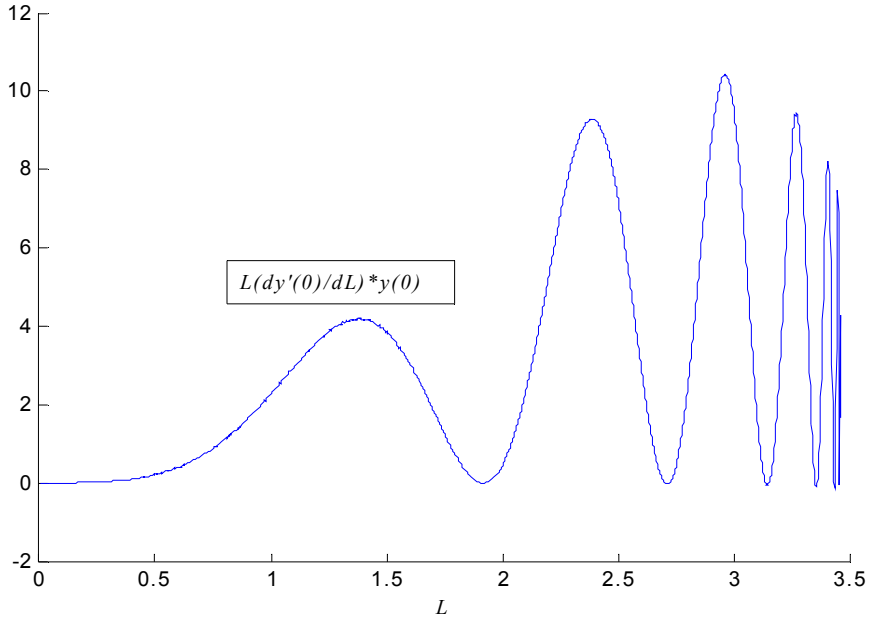

Figure 9(d): The VEV of the trace energy momentum tensor for mass dimension $\delta_+ = 2$, q=1, $\boldsymbol{Q}$=1

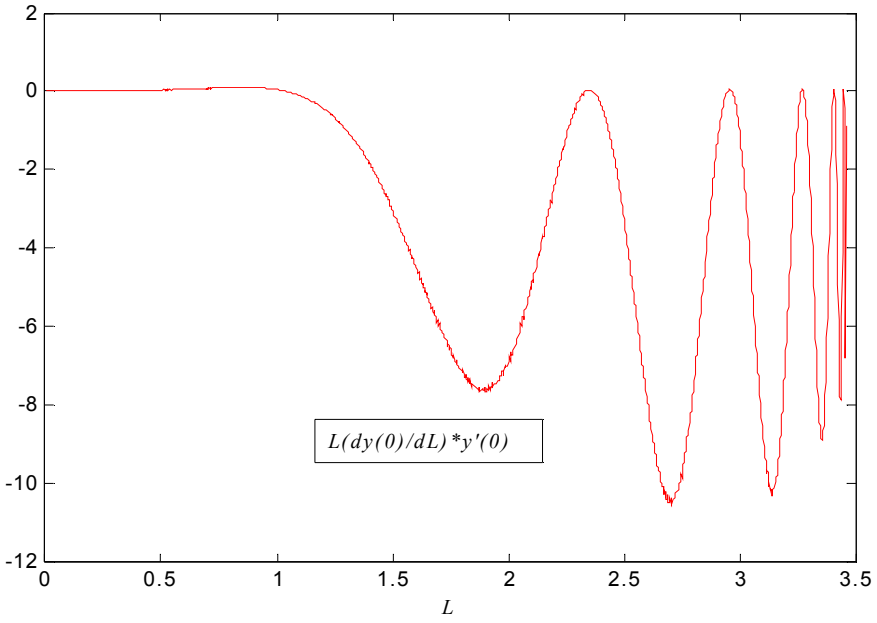

Figure 9(e): The VEV of the trace energy momentum tensor for mass dimension $\delta = 1$, $q=1$, $\boldsymbol{Q}=1$

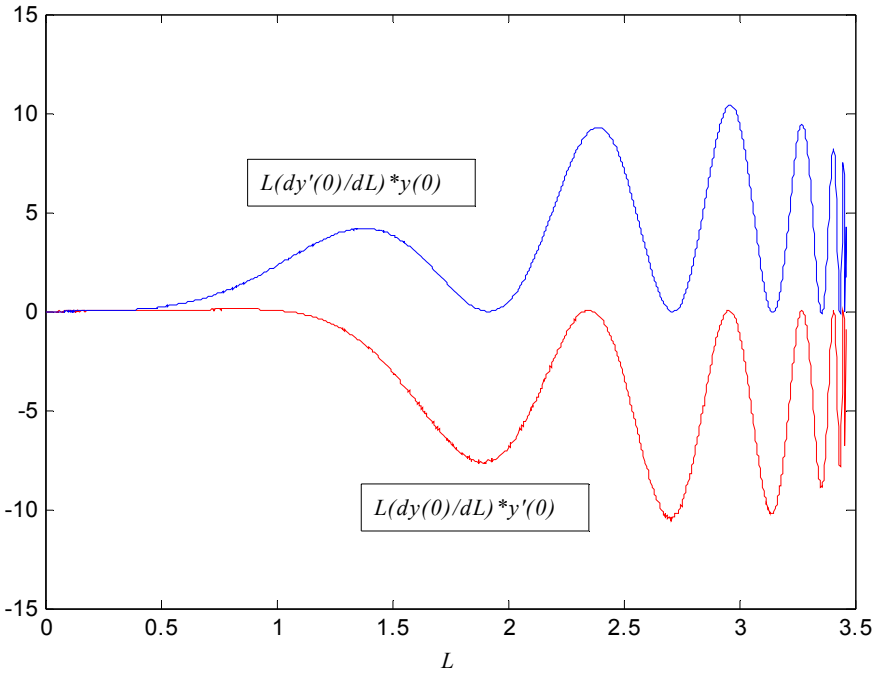

Figure 9(f): Plot of 9(d) and 9(e) back to back

It is interesting to see both vevs plotted back to back, as although they are out of phase with each other they seem to mirror one other in a sense.

2.4 Time dependent scalar field

Equations of Motion

We now attempt to find a dispersion relation for the field. This will again be a purely numerical endeavour. We must however re-derive the equation of motion with the appropriate boundary conditions. Firstly we assume the scalar has a time dependence and rewrite the field as

$$\varphi(t,r,x) = \varphi(r)e^{-i(\omega t - Kx)} \tag{2.77}$$

where for our purposes it is sufficient to take the wave-vector K to be purely in the x-direction and transverse to the radial coordinate r. Inserting (2.74) into (2.14) one finds

$$\frac{1}{r^2}\left\{D_0(r^2 g^{00} D_0\varphi) + D_r(r^2 g^{rr} D_r\varphi) + D_x(r^2 g^{xx} D_x\varphi) + D_y(r^2 g^{yy} D_y\varphi)\right\} - \mathrm{m}^2\varphi = 0 \tag{2.78}$$

The field has no y-dependence so the scalar derivative in that direction is accordingly zero. If we set $A_x = A_y = 0$ in the electric potential (it should be noted that here A_y denotes the y-component of the electric potential and not the operator of the last section), (2.75) becomes

$$\Rightarrow \qquad -\frac{1}{\Delta}\left(\partial_0^2 - 2iqA_0\partial_0 + q^2A_0^2\right)\varphi + \frac{1}{r^2}\partial_r(r^2\Delta\partial_r\varphi) + \frac{1}{r^2}\partial_x^2\varphi - \mathrm{m}^2\varphi = 0 \tag{2.79}$$

$$\Rightarrow \qquad \frac{1}{r^2}\partial_r(r^2\Delta\partial_r\varphi) + \left\{\frac{\omega^2 - 2\omega qA_0 + q^2A_0^2}{\Delta} - \frac{K^2}{r^2} - \mathrm{m}^2\right\}\varphi = 0 \tag{2.80}$$

The first term in (2.80) is the same as that of our original analysis in §2.2 so we focus on the term linear in φ. We again make the definitions (2.16) and (2.22) and in what follows we shall only consider the case where the curvature constant $k = 0$. Equation (2.80) then becomes

$$\frac{u^2}{r_+^2}\left\{-\frac{u^2}{r_+}\frac{d}{du}(-r_+\Delta\frac{d}{du}(u\cdot y))\right\}+\frac{1}{r_+^2}\left\{\frac{\omega^2 r_+^2-2\omega r_+^2 qA_0+r_+^2q^2A_0^2}{\Delta}-\frac{K^2r_+^2}{r^2}-\mathrm{m}^2r_+^2\right\}u\cdot y=0$$

$$\Rightarrow\quad \frac{u^2}{r_+^2}\left\{-\frac{u^2}{r_+}\frac{d}{du}(-r_+\Delta\frac{d}{du}(u\cdot y))\right\}+\frac{1}{r_+^2}\left\{\frac{\tilde{\omega}^2-2\tilde{\omega}Q(1-u)+Q^2(1-u)^2}{\Delta}-K^2u^2-m^2\right\}u\cdot y=0$$

$$\Rightarrow\quad u^4\frac{d}{du}\left\{\Delta(y+u\frac{dy}{du})\right\}+\left\{\frac{\tilde{\omega}^2-2\tilde{\omega}Q(1-u)+Q^2(1-u)^2}{\Delta}-K^2u^2-m^2\right\}u\cdot y=0$$

$$\Rightarrow\quad u^3\left\{\Delta uy''+(2\Delta+\Delta' u)y'+\Delta' y\right\}+\left\{\frac{\tilde{\omega}^2-2\tilde{\omega}Q(1-u)+Q^2(1-u)^2}{\Delta}-K^2u^2-m^2\right\}y=0$$

Giving

$$\left(u^4\Delta\right)y''+u^3(2\Delta+\Delta' u)y'+\left\{u^3\Delta'+\frac{\tilde{\omega}^2-2\tilde{\omega}Q(1-u)+Q^2(1-u)^2}{\Delta}-K^2u^2-m^2\right\}y=0 \tag{2.81}$$

Where again all parameters have been rescaled as follows to make them dimensionless

$$L=\frac{\boldsymbol{L}}{r_+},\qquad Z=\frac{\boldsymbol{Z}}{r_+},\quad \tilde{\omega}=\omega r_+,\qquad m=\mathrm{m}r_+,\qquad Q=q\boldsymbol{Q},\qquad K=K_x \tag{2.82}$$

Recalling the definition of the horizon function (2.18) our equation of motion becomes.

$$\begin{aligned}&(1-u)(1+u+u^2-u^3Z^2L^2)\frac{d^2}{du^2}y(u)+u\left\{4Z^2L^2u^2-3(1+Z^2L^2)u\right\}\frac{d}{du}y(u)\\&+\left\{\frac{L^4(Q^2(1-u)^2-2\tilde{\omega}Q(1-u)+\tilde{\omega}^2)}{(1-u)(1+u+u^2-u^3Z^2L^2)}+2Z^2L^2u^2-u(1+Z^2L^2)-K^2L^2-\frac{1}{u^2}(m^2L^2+2)\right\}y(u)=0\end{aligned} \tag{2.83}$$

There is one problem with this equation however. The squared frequency term in the prefactor of $y(u)$ diverges at the horizon where $u = 1$. We deal with this by looking for solutions to (2.83) of the form

$$y(u)=(1-u)^{\nu}x(u) \tag{2.84}$$

The value of the exponent ν is to be determined so that it rids the singularity in $y(u)$.

Due to the fact that (2.83) is a second order differential equation we expect ν to take on two separate values $\nu_{\pm}$ corresponding to ingoing and outgoing waves (or visa versa) at the outer horizon. Due to the premise that matter cannot escape the black hole once its outer horizon is reached, we will concern ourselves with the appropriate value of ν obeying ingoing boundary conditions at the outer horizon. From (2.84) the u-derivatives of the scalar are given as

$$y'(u) = -\nu(1-u)^{\nu-1}x(u) + (1-u)^{\nu}x'(u) \tag{2.85}$$

and

$$y''(u) = \nu(\nu-1)(1-u)^{\nu-2}x(u) - 2\nu(1-u)^{\nu-1}x'(u) + (1-u)^{\nu}x''(u) \tag{2.86}$$

To simplify what follows, we again rewrite equation (2.83) shorthand as

$$f(u)y''(u) + g(u)y'(u) + h(u)y(u) = 0 \tag{2.87}$$

Where all prefactors are defined as in (2.83) Inserting (2.84)→(2.86), (2.87) becomes

$$\begin{aligned} &f(u)\left\{\nu(\nu-1)(1-u)^{\nu-2}x(u) - 2\nu(1-u)^{\nu-1}x'(u) + (1-u)^{\nu}x''(u)\right\} \\ &+g(u)\left\{-\nu(1-u)^{\nu-1}x(u) + (1-u)^{\nu}x'(u)\right\} + h(u)\left\{(1-u)^{\nu}x(u)\right\} = 0 \end{aligned} \tag{2.88}$$

We rewrite the following prefactors as

$$f(u) = (1-u)F(u), \qquad \text{and} \qquad h(u) = \frac{\tilde{h}(u)}{(1-u)} + J(u) \tag{2.89}$$

where

$$F(u) = 1 + u + u^2 - u^3Z^2L^2$$

$$\tilde{h}(u) = \frac{L^4(Q^2(1-u)^2 - 2\tilde{\omega}Q(1-u) + \tilde{\omega}^2)}{(1+u+u^2-u^3Z^2L^2)}$$

$$J(u) = 2Z^2L^2u^2 - u(1+Z^2L^2) - K^2L^2 \tag{2.90}$$

Inserting (2.89) into (2.88) and rearranging, one finds

$$F(1-u)^{\nu+1}x''(u)+(1-u)^{\nu}\left(g-2F\nu\right)x'(u)+(1-u)^{\nu-1}\left(F\nu(\nu-1)-g\nu+\tilde{h}+J(1-u)\right)x(u)=0 \tag{2.91}$$

Dividing this through by a factor of $(1-u)^{\nu}$ gives

$$f(u)x''(u)+\left(g-2F\nu\right)x'(u)+\left\{\frac{F\nu^2-(g+F)\nu+\tilde{h}}{(1-u)}+J\right\}x(u)=0 \tag{2.92}$$

We can now solve for ν in the quadratic in the prefactor of $x(u)$ at $u = 1$, such that it cancels out the divergence there. We note that at the horizon, $g(1) = -F(1)$, thus ν takes on the solutions

$$\nu^2=-\frac{\tilde{h}(1)}{F(1)}$$

$$\Rightarrow \qquad \nu=\frac{\pm i\tilde{\omega}L^2}{(3-Z^2L^2)} \tag{2.93}$$

We find the negative choice of (2.93) to correspond to an ingoing wave at the outer horizon of the black hole. We now write (2.92) longhand

$$(1-u)(1+u+u^2-u^3Z^2L^2)\frac{d^2}{du^2}x(u)+\left\{4Z^2L^2u^3-3(1+Z^2L^2)u^2-2\nu(1+u+u^2-u^3Z^2L^2)\right\}\frac{d}{du}x(u)$$

$$+\left\{\frac{\nu(\nu-1)}{(1-u)}(1+u+u^2-u^3Z^2L^2)-\frac{\nu}{(1-u)}(4Z^2L^2u^3-3(1+Z^2L^2)u^2)\right.$$

$$\left.+\frac{L^4(Q^2(1-u)^2-2\tilde{\omega}Q(1-u)+\tilde{\omega}^2)}{(1-u)(1+u+u^2-u^3Z^2L^2)}+2Z^2L^2u^2-u(1+Z^2L^2)-K^2L^2\right\}x(u)=0 \tag{2.94}$$

Although slightly tedious, it benefits to write (2.94) as

$$f(u)x''(u)+G(u)x'(u)+H(u)x(u)=0 \tag{2.95}$$

and for a moment we shall focus purely on the function $H(u)$ in (2.92) above. Using the following relation's

$$F(u)-F(1)=(1-u)\hat{F}(u)$$

$$g(u)-g(1)=(1-u)\hat{g}(u)$$

$$\tilde{h}(u)-\tilde{h}(1)=(1-u)\tilde{H}(u) \tag{2.96}$$

we can rewrite the prefactor $H(u)$ using $\hat{F}(u)$, $\hat{g}(u)$, and $\tilde{H}(u)$ defined above as

$$H(u)=\Bigg\{\frac{\nu(\nu-1)}{(1-u)}(1+u+u^2-u^3Z^2L^2-3+Z^2L^2)-\frac{\nu}{(1-u)}(4Z^2L^2u^3-3(1+Z^2L^2)u^2+3-Z^2L^2)$$
$$+\frac{L^4(Q(1-u)-\tilde{\omega})^2}{(1-u)(1+u+u^2-u^3Z^2L^2)}-\frac{\tilde{\omega}^2L^4}{(1-u)(3-Z^2L^2)}+2Z^2L^2u^2-u(1+Z^2L^2)-K^2L^2$$

$$+\frac{(3-Z^2L^2)^2\nu^2+\tilde{\omega}^2L^4}{(1-u)(3-Z^2L^2)}\Bigg\}x(u)=0 \tag{2.97}$$

The singularity is now confined to the last term on the third line of (2.97) above, and one can clearly see that inserting equation (2.93) into this successfully rids this term. We can tidy up the remaining terms by extracting a factor of $(1-u)$ in everything bar $J(u)$, giving

$$H(u)=\Bigg\{L^4\left(\frac{\tilde{\omega}^2(4-Z^2L^2+u+u^2-Z^2L^2u^3)(2+u-Z^2L^2(1+u+u^2))}{(3-Z^2L^2)^2(1+u+u^2-u^3Z^2L^2)}+\frac{Q^2(1-u)-2Q\tilde{\omega}}{1+u+u^2-u^3Z^2L^2}\right)$$

$$+\nu(3Z^2L^2u^2-2u-1)+2Z^2L^2u^2-u(1+Z^2L^2)-K^2L^2\Bigg\} \tag{2.98}$$

With this prefactor, equation (2.95) is now perfectly regular at the horizon of the black hole. For simplicity in notation we may absorb all factors of L into the other parameters by defining the following

$$\bar{Z}=ZL,\quad \bar{Q}=QL^2,\quad \bar{\omega}=\tilde{\omega}L^2,\quad \bar{K}=KL \tag{2.99}$$

and (2.94) becomes

$$(1-u)(1+u+u^2-u^3\bar{Z}^2)\frac{d^2}{du^2}x(u)+\left\{4\bar{Z}^2u^3-3(1+\bar{Z}^2)u^2-2\nu(1+u+u^2-u^3\bar{Z}^2)\right\}\frac{d}{du}x(u)$$

$$+\left\{\frac{\bar{\omega}^2(4-\bar{Z}^2+u+u^2-\bar{Z}^2u^3)(2+u-\bar{Z}^2(1+u+u^2))}{(3-\bar{Z}^2)^2(1+u+u^2-u^3\bar{Z}^2)}+\frac{\bar{Q}^2(1-u)-2\bar{Q}\bar{\omega}}{1+u+u^2-u^3\bar{Z}^2}+\right.$$

$$\left.+\ \nu(3\bar{Z}^2u^2-2u-1)+2\bar{Z}^2u^2-u(1+\bar{Z}^2)-\bar{K}^2\right\}x(u)=0 \tag{2.100}$$

Boundary Conditions

We now need to work out the appropriate boundary conditions. Again because of the linearity of the equation we may choose $x(1)=1$ at the horizon of the black hole without a loss of generality. We again let $u=1-\varepsilon$ and Taylor expand the scalar and its coefficients about $u=1$. The results are completely analogous to those in §2.2. We have

$$x(1-\varepsilon)=x_0-\varepsilon x_1+\frac{1}{2}\varepsilon^2x_2+o(\varepsilon^3)+\cdots \tag{2.101}$$

where we take $x_0=x(1)=1$. Expanding the prefactors gives

$$\begin{aligned} f(1-\varepsilon)&=-\varepsilon f_1+o(\varepsilon^2)+\ldots \\ G(1-\varepsilon)&=G_0-\varepsilon G_1+o(\varepsilon^2)+\cdots \\ H(1-\varepsilon)&=H_0-\varepsilon H_1+o(\varepsilon^2)+\cdots \end{aligned} \tag{2.102}$$

and the x_i are given as

$$x_1=-\frac{H_0}{G_0} \tag{2.103}$$

and

$$x_2=\frac{(G_1+H_0)\left(\frac{H_0}{G_0}\right)-H_1}{(f_1+G_0)} \tag{2.104}$$

$$\Rightarrow \qquad x_2=\frac{G_0^{-1}(H_0^2+G_1H_0)-H_1}{(f_1+G_0)} \tag{2.105}$$

The subscript "$_0$" again represents each coefficient evaluated at the black hole horizon,

while the subscript "$_1$" represents its derivative evaluated there. Equation (2.105) does not reduce to the equivalent of (2.48), as now $f_1 \neq G_0$. The coefficients are worked out to be

$$f_1 = \bar{Z}^2 - 3$$

$$G_0 = (\bar{Z}^2 - 3)(1 + 2\nu)$$

$$G_1 = 6\left\{(\bar{Z}^2 - 1)(1 + \nu)\right\}$$

$$H_0 = (1 - \bar{Z}^2)\left\{\frac{6\bar{\omega}^2}{(3 - \bar{Z}^2)^2} - 3\nu - 1\right\} - \frac{2\bar{Q}\bar{\omega}}{(3 - \bar{Z}^2)} - \bar{K}^2$$

$$H_1 = -\frac{\bar{\omega}^2(3\bar{Z}^4 + 2\bar{Z}^2 + 3)}{(3 - \bar{Z}^2)^3} + \frac{6\bar{Q}\bar{\omega}(1 - \bar{Z}^2)}{(3 - \bar{Z}^2)^2} - \frac{\bar{Q}^2}{(3 - \bar{Z}^2)} - (1 - 3\bar{Z}^2)(1 + 2\nu) \tag{2.106}$$

Thus to first order in ε we have

$$f(1 - \varepsilon) = (3 - \bar{Z}^2)\varepsilon + \cdots$$

$$G(1 - \varepsilon) = (\bar{Z}^2 - 3)(1 + 2\nu) + \left(6\left\{(1 - \bar{Z}^2)(1 + \nu)\right\}\right)\varepsilon + \cdots$$

$$H(1 - \varepsilon) = \left\{(1 - \bar{Z}^2)\left\{\frac{6\bar{\omega}^2}{(3 - \bar{Z}^2)^2} - 3\nu - 1\right\} - \frac{2\bar{Q}\bar{\omega}}{(3 - \bar{Z}^2)} - \bar{K}^2\right\}$$

$$+\left(\frac{\bar{\omega}^2(3\bar{Z}^4 + 2\bar{Z}^2 + 3)}{(3 - \bar{Z}^2)^3} - \frac{6\bar{Q}\bar{\omega}(1 - \bar{Z}^2)}{(3 - \bar{Z}^2)^2} + \frac{\bar{Q}^2}{(3 - \bar{Z}^2)} + (1 - 3\bar{Z}^2)(1 + 2\nu)\right)\varepsilon + \cdots \tag{2.107}$$

We may now plug these results into (2.103) and (2.104) to find the appropriate boundary terms. The calculation of the resulting x_i is rather tedious and long-winded. For brevity we make the following definition's before writing them down.

$$\alpha = \frac{1}{(3 - \bar{Z}^2)}$$

$$\gamma = (1-\bar{Z}^2)$$

$$\rho = (1+\nu)$$

$$\sigma = (1+2\nu) \tag{2.108}$$

With these in place, we find

$$x_1 = \frac{\alpha}{\sigma}\left\{\gamma(6\bar{\omega}^2\alpha^2 - 3\nu - 1) - 2\bar{Q}\bar{\omega}\alpha - \bar{K}^2\right\} \tag{2.109}$$

and

$$x_2 = \alpha(2\rho)^{-1}\left\{\alpha\rho^{-1}\left[\left(\gamma(6\bar{\omega}^2\alpha^2 - 3\nu - 1) - 2\bar{Q}\bar{\omega}\alpha - \bar{K}^2\right)^2 - 6\rho\gamma\left(\gamma(6\bar{\omega}^2\alpha^2 - 3\nu - 1) - 2\bar{Q}\bar{\omega}\alpha - \bar{K}^2\right)\right]\right.$$

$$\left. -\alpha^3\bar{\omega}^2(3\bar{Z}^4 + 2\bar{Z}^2 + 3) + \alpha^2 6\bar{Q}\bar{\omega}\gamma - \alpha\bar{Q}^2 - \sigma(1-3\bar{Z}^2)\right\} \tag{2.110}$$

Thus to first order in ε our boundary conditions are

$$x(1-\varepsilon) = 1 - \varepsilon\left[\frac{\alpha}{\sigma}\left\{\gamma(6\bar{\omega}^2\alpha^2 - 3\nu - 1) - 2\bar{Q}\bar{\omega}\alpha - \bar{K}^2\right\}\right] \tag{2.111}$$

and

$$x'(1-\varepsilon) = \frac{\alpha}{\sigma}\left\{\gamma(6\bar{\omega}^2\alpha^2 - 3\nu - 1) - 2\bar{Q}\bar{\omega}\alpha - \bar{K}^2\right\}$$

$$-\varepsilon\left(\alpha(2\rho)^{-1}\left\{\alpha\rho^{-1}\left[\left(\gamma(6\bar{\omega}^2\alpha^2 - 3\nu - 1) - 2\bar{Q}\bar{\omega}\alpha - \bar{K}^2\right)^2 - 6\rho\gamma\left(\gamma(6\bar{\omega}^2\alpha^2 - 3\nu - 1) - 2\bar{Q}\bar{\omega}\alpha - \bar{K}^2\right)\right]\right.\right.$$

$$\left.\left. -\alpha^3\bar{\omega}^2(3\bar{Z}^4 + 2\bar{Z}^2 + 3) + \alpha^2 6\bar{Q}\bar{\omega}\gamma - \alpha\bar{Q}^2 - \sigma(1-3\bar{Z}^2)\right\}\right) \tag{2.112}$$

It can be readily seen as another consistency check, that in the limit where $\omega = K = 0$, the boundaries, (2.111) and (2.112) reduce down to (2.52) and (2.53). We are now in a position to modify the previous matlab routine to include a frequency and wave vector dependence (See Appendix), and can start formulating pictures of how the scalar varies with respect to both, ultimately determining the dispersion relation for the

boundary field.

2.5 Dispersion relations

As before, the AdS/CFT dictionary requires that we assign operators on the boundary theory which have corresponding duals in the bulk gravitational theory. By examining how the scalar behaves with respect to a varying frequency and momentum, we can extract the value's of the field and its derivative at $u = 0$ to act as these operators. If one increases the momentum K in a low energy regime, the field seems to manifest itself in the appearance of quasiparticle peaks in a momentum space representation. This will be shown in a succession of plots given in the numerical results below.

Information regarding the behaviour of a bosonic field can be obtained from the fields propagator, which in a momentum space representation gives the probability amplitude that the field travels with a certain energy and momentum. It can be written as

$$G_R(\omega,K) = \left\langle \mathcal{O}(\omega,K)\mathcal{O}(0,K) \right\rangle \tag{2.113}$$

for field operators $\mathcal{O}(\omega,K)$ living in Anti de-Sitter space. We note the propagator for a free field in momentum space is given as

$$G_R(\omega,K) = \frac{i}{\omega^2 - K^2 - m^2} \underset{K=0}{=} \frac{i}{(\omega^2 - m^2)} \tag{2.114}$$

ie, It can be considered as the inverse of the wave operator appropriate to the field. For brevity in the notation, I have dropped the bars from ω and K. Now, we are interested in finding the Greens functions for the quantum field at the conformal bound of Anti de-Sitter space. It is a difficult matter to compute the two-point function (2.113) directly. A reasonable approximation [12] however, would be to calculate the Greens function

$$G_Q^{(\delta)}(\omega,K) = \mathrm{Re}\left[\frac{A(\omega,K)}{B(\omega,K)} \right] \tag{2.115}$$

In (2.115) the two functions in the quotient on the r.h.s are defined by

$$A(\omega, K) = \left\langle x^{(0)}(\omega, K) \right\rangle \tag{2.116}$$

and

$$B(\omega, K) = \left\langle x'^{(0)}(\omega, K) \right\rangle \tag{2.117}$$

where the r.h.s of (2.116) and (2.117) are the vev and its coupling of the scalar field evaluated on the boundary of AdS. The superscript '$^{(0)}$' denotes the fact that the AdS boundary corresponds to where u=0. The superscript 'δ' on the left hand side of (2.115) will represent the mass dimension of the operators. The spectral functions for the system are given as

$$\Pi_Q^{(\delta)}(\omega, K) = \mathrm{Im}\left[\frac{A(\omega, K)}{B(\omega, K)}\right] \tag{2.118}$$

and are of physical importance as they measure how much spectral weight a particle with momentum K has at energy ω. It is Anticipated in this analysis that at zero frequency the spectral functions will vanish everywhere no matter what value of the other parameters are chosen. This can be seen if one looks back to the equations of motion, where the only complex component lies in the exponent ν which is directly proportional to the fields energy. For all Greens functions, and consequently dispersion relations calculated below, I shall work with mass dimension two, ie, the positive root of (2.61). The subscript 'Q' represents the charge of the system, and it will come in handy later when I evaluate this Greens function at different temperatures.

I shall now provide a series of plots of both the real and imaginary parts of (2.116) and (2.117) for a range of frequency values at zero momentum. I begin by setting the charge of the system to unity, then increasing it until the black hole is almost extremal. As the parameter L was absorbed into the other parameters, the charge now sets the temperature of the system, and one will see that close to extremality, ie, Q=3.4, the field becomes highly unstable. I shall give the temperature value for each set of plots given. It is worth remembering at this point that we are working for the case of a conformally coupled scalar field here, so we still have $m^2L^2 = -2$, and q=1.

2.6 Numerical Results

$K=0, \quad Q=1, \quad Z=1/2, \quad T=0.219$

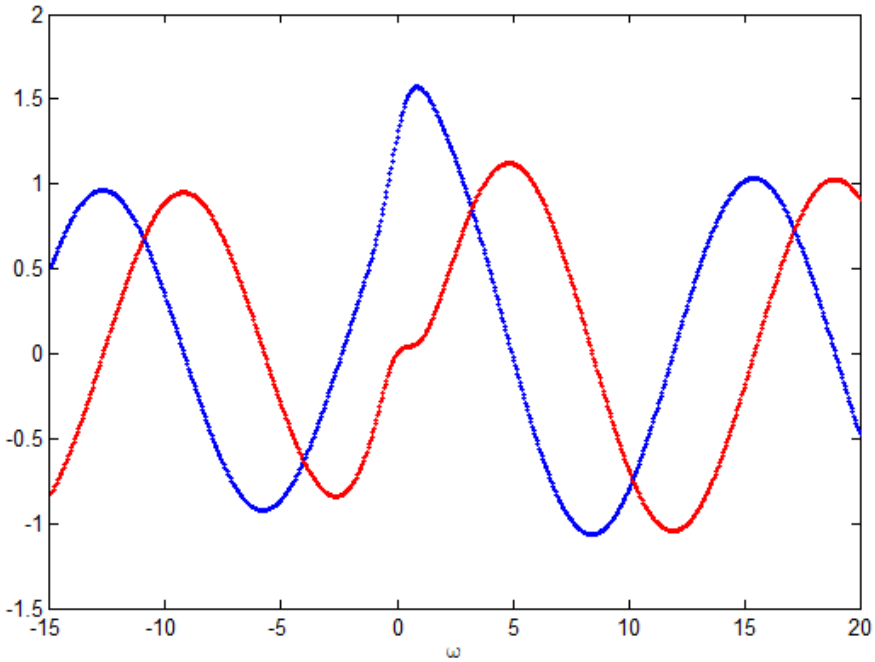

Figure 10(a): Re[$A(\omega,K)$] ~ blue, Im[$A(\omega,K)$] ~ red, corresponding to zero momentum and $Q=1$

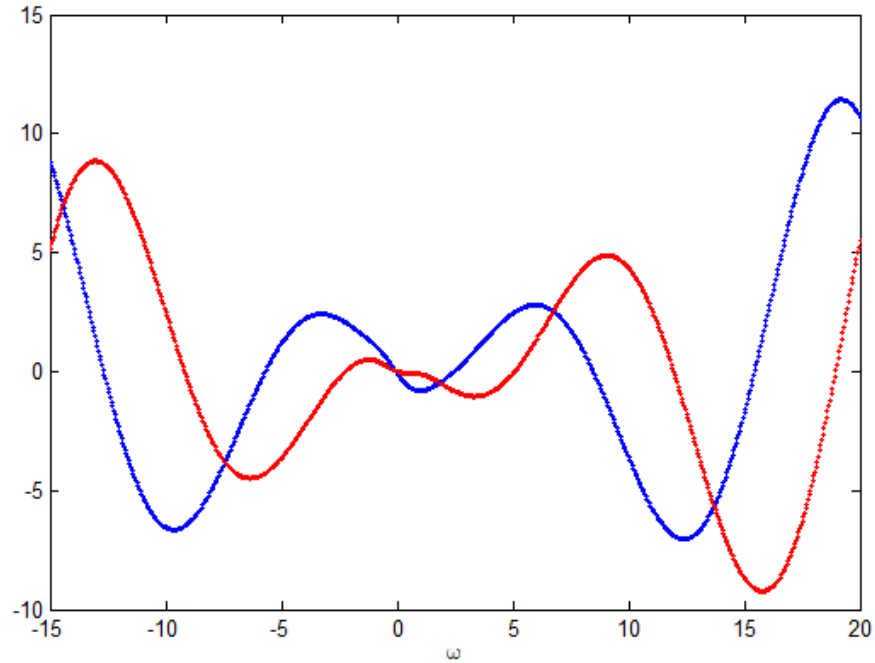

Figure 10(b): Re[$B(\omega,K)$] ~ blue, Im[$B(\omega,K)$] ~ red, corresponding to zero momentum and $Q=1$

$K=0, \quad Q=2, \quad Z=1, \quad T=0.159$

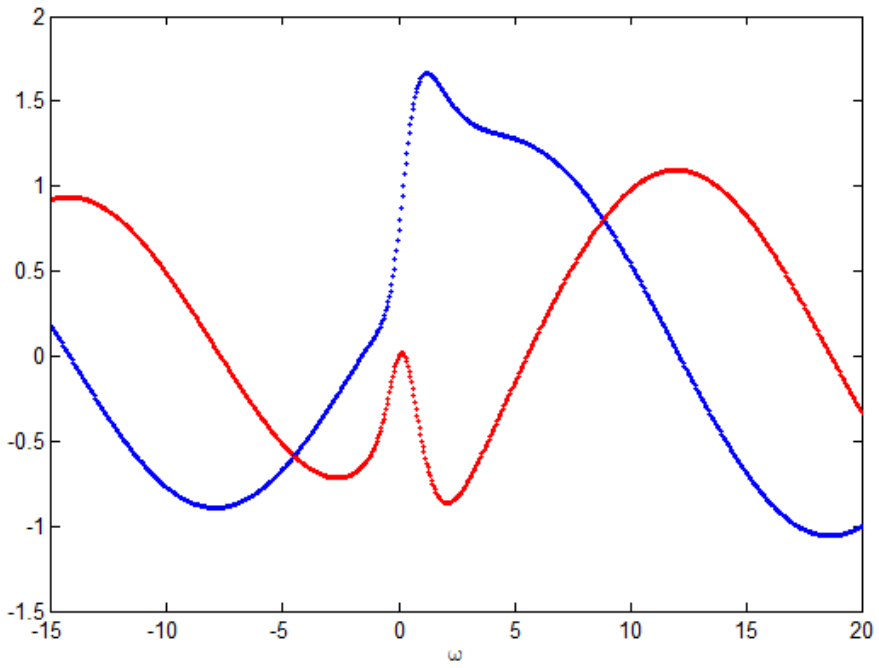

Figure 10(c): Re[$A(\omega,K)$] ~ blue, Im[$A(\omega,K)$] ~ red, corresponding to zero momentum and $Q=2$

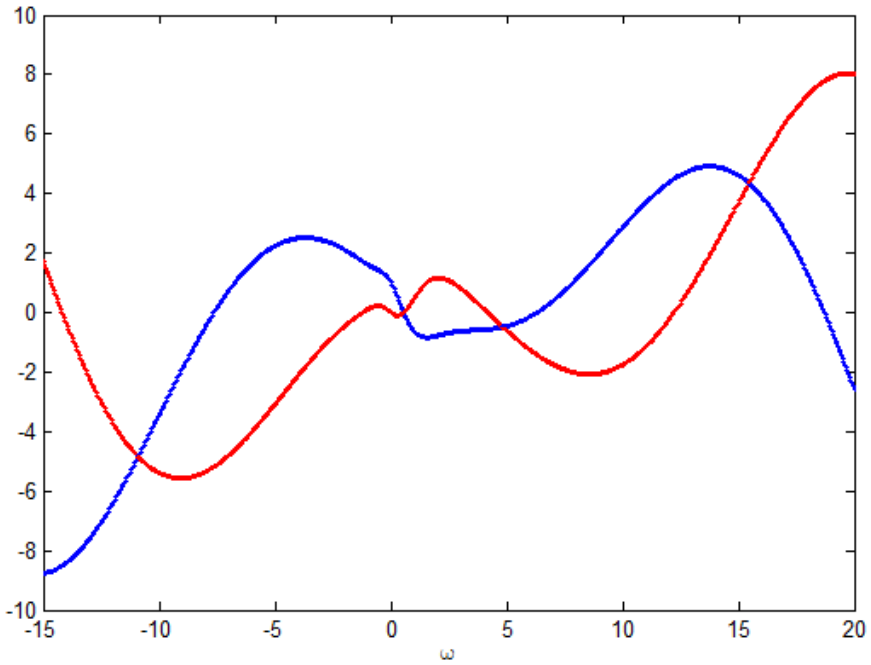

Figure 10(d): Re[$B(\omega,K)$] ~ blue, Im[$B(\omega,K)$] ~ red, corresponding to zero momentum and $Q=2$

$K=0, \quad Q=3, \quad Z=3/2, \quad T=0.0597$

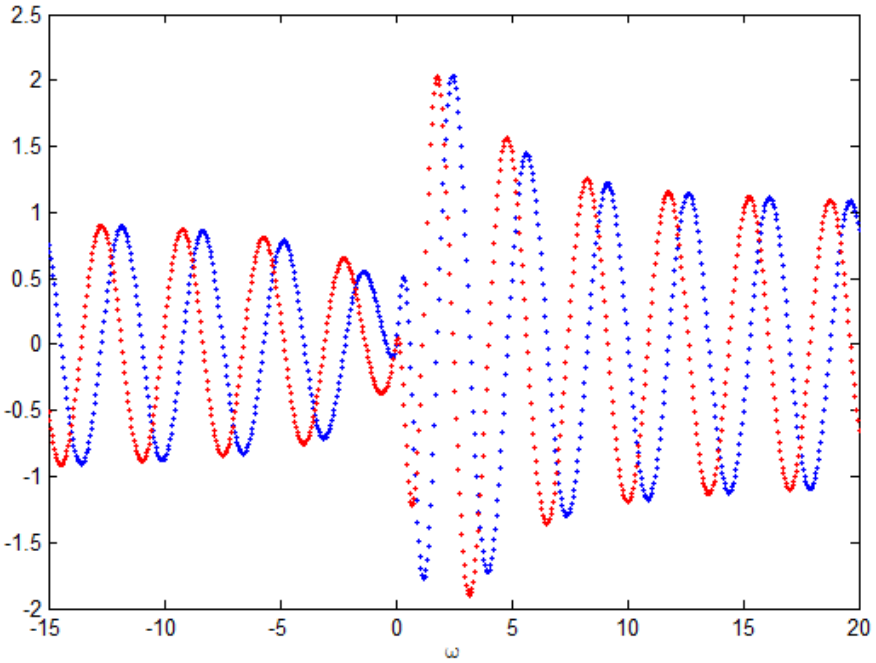

Figure 10(e): Re[$A(\omega,K)$] ~ blue, Im[$A(\omega,K)$] ~ red, corresponding to zero momentum and $Q=3$

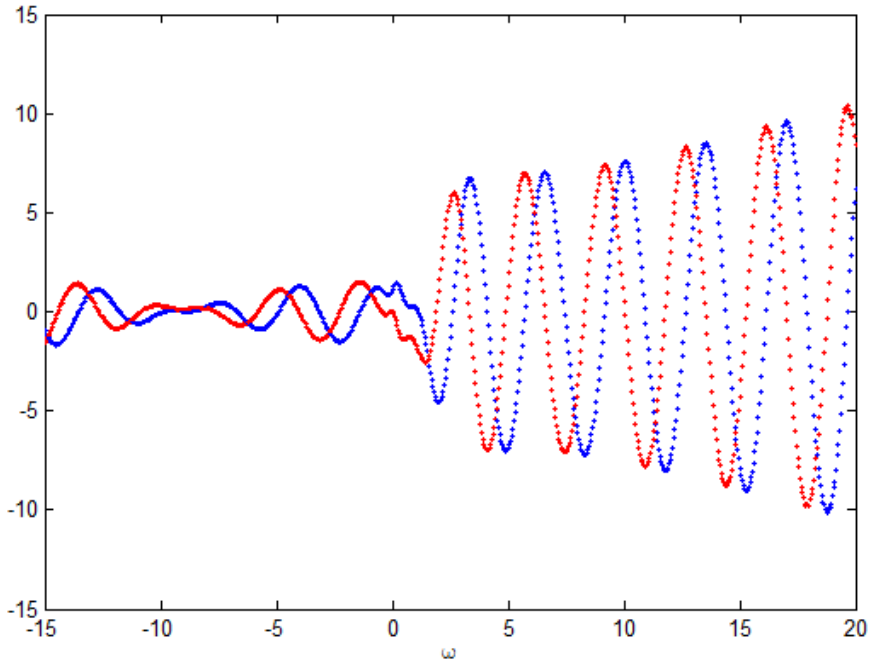

Figure 10(f): Re[$B(\omega,K)$] ~ blue, Im[$B(\omega,K)$] ~ red, corresponding to zero momentum and $Q=3$

K=0, Q=3.4, Z=1.7, T=0.0088

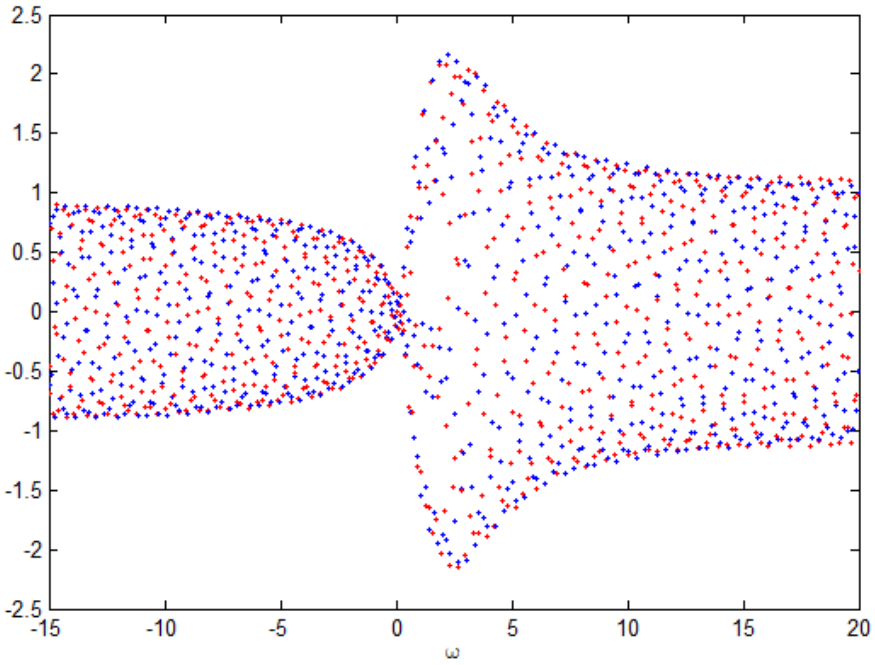

Figure 10(g): Re[$A(\omega,K)$] ~ blue, Im[$A(\omega,K)$] ~ red, corresponding to zero momentum and Q=3.4

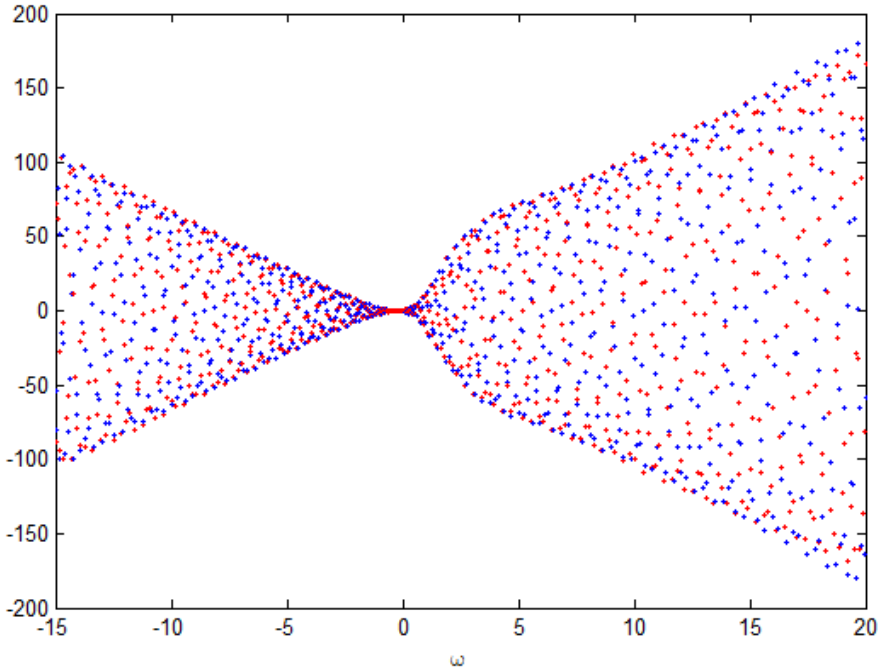

Figure 10(h): Re[$B(\omega,K)$] ~ blue, Im[$B(\omega,K)$] ~ red, corresponding to zero momentum and Q=3.4

In Figures 10(g) and (h) above the black hole is very close to being extremal, with Q_{max}=3.4641. Beyond the value we have taken for Q, the field becomes even more unstable until (2.36), which now of course reads

$$\bar{Z} < \sqrt{3} \tag{2.119}$$

becomes saturated and the numerics of the system go crazy. One can grasp a better idea of how both the operator and its coupling behave in momentum space from a 3D perspective, and to that end I provide a complete graphical representation of the behaviour of the vev's (2.116) and (2.117). It will be seen that as one lowers the temperature of the black hole, which now corresponds to increasing the coupled charge of the system, the boundary field begins to develop into quaisparticle peaks at large momentum.

Q=1, Z=1/2, T=0.219

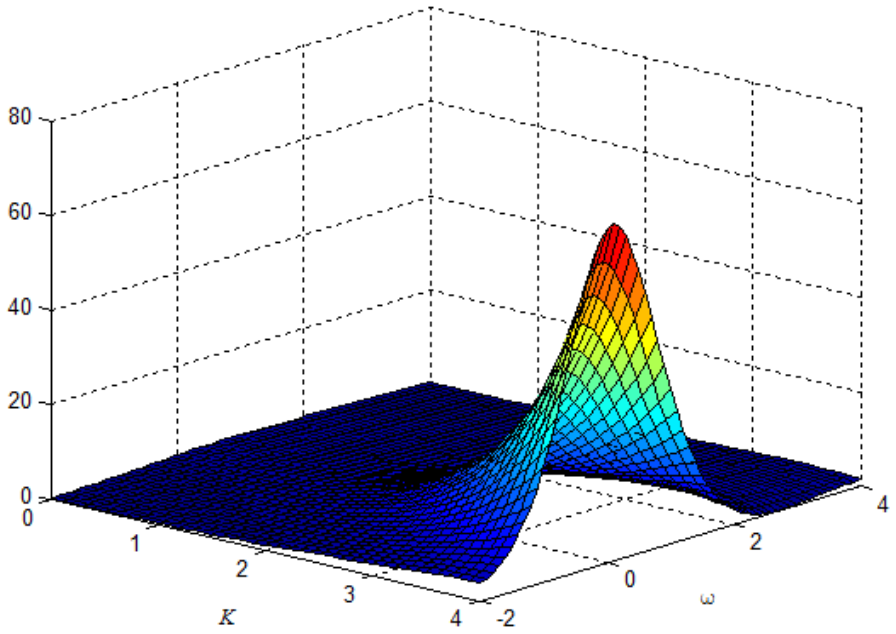

Figure 11(a): Surface plot of Re[$A(\omega,K)$]

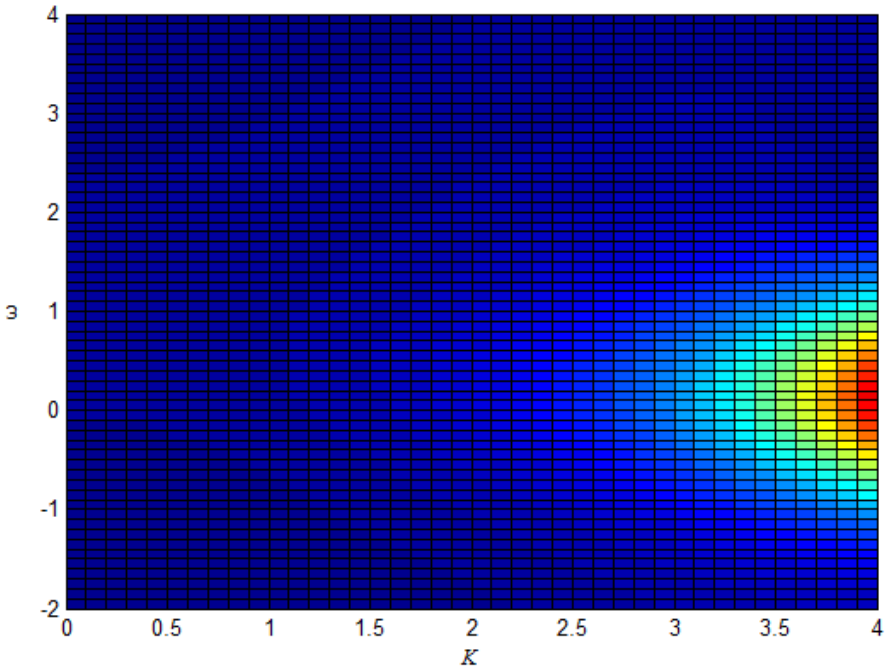

Figure 11(b): Contour plot of Re[$A(\omega,K)$]

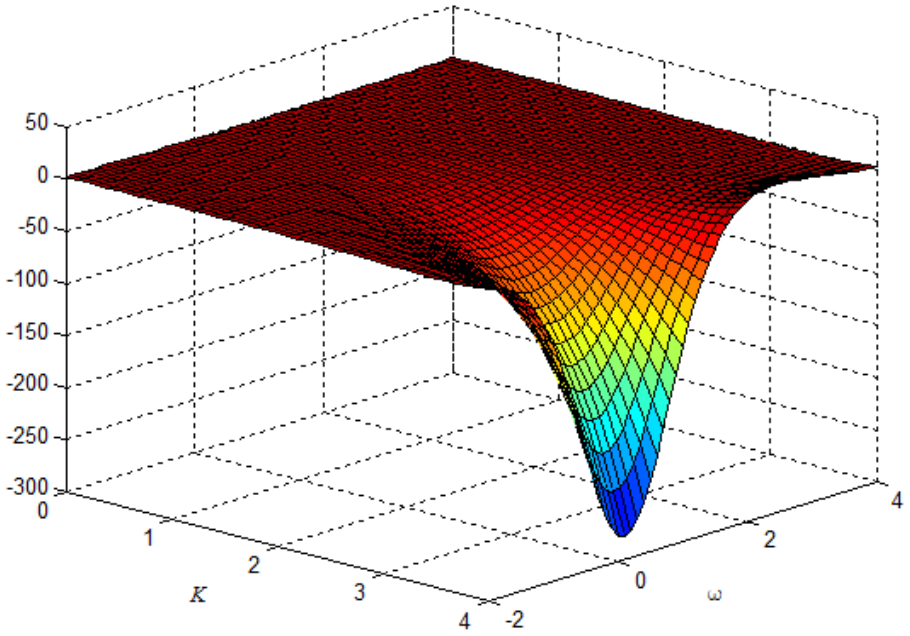

Figure 11(c): Surface plot of Re[$B(\omega,K)$]

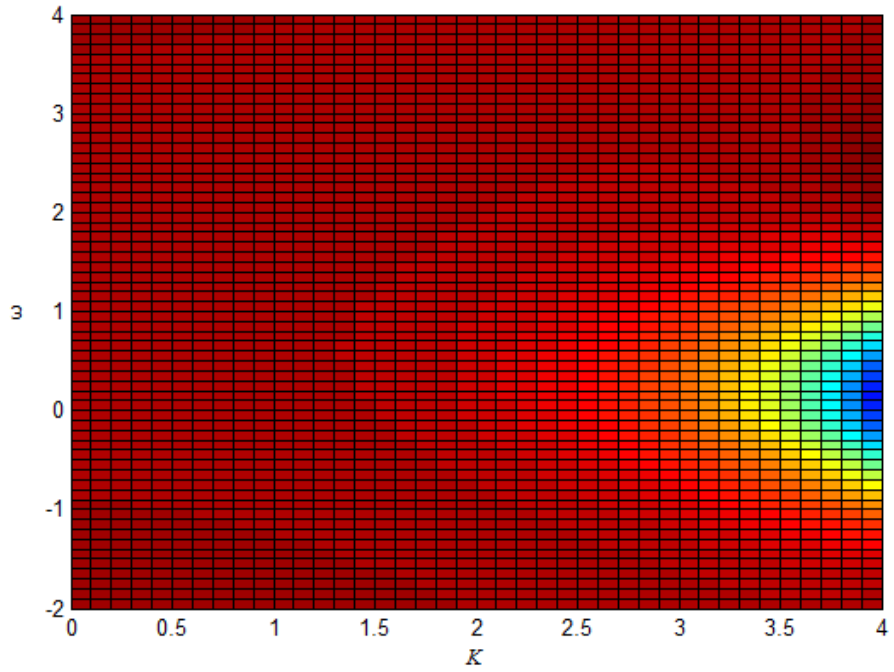

Figure 11(d): Contour plot of Re[$B(\omega,K)$]

Q=2, Z=1, T=0.159

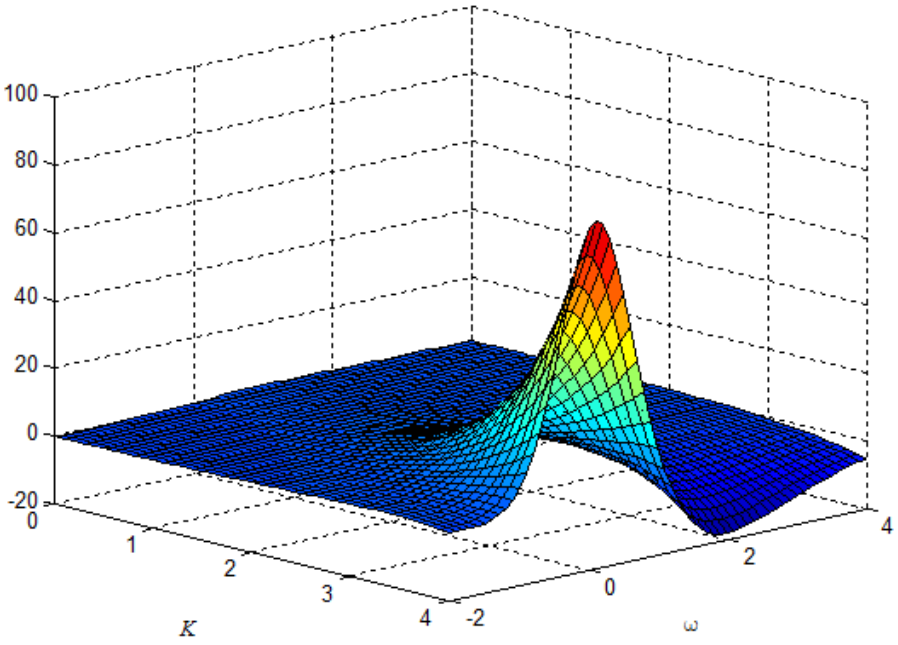

Figure 11(e): Surface plot of Re[$A(\omega,K)$]

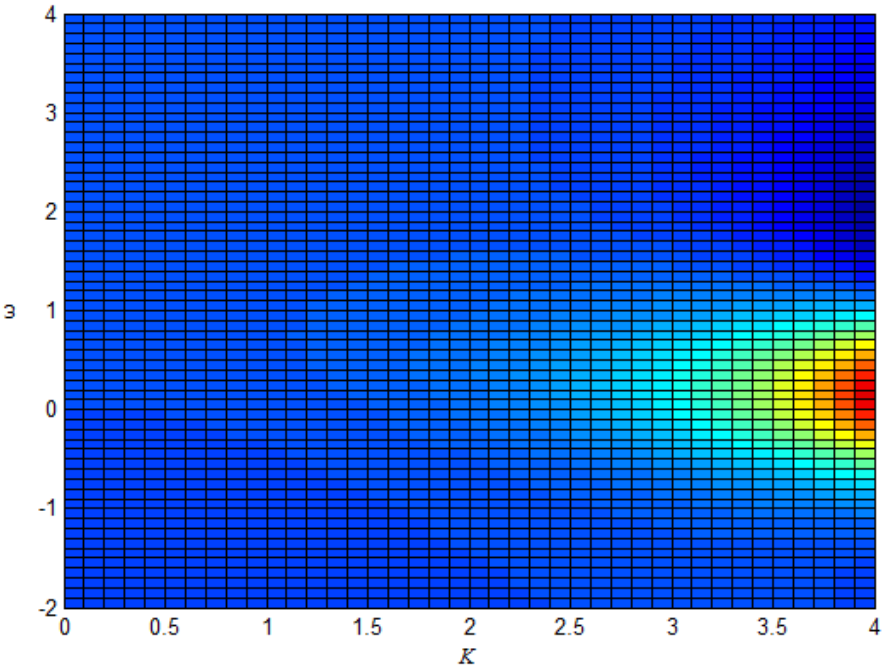

Figure 11(f): Contour plot of Re[$A(\omega,K)$]

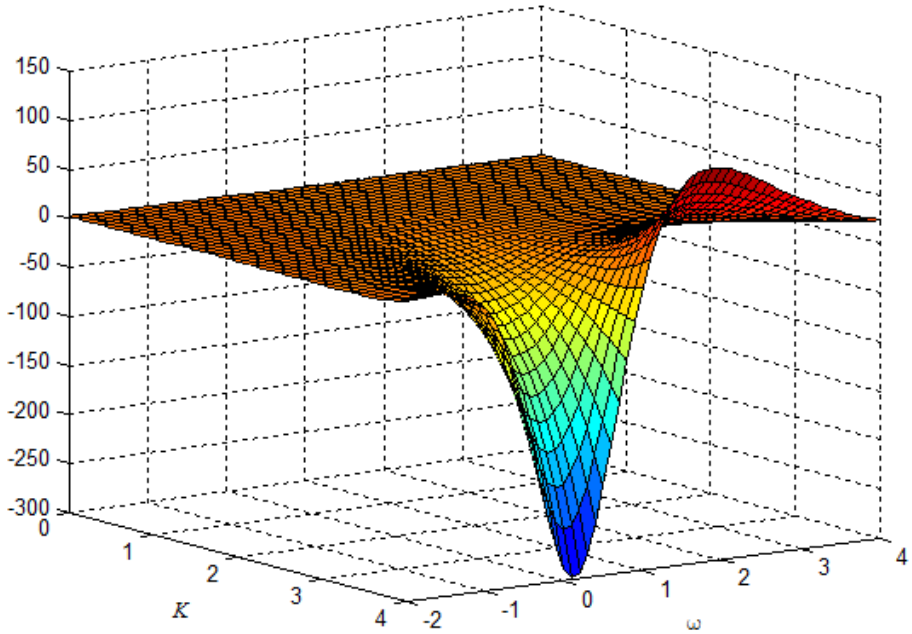

Figure 11(g): Surface plot of Re[$B(\omega,K)$]

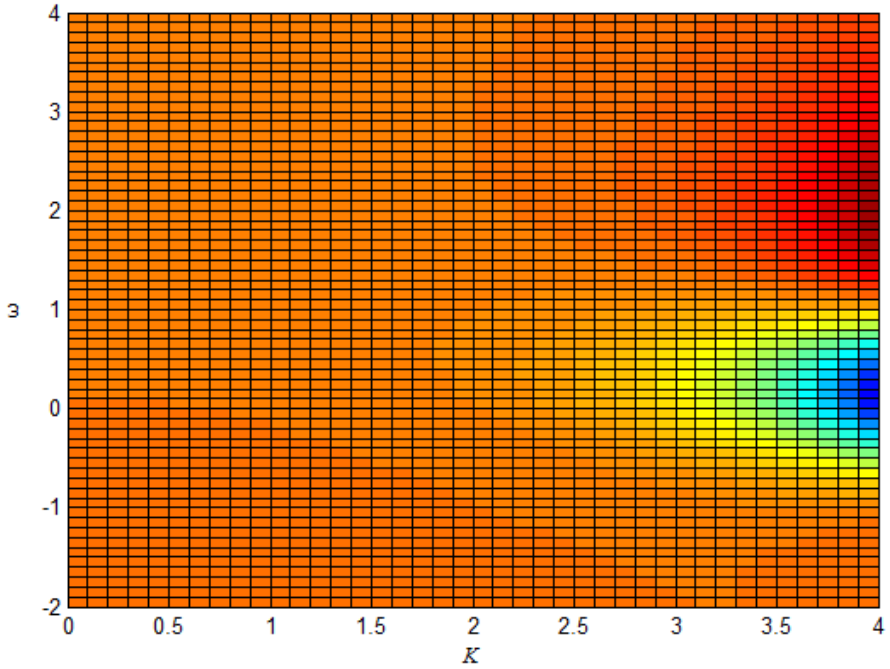

Figure 11(h): Contour plot of Re[$B(\omega,K)$]

Q=3, Z=3/2, T=0.0597

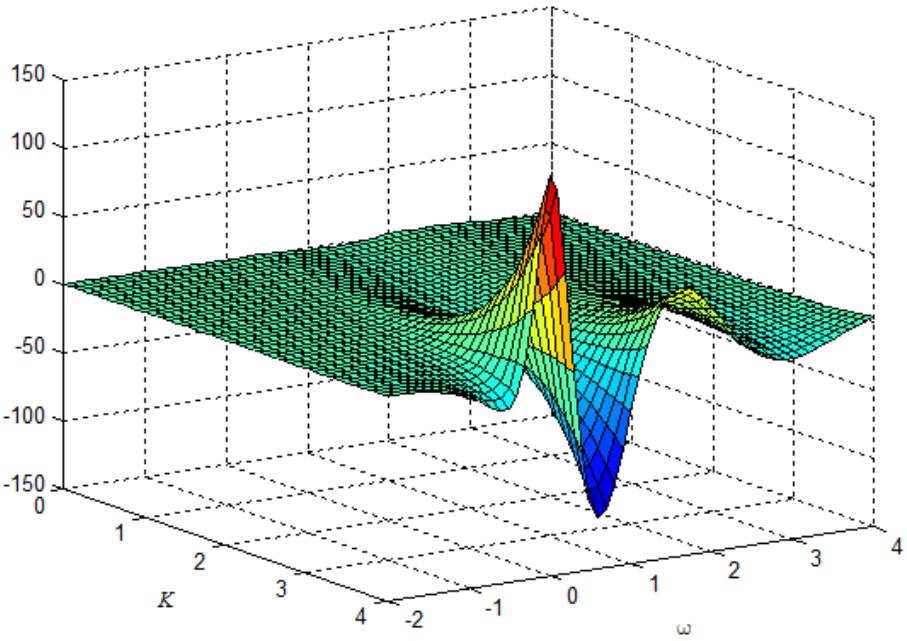

Figure 11(i): Surface plot of Re[$A(\omega,K)$]

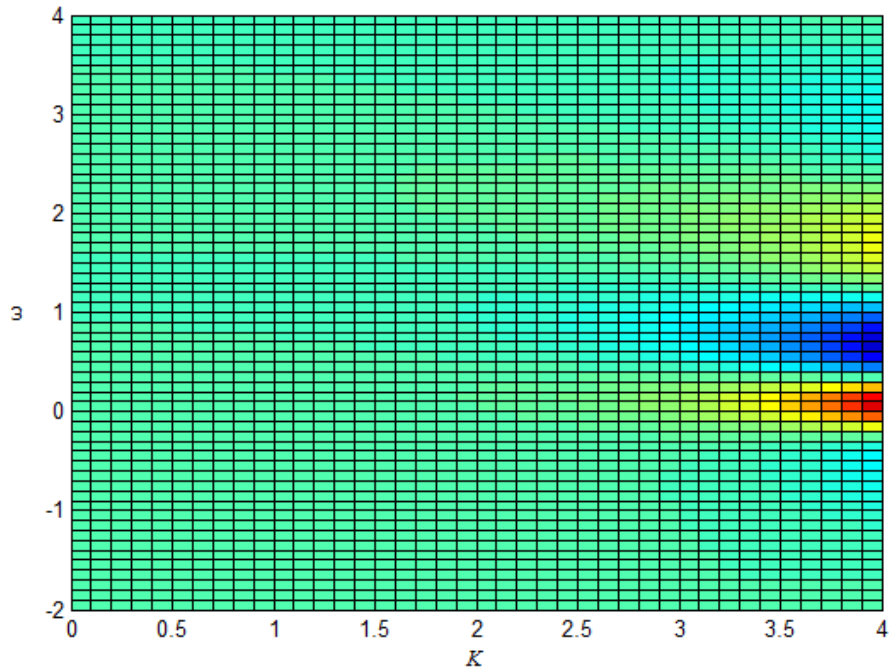

Figure 11(j): Contour plot of Re[$A(\omega,K)$]

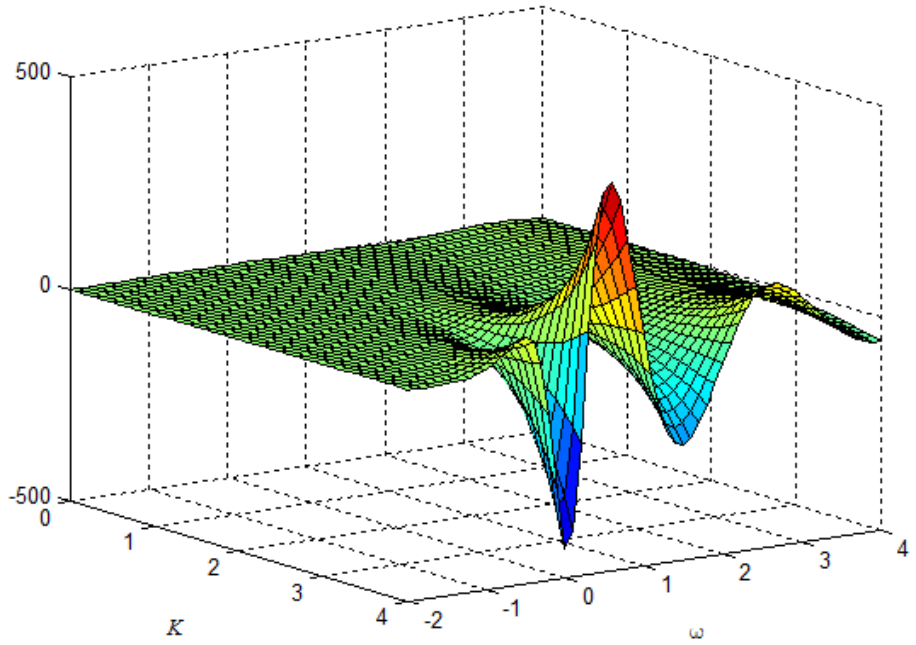

Figure 11(k): Surface plot of Re[$B(\omega,K)$]

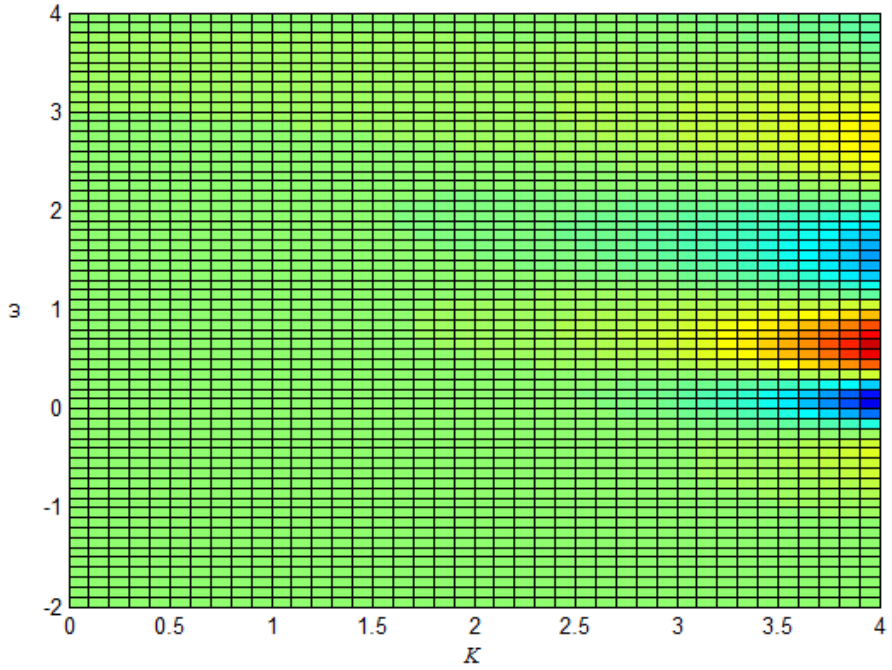

Figure 11(l): Contour plot of Re[$B(\omega,K)$]

Q=3.4, Z=1.7, T=0.0088

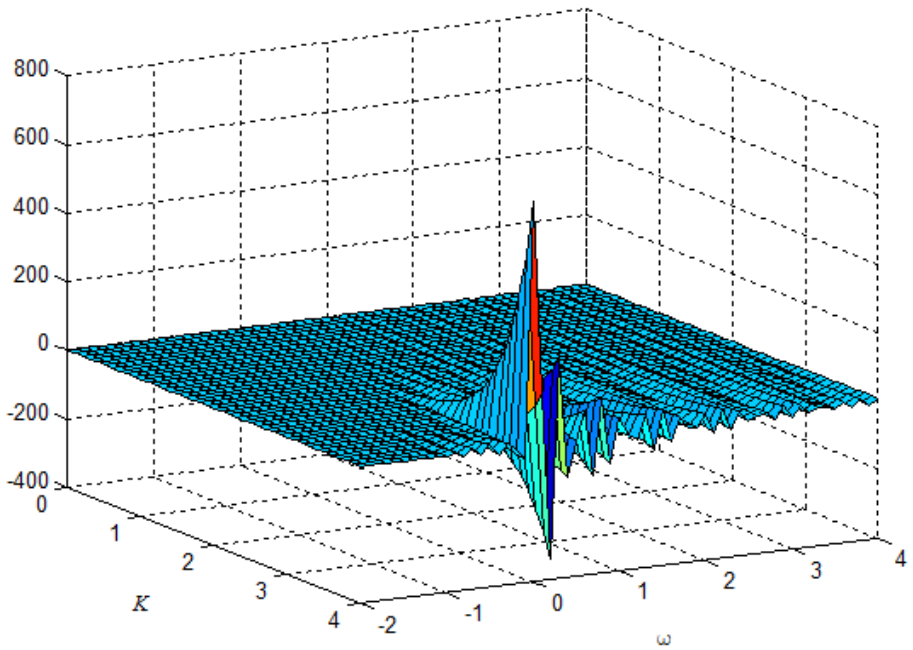

Figure 11(m): Surface plot of Re[$A(\omega,K)$]

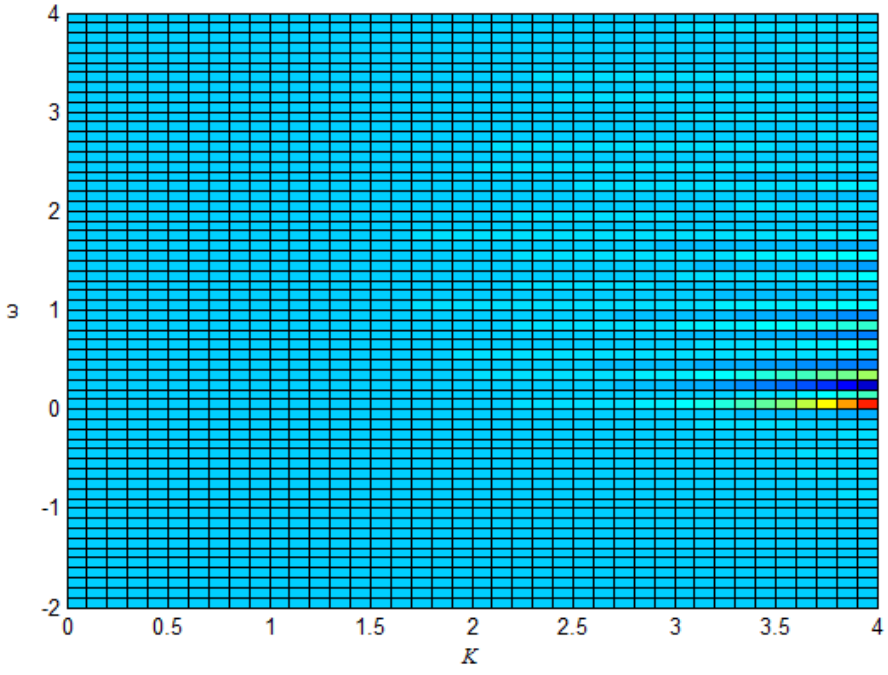

Figure 11(n): Contour plot of Re[$A(\omega,K)$]

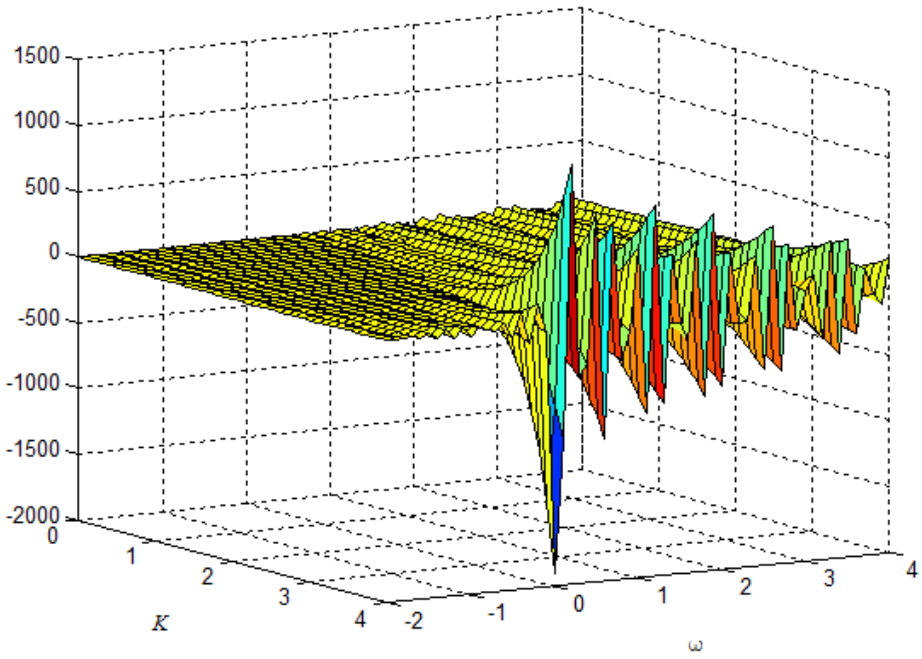

Figure 11(o): Surface plot of Re[$B(\omega,K)$]

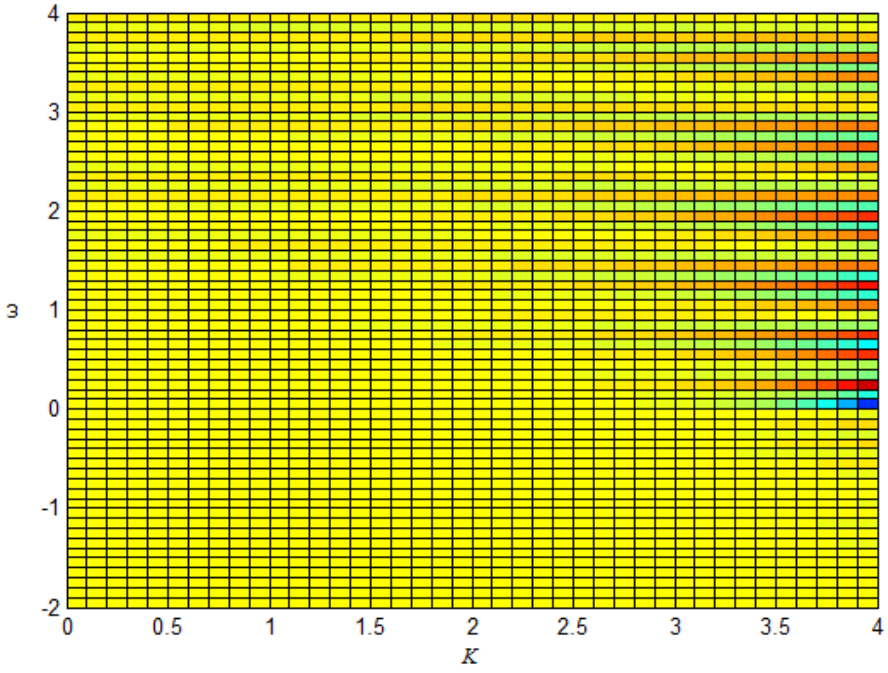

Figure 11(p): Contour plot of Re[$B(\omega,K)$]

As one increases the charge of the system, and consequently reduces the temperature of the black hole, we see the field begins to develop into quasiparticle peaks at large momentum. For the unfamiliar reader, a quasiparticle should be thought of as more of an effect from the particles its surroundings. Its behaviour is a result of the composition of the field/medium to which it belongs; one might use the analogy of a bubble in a glass of beer. They are formed here at large momentum as one increases the charge of the system. Close to extremality we see the formation of multiple quasiparticle peaks. This can be seen in Figure 11:(o),(p) above where the charge Q is taken almost at its upper limit. The amplitude of these peaks decrease from some value of ω to lower values as one takes the frequency of the field to be more positive or more negative. Similar behaviour will be seen in the plots of the imaginary part of the boundary field and its derivative in the next series of surface and contour plots, however the most obvious quasiparticle peaks will be seen in the Greens function plots taken after what follows. These peaks will represent the resonant frequencies in the boundary field.

Allow me first to present the imaginary part of the vev (2.118) and its coupling (2.119) at the AdS boundary. Again, I will evaluate these functions for an increasing coupled charge until the black hole is just about extremal.

Q=1, Z=1/2, T=0.219

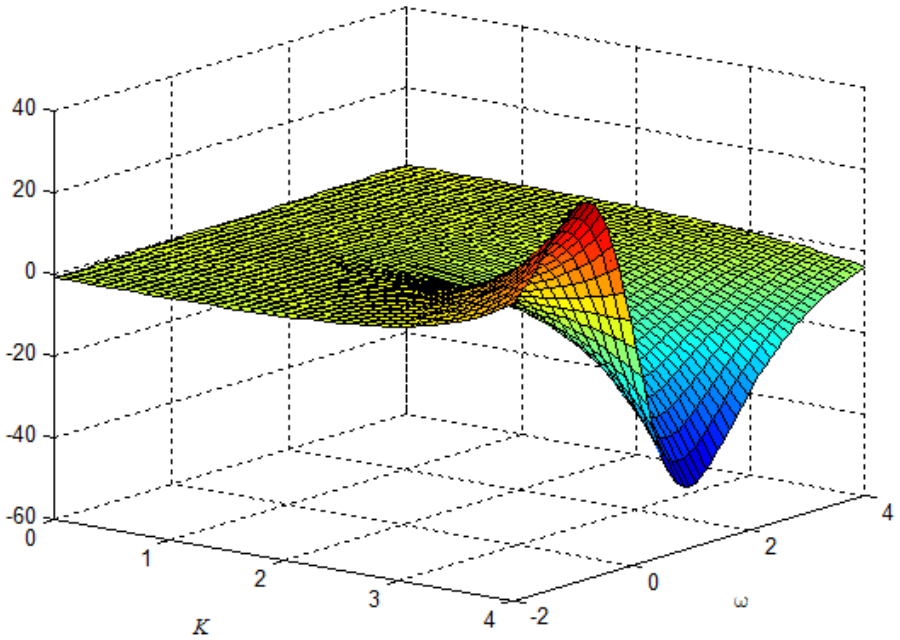

Figure 12(a): Surface plot of Im[$A(\omega,K)$]

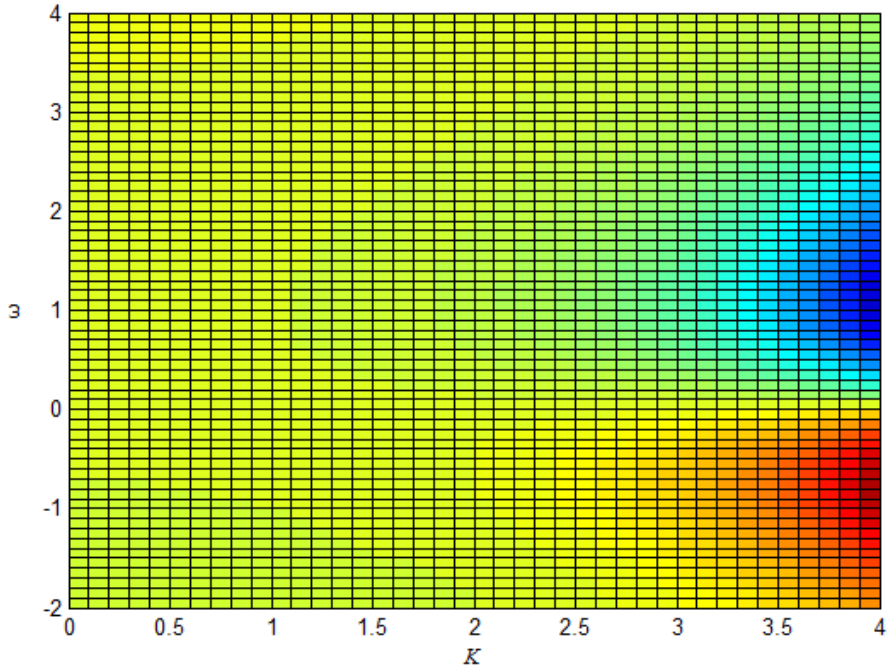

Figure 12(b): Contour plot of Im[$A(\omega,K)$]

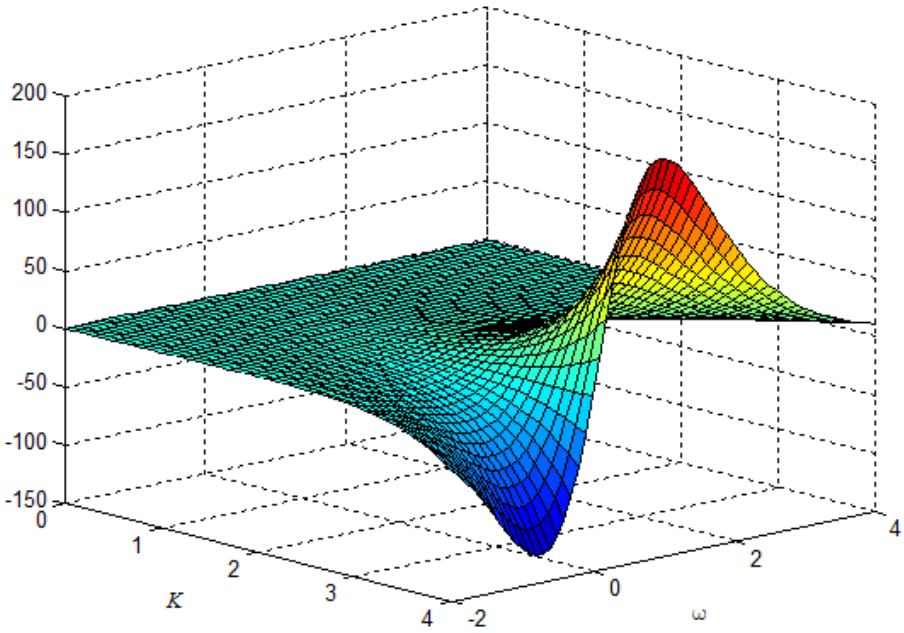

Figure 12(c): Surface plot of Im[$B(\omega,K)$]

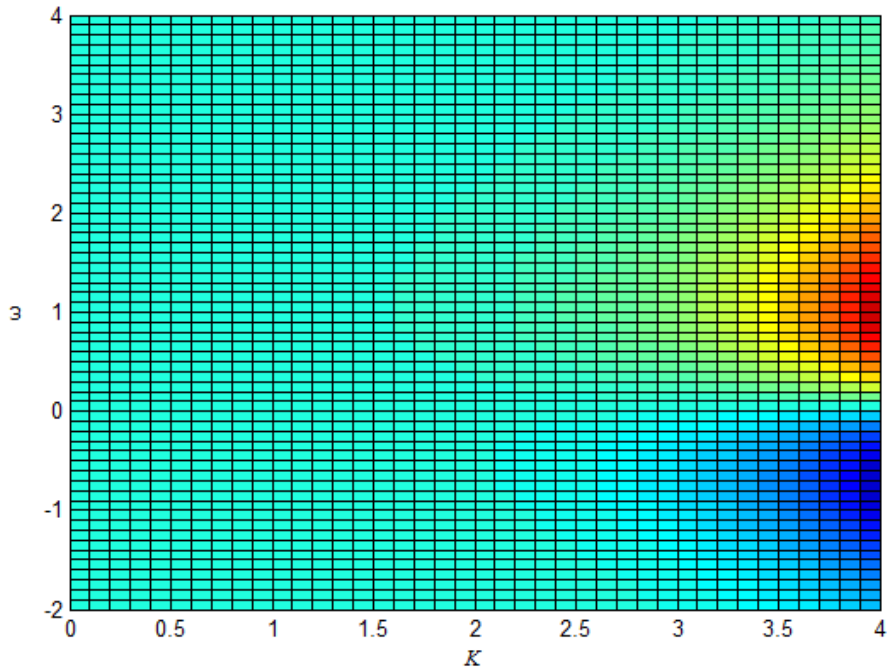

Figure 12(d): Contour plot of Im[$B(\omega,K)$]

Q=2, Z=1, T=0.159

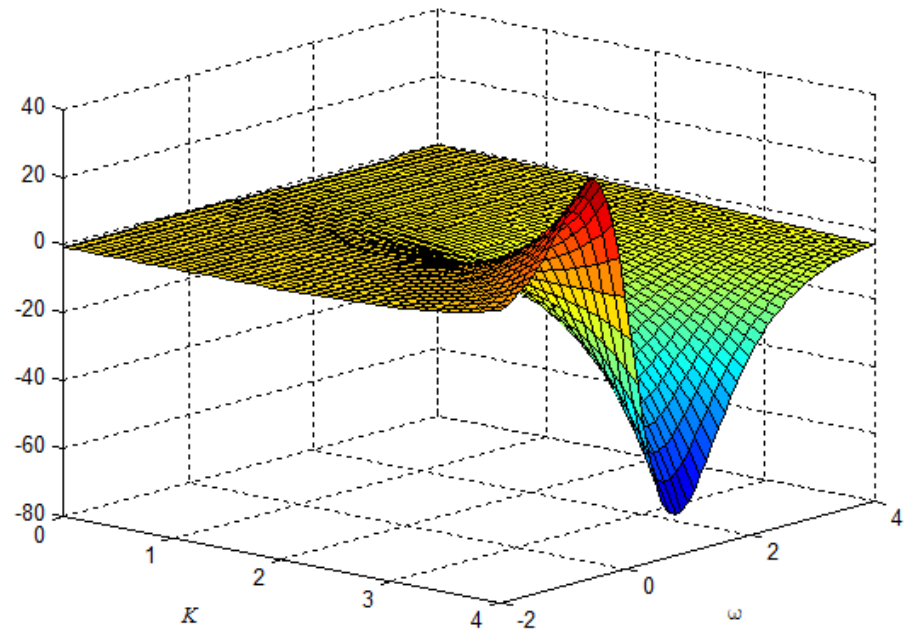

Figure 12(e): Surface plot of Im[$A(\omega,K)$]

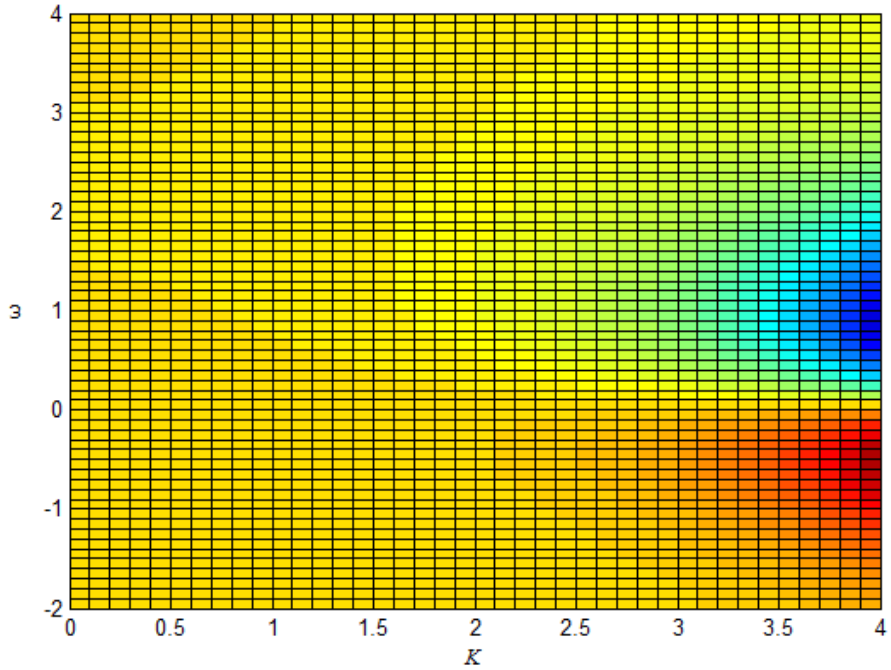

Figure 12(f): Contour plot of Im[$A(\omega,K)$]

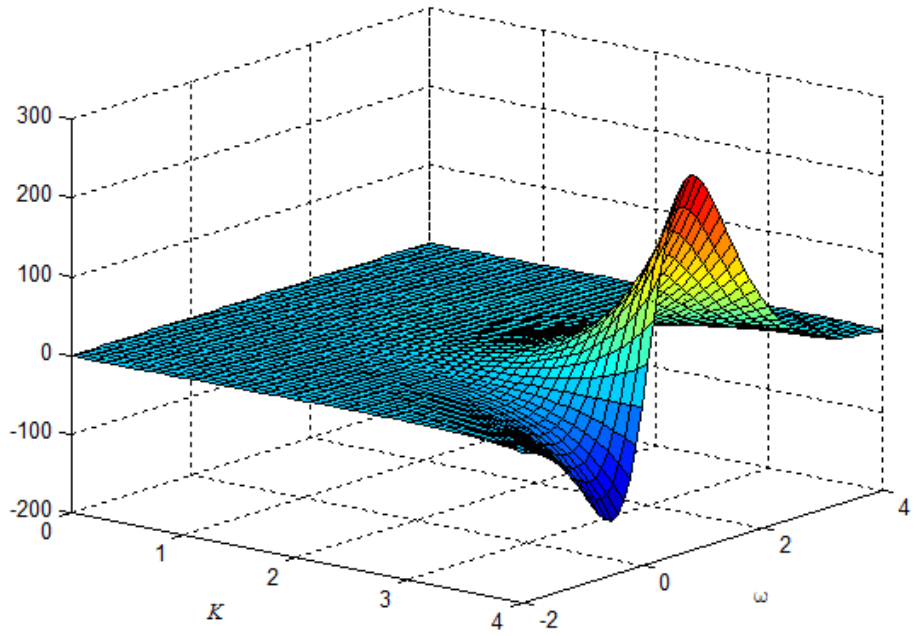

Figure 12(g): Surface plot of Im[$B(\omega,K)$]

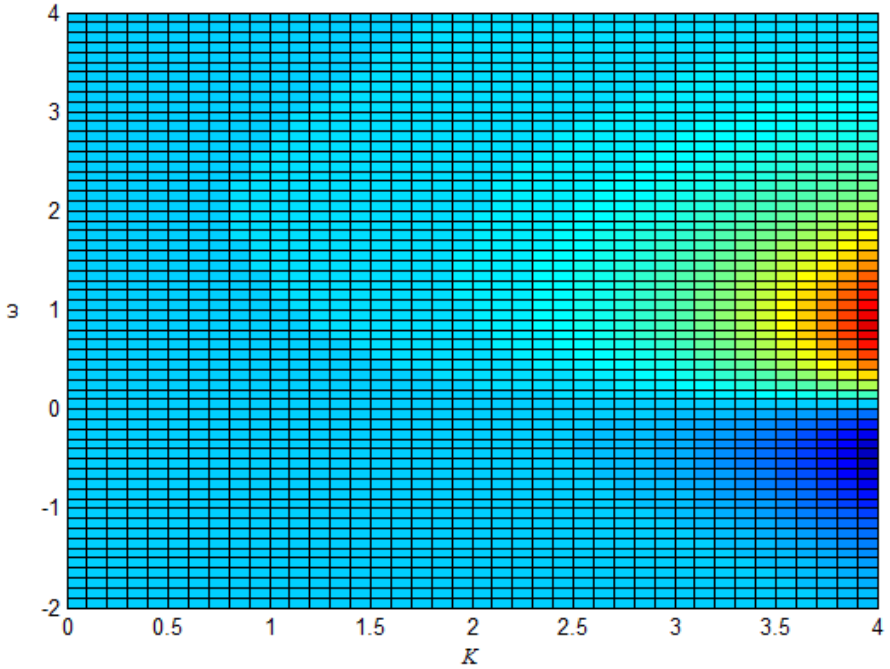

Figure 12(h): Contour plot of Im[$B(\omega,K)$]

Q=3, Z=3/2, T=0.0597

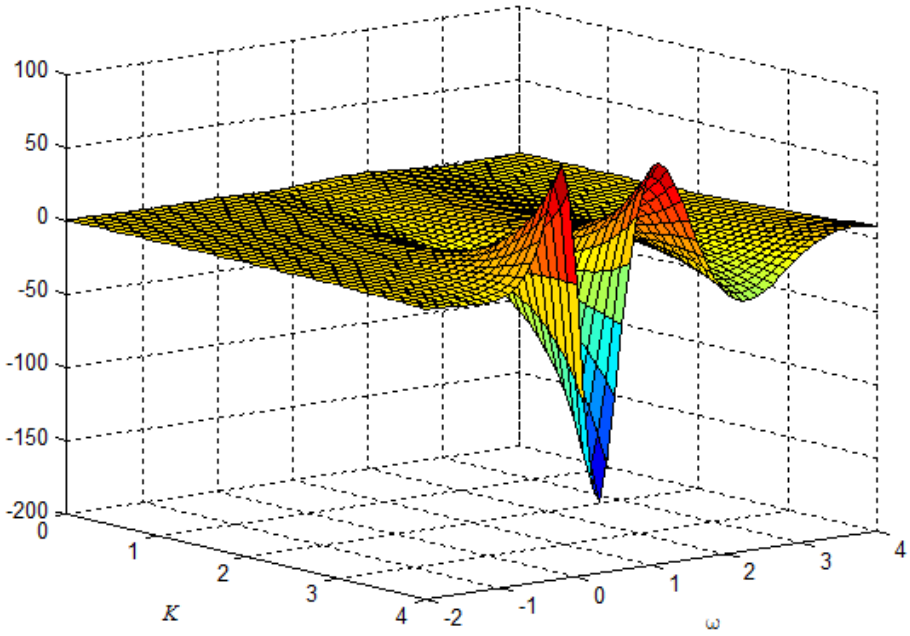

Figure 12(i): Surface plot of Im[$A(\omega,K)$]

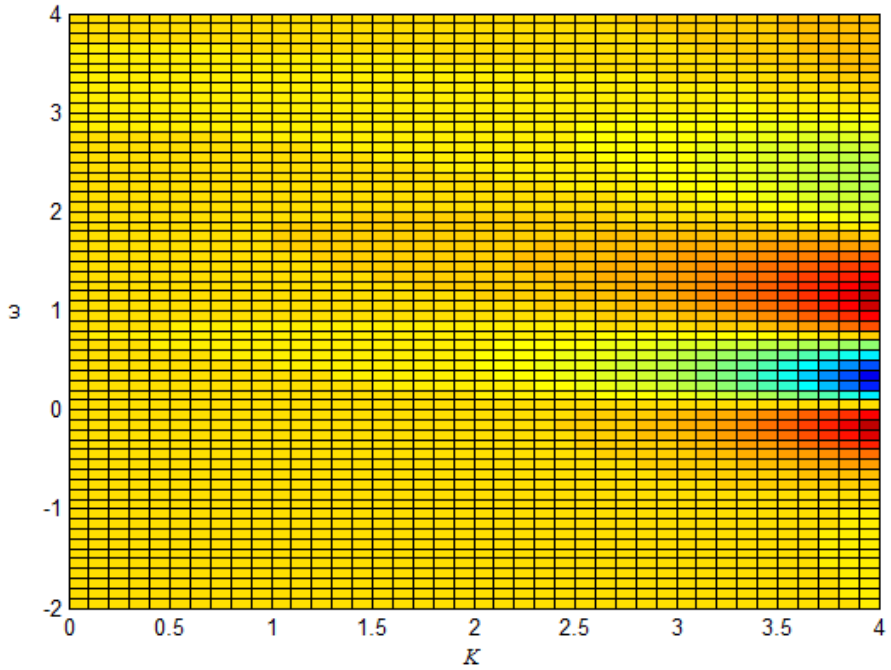

Figure 12(j): Contour plot of Im[$A(\omega,K)$]

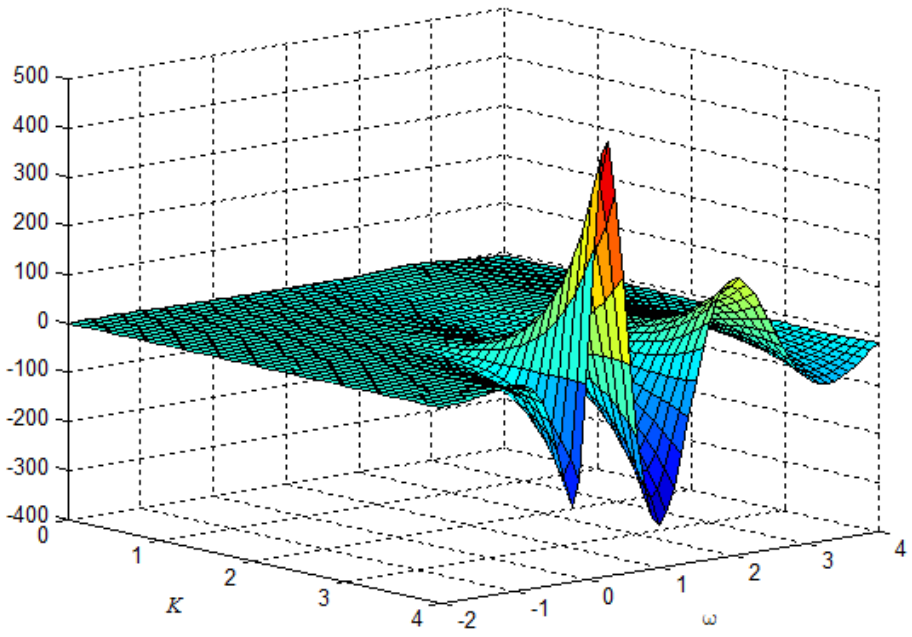

Figure 12(k): Surface plot of Im[$B(\omega,K)$]

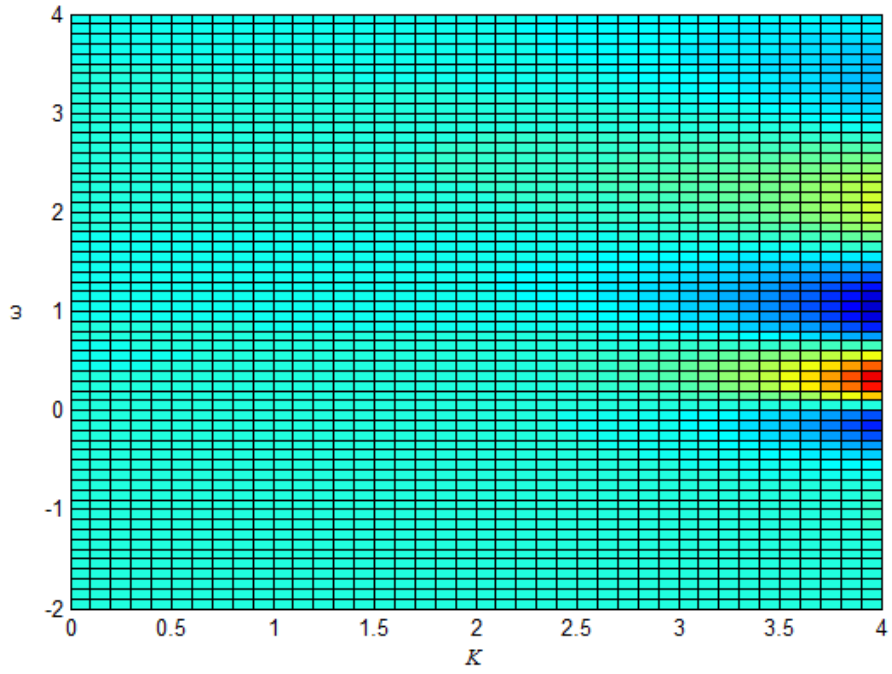

Figure 12(l): Contour plot of Im[$B(\omega,K)$]

Q=3.4, Z=1.7, T=0.0088

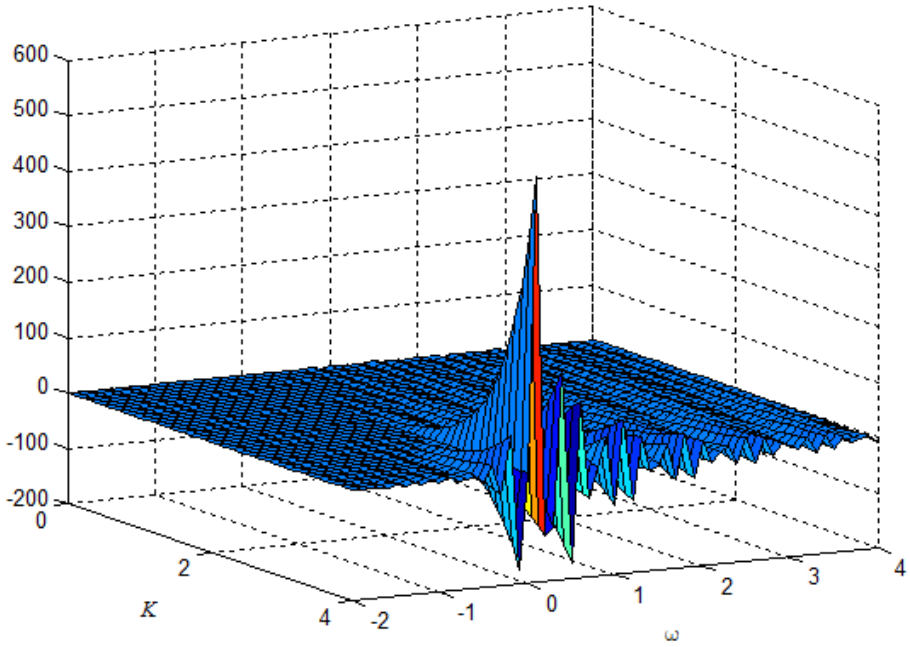

Figure 12(m): Surface plot of Im[$A(\omega,K)$]

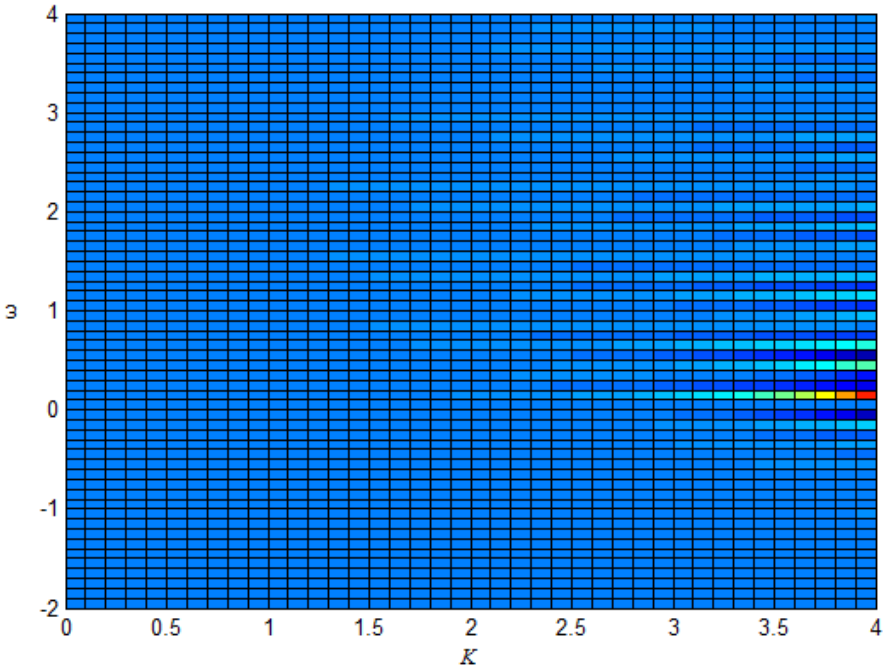

Figure 12(n): Contour plot of Im[$A(\omega,K)$]

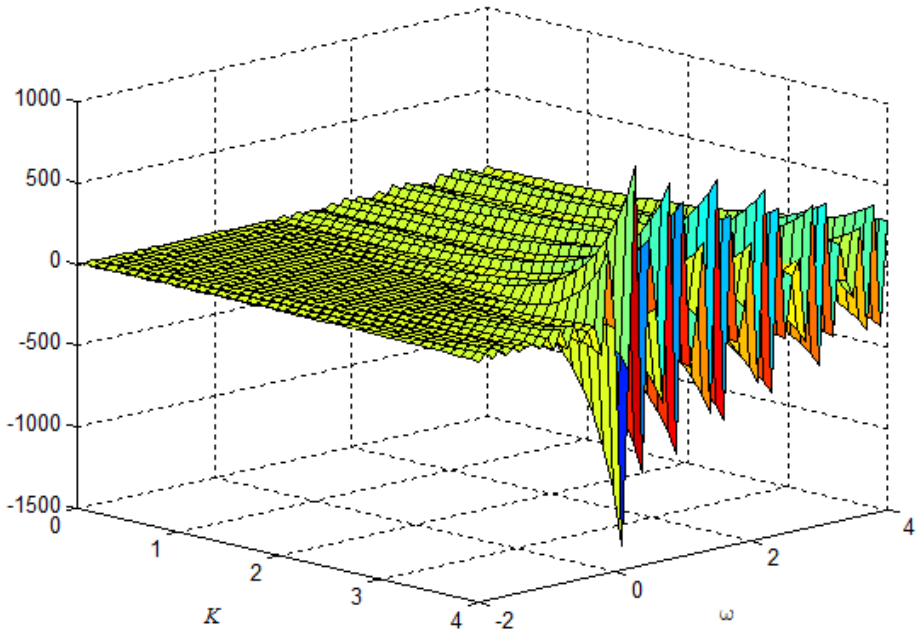

Figure 12(o): Surface plot of Im[$B(\omega,K)$]

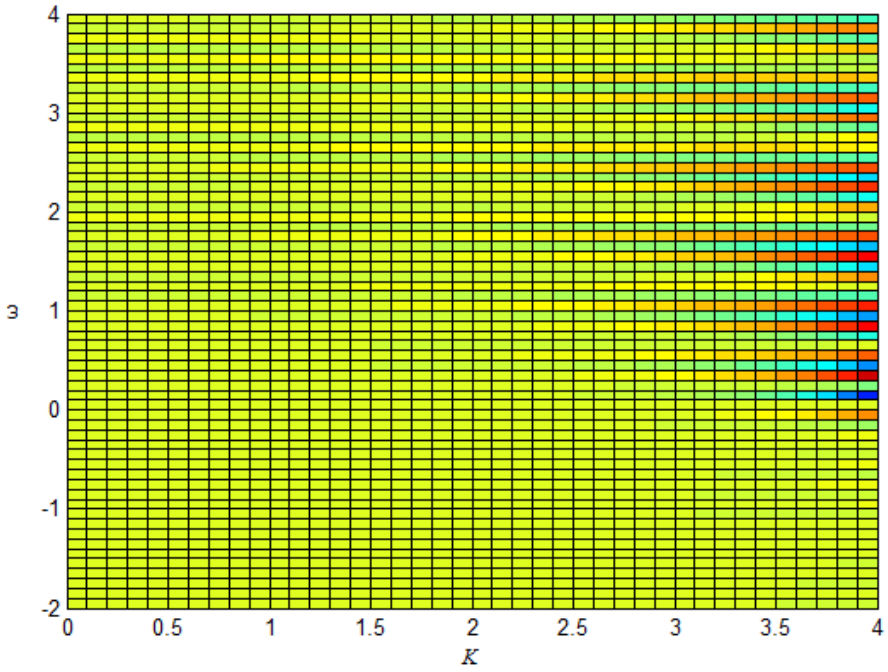

Figure 12(p): Contour plot of Im[$B(\omega,K)$]

Greens Functions: Eq (2.115)

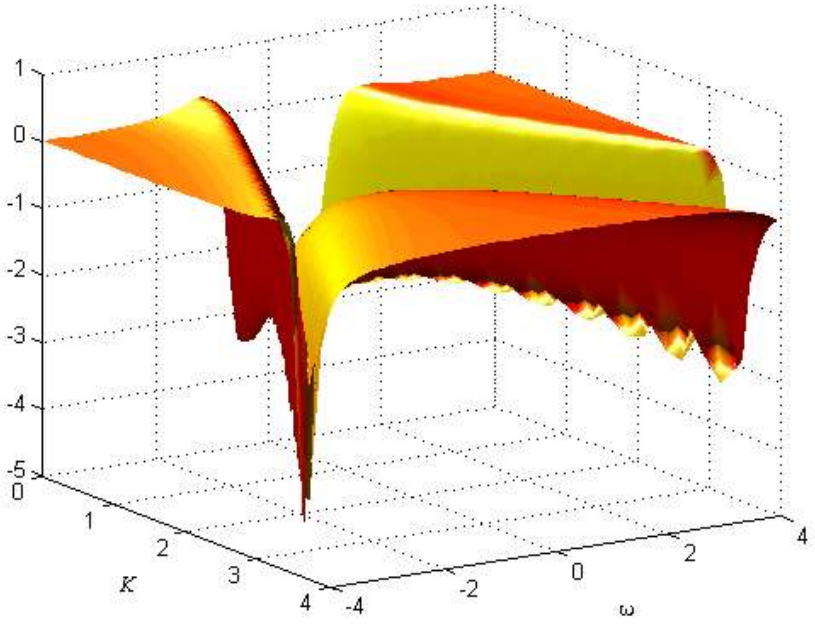

Figure 13(a): Greens function; $G = \mathrm{Re}[A(\omega,K) / B(\omega,K)]$, Q=0.1, Z=0.05, T=0.239

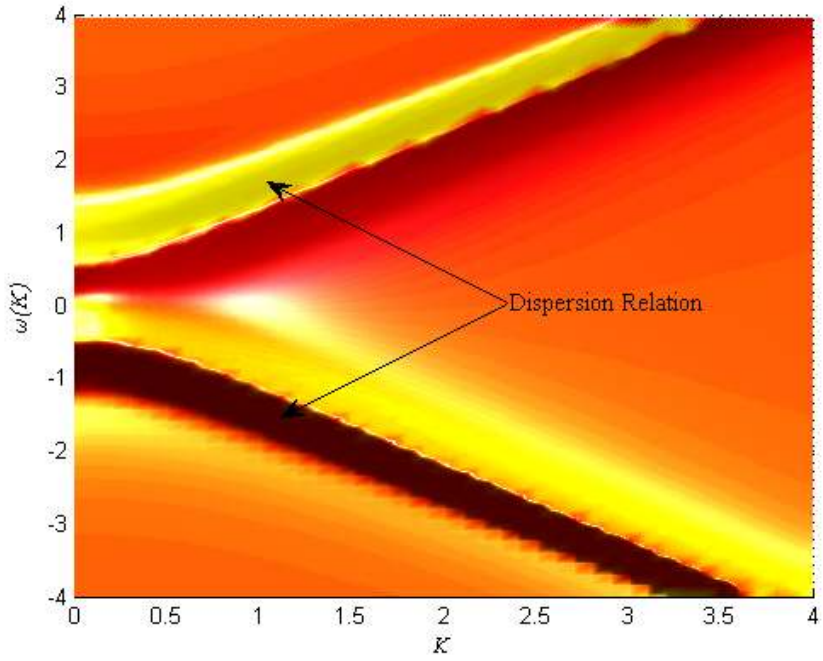

Figure 13(b): Contour of Fig 13(a),showing Dispersion Relations

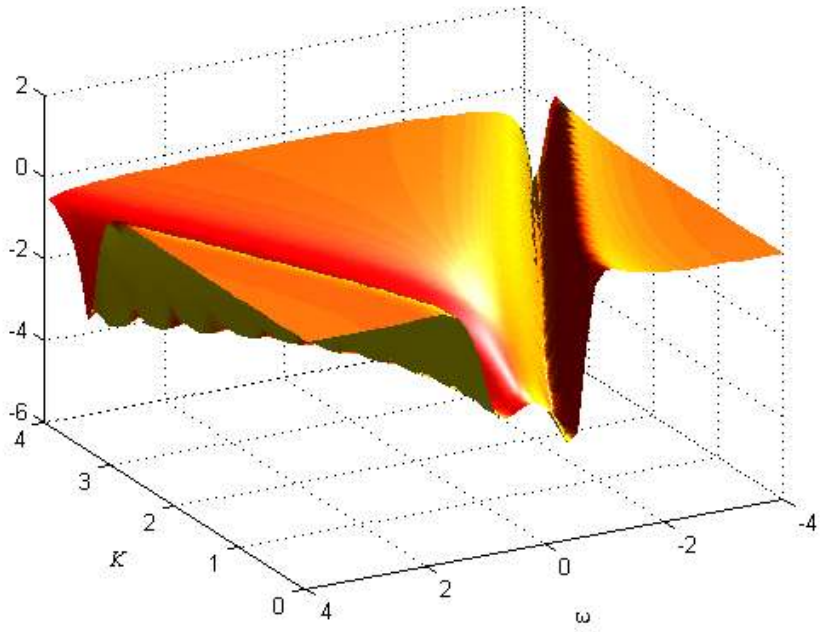

Figure 13(c): Greens function; G = Re[$A(\omega,K) / B(\omega,K)$], Q=0.185, Z=0.0086, T=0.238

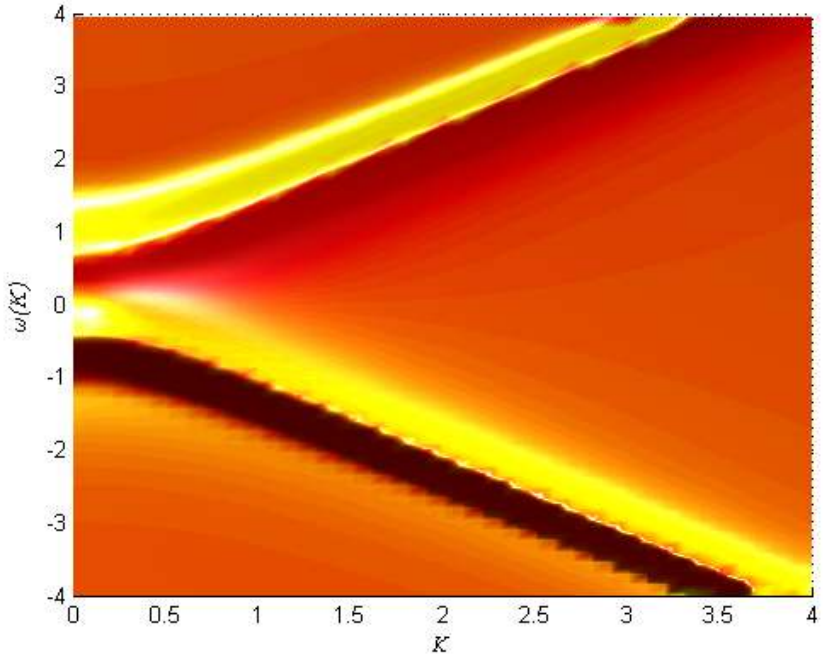

Figure 13(d): Contour of Fig 13(c),showing Dispersion Relations

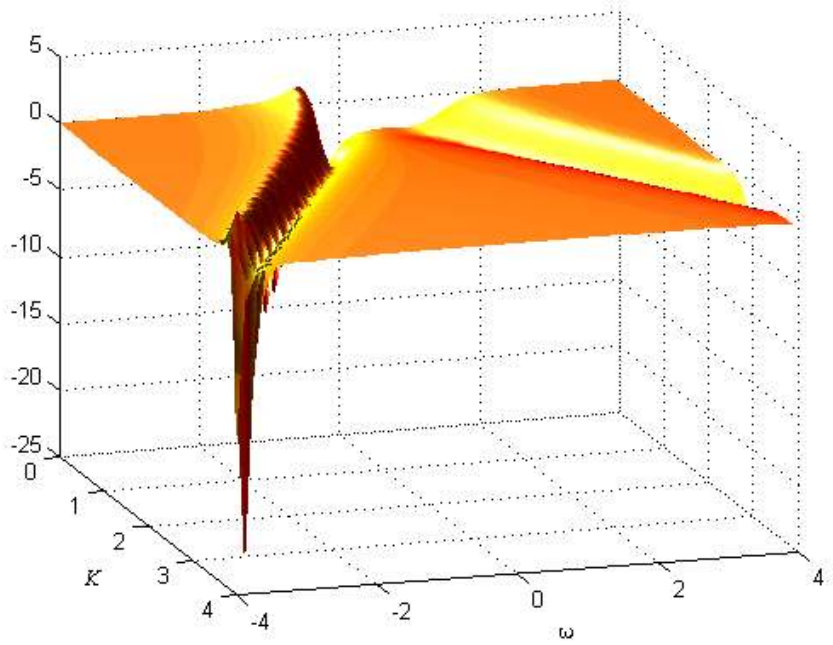

Figure 13(e): Greens function; G = Re[$A(\omega,K) / B(\omega,K)$], , Q=0.5, Z=0.25, T=0.234

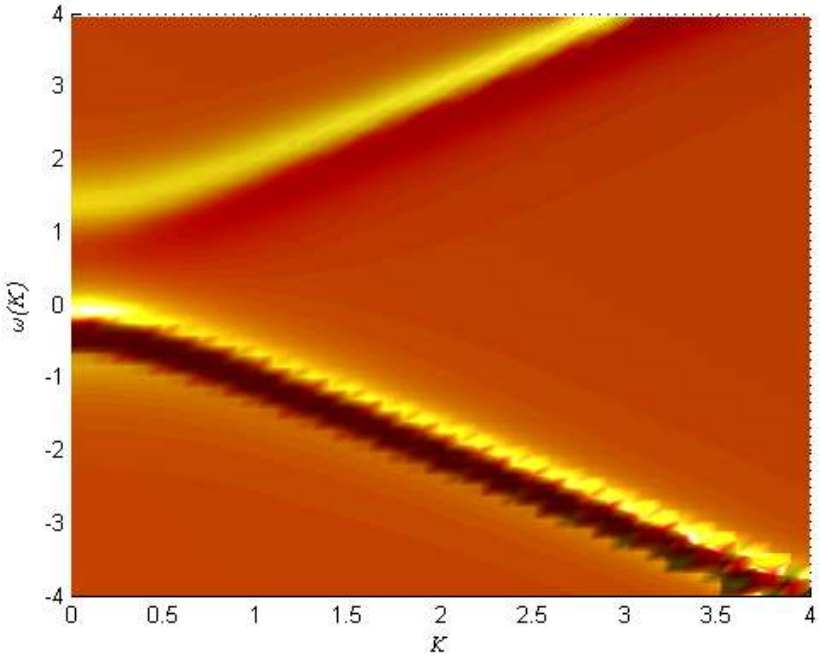

Figure 13(f): Contour of Fig 13(e),showing Dispersion Relations

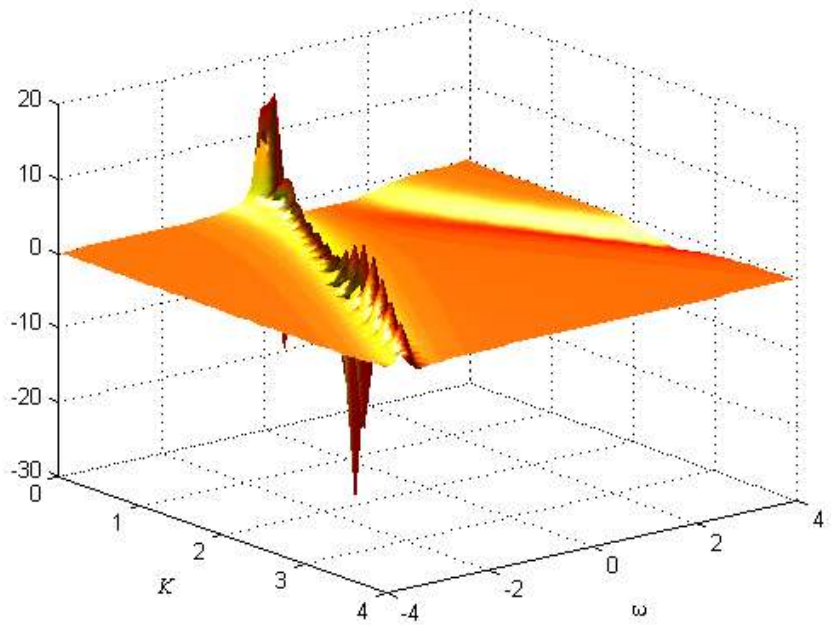

Figure 13(g): Greens function; $G = \mathrm{Re}[A(\omega,K) / B(\omega,K)]$, , Q=1, Z=0.5, T=0.219

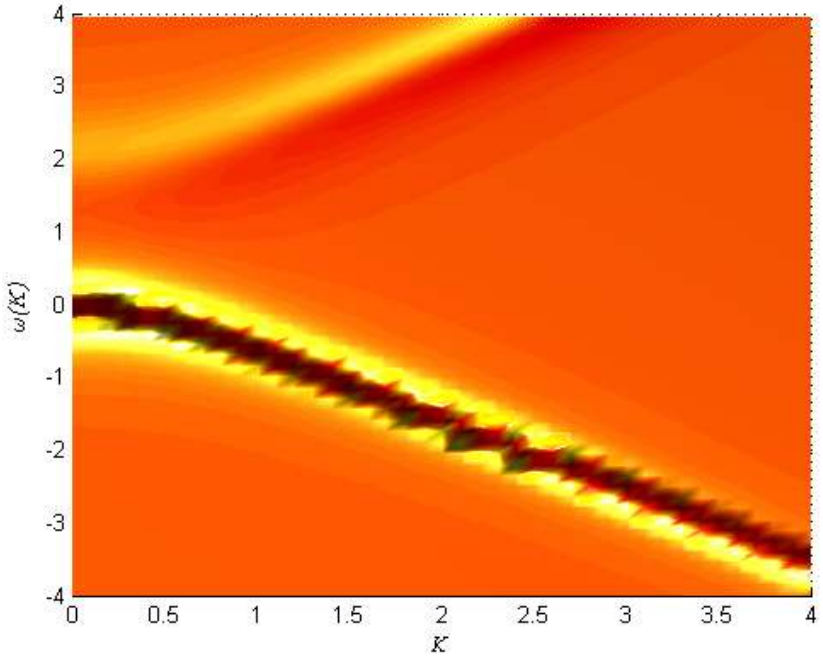

Figure 13(h): Contour of Fig 13(e),showing Dispersion Relations

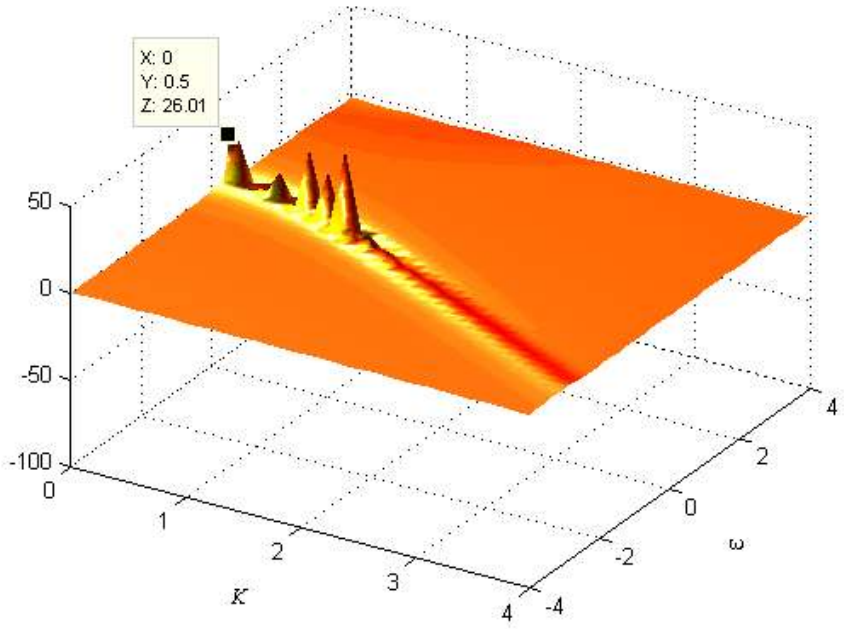

Figure 13(i): Greens function; $G = \mathrm{Re}[A(\omega,K) / B(\omega,K)]$, , Q=1.93, Z=0.97, $T=T_c$=0.165

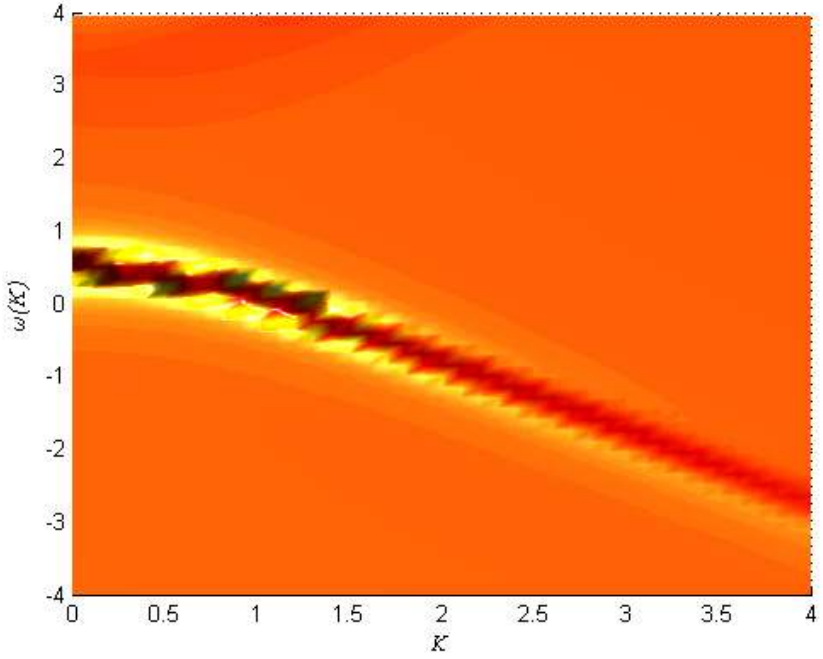

Figure 13(j): Contour of Fig 13(i),showing Dispersion Relations

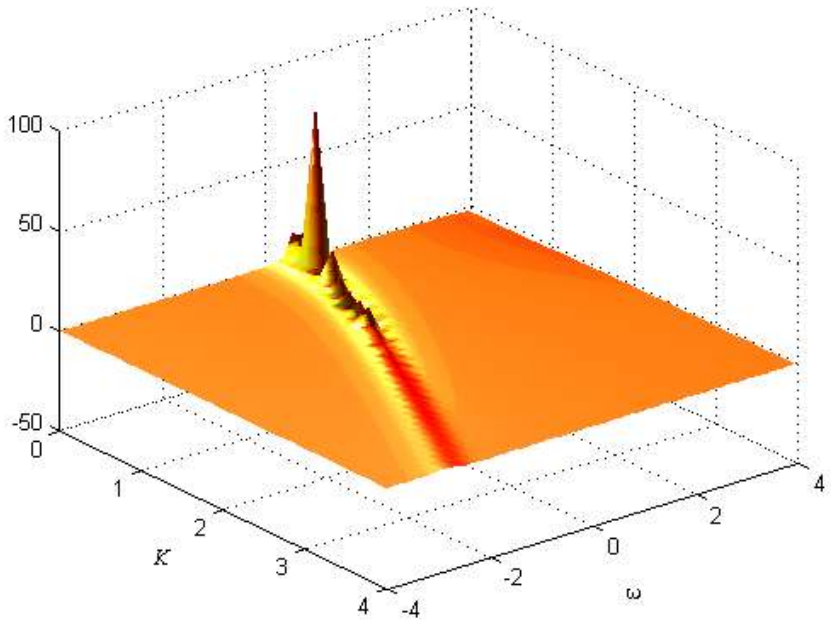

Figure 13(k): Greens function; $G = \mathrm{Re}[A(\omega,K) / B(\omega,K)]$, , Q=2, Z=1, T=0.159

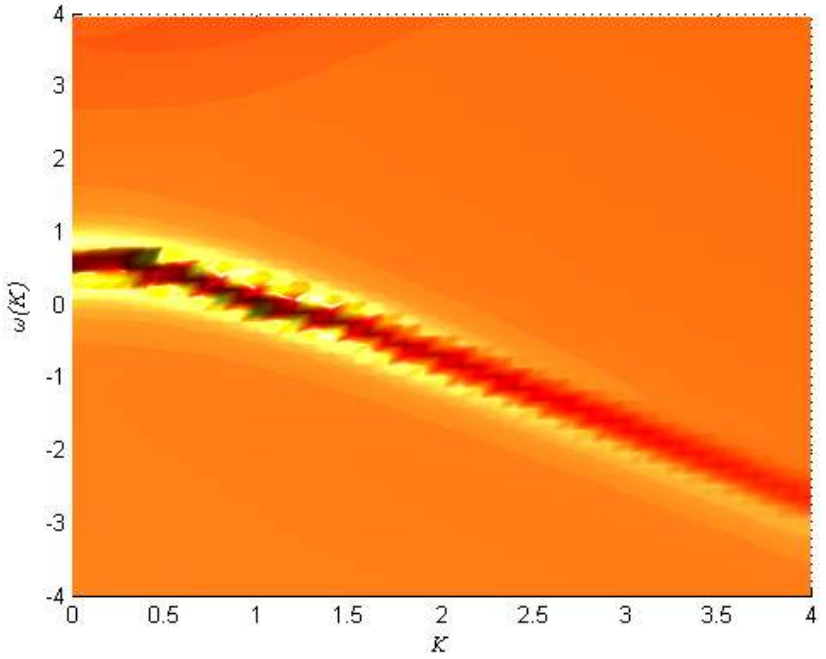

Figure 13(l): Contour of Fig 13(i),showing Dispersion Relation

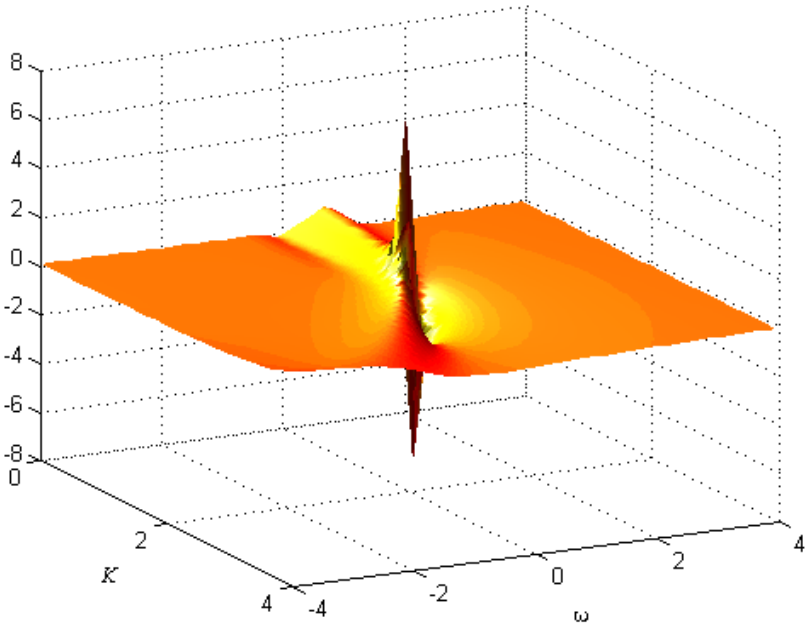

Figure 13(m): Greens function; $G = \mathrm{Re}[A(\omega,K) / B(\omega,K)]$, Q=3, Z=3/2, T=0.0597

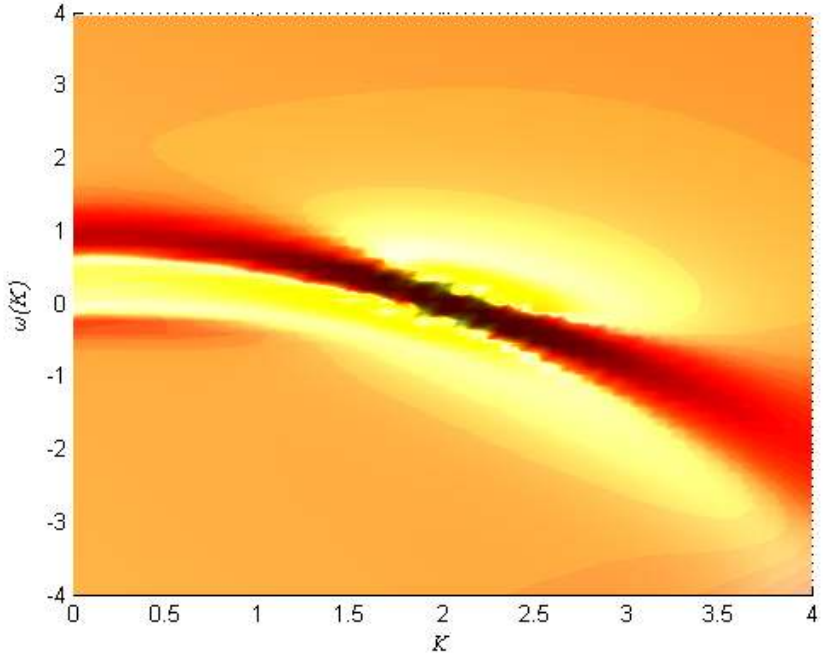

Figure 13(n): Contour of Fig 13(k),showing Dispersion Relation

Spectral Functions: Eq (2.118)

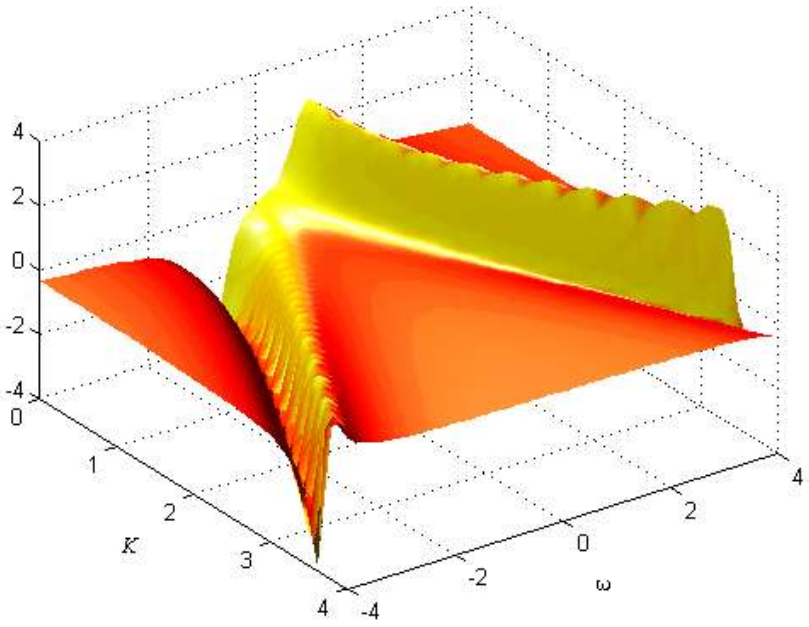

Figure 14(a): Spectral function; $\Pi = \mathrm{Im}[A(\omega,K) / B(\omega,K)]$, Q=0.1, Z=0.05, T=0.239

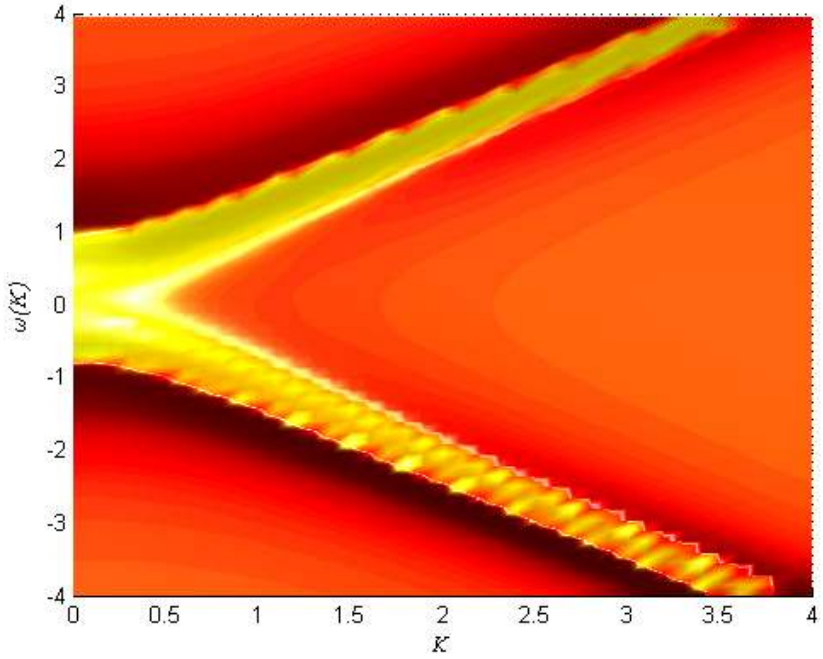

Figure 14(b): Contour of Fig 14(a),showing Dispersion Relations

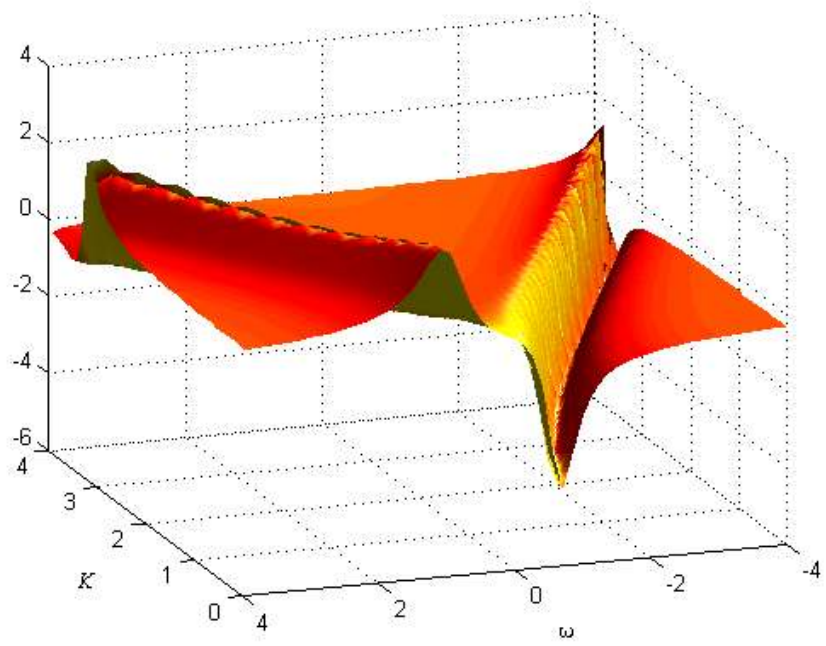

Figure 14(c): Spectral function; $\Pi = \mathrm{Im}[A(\omega,K) / B(\omega,K)]$, Q=0.185, Z=0.0086, T=0.238

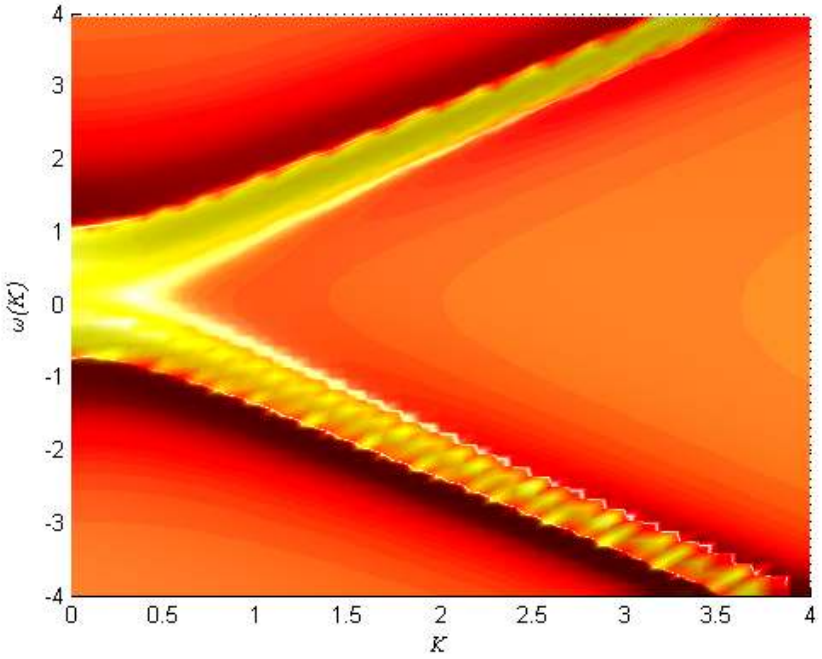

Figure 14(d): Contour of Fig 14(c),showing Dispersion Relations

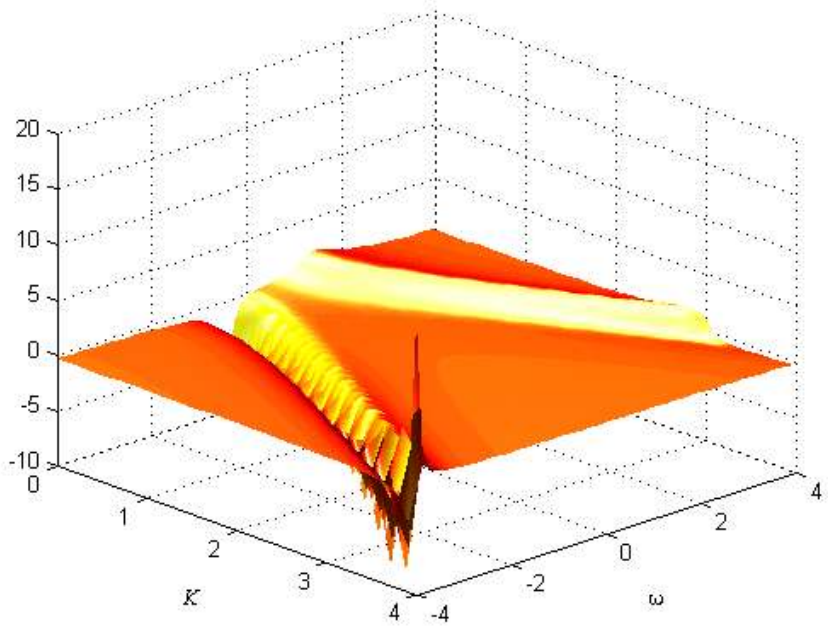

Figure 14(e): Spectral function; $\Pi = \mathrm{Im}[A(\omega,K) / B(\omega,K)]$, Q=0.5, Z=0.25, T=0.234

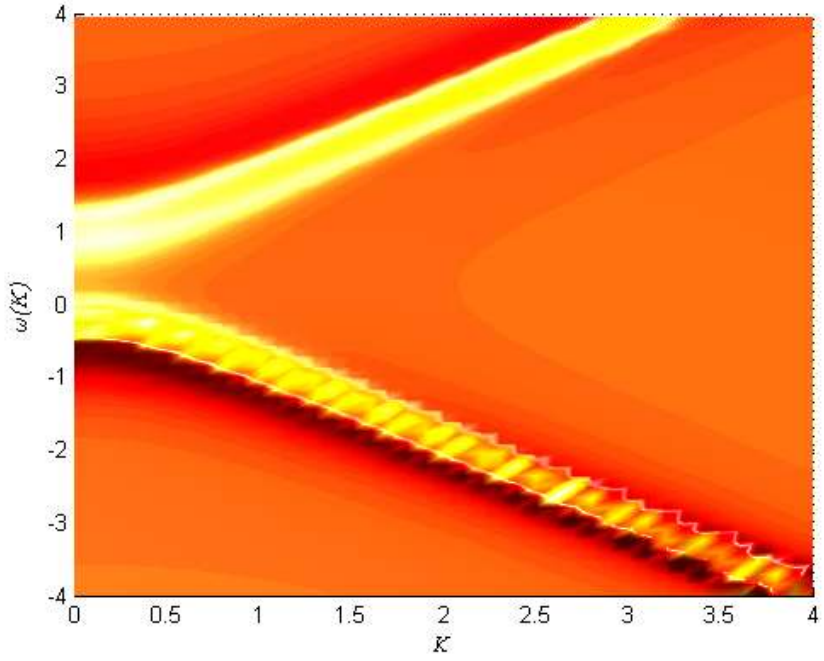

Figure 14(f): Contour of Fig 14(e),showing Dispersion Relations

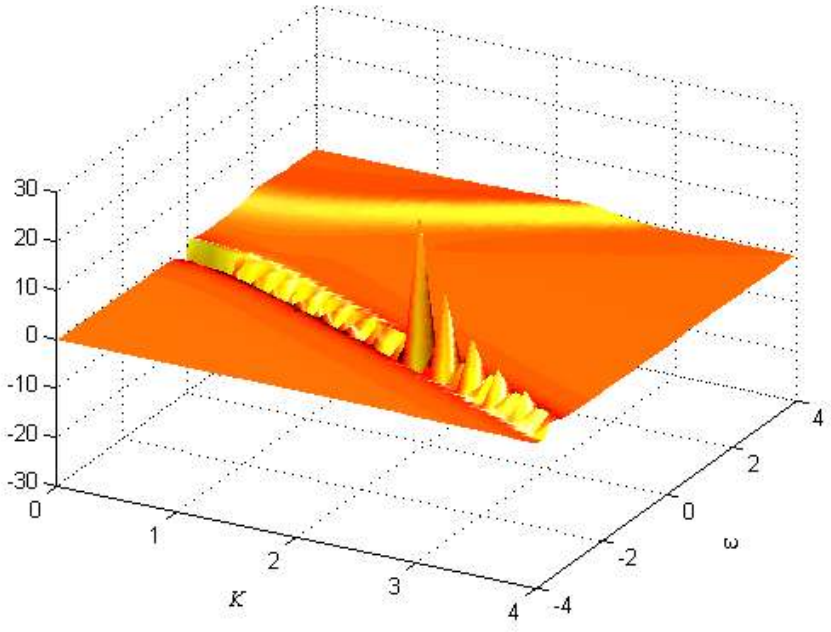

Figure 14(g): Spectral function; $\Pi = \mathrm{Im}[A(\omega,K) / B(\omega,K)]$, Q=1, Z=0.5, T=0.219

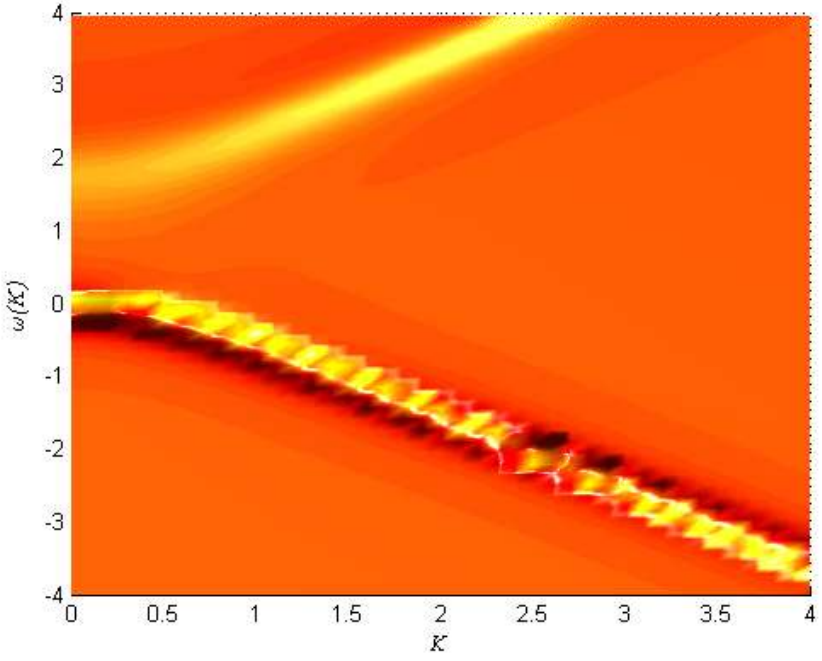

Figure 14(h): Contour of Fig 14(g),showing Dispersion Relations

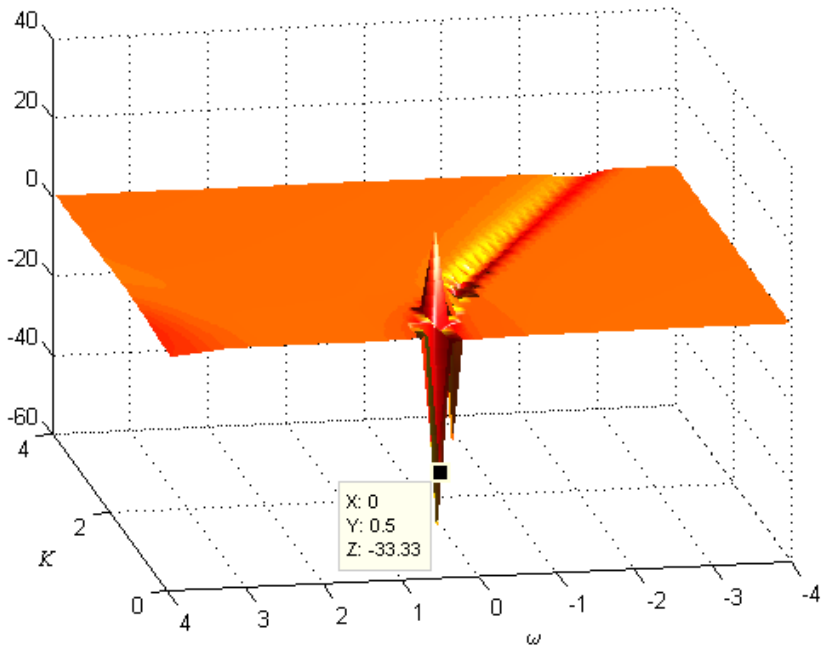

Figure 14(i): Spectral function; $\Pi = \mathrm{Im}[A(\omega,K)/B(\omega,K)]$, Q=1.93, Z=0.97, $T=T_c$ =0.165

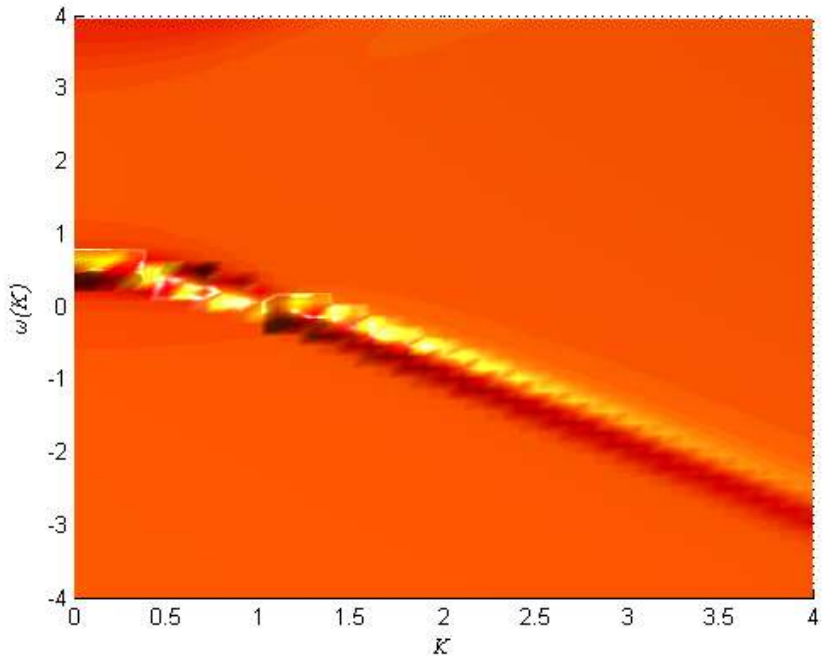

Figure 14(j): Contour of Fig 14(i),showing Dispersion Relations

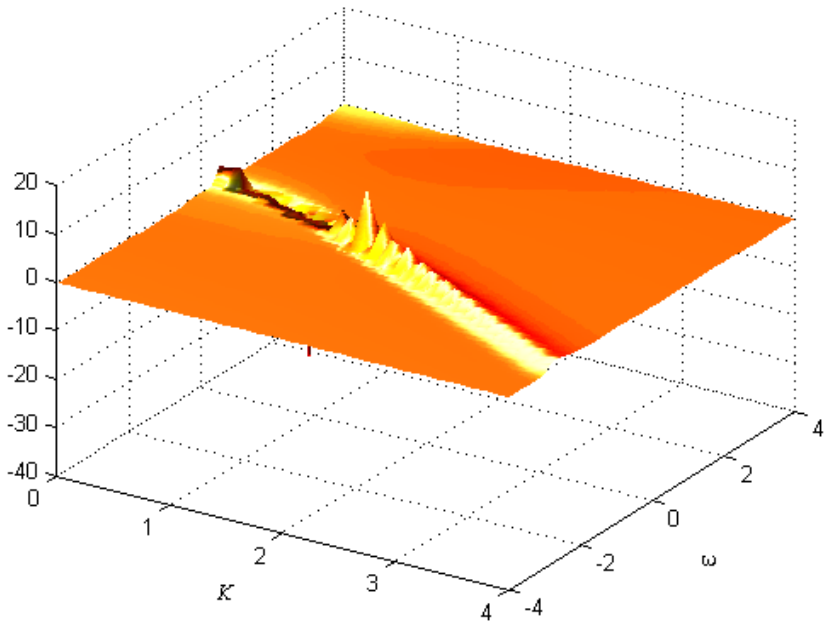

Figure 14(k): Spectral function; $\Pi = \mathrm{Im}[A(\omega,K) / B(\omega,K)]$, Q=2, Z=1, T=0.159

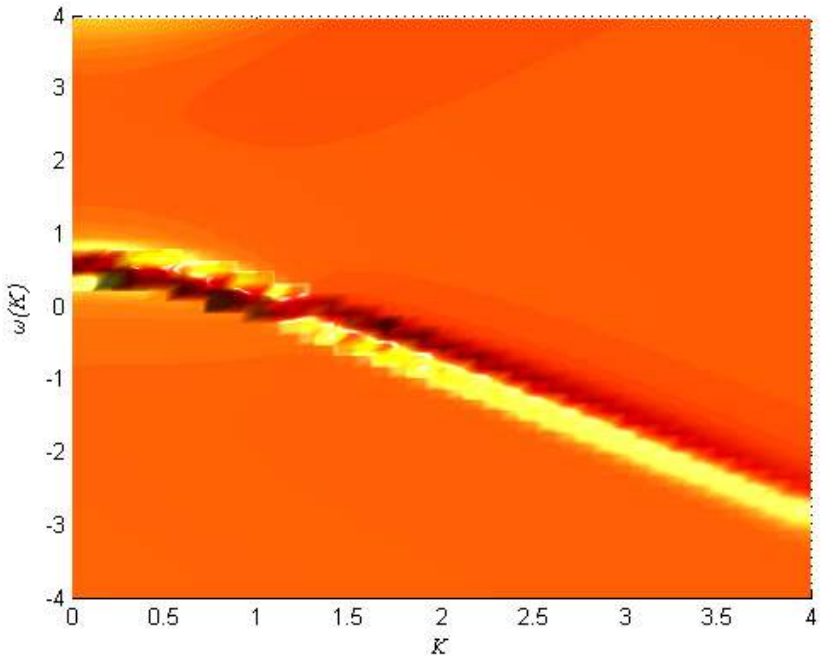

Figure 14(l): Contour of Fig 14(k),showing Dispersion Relations

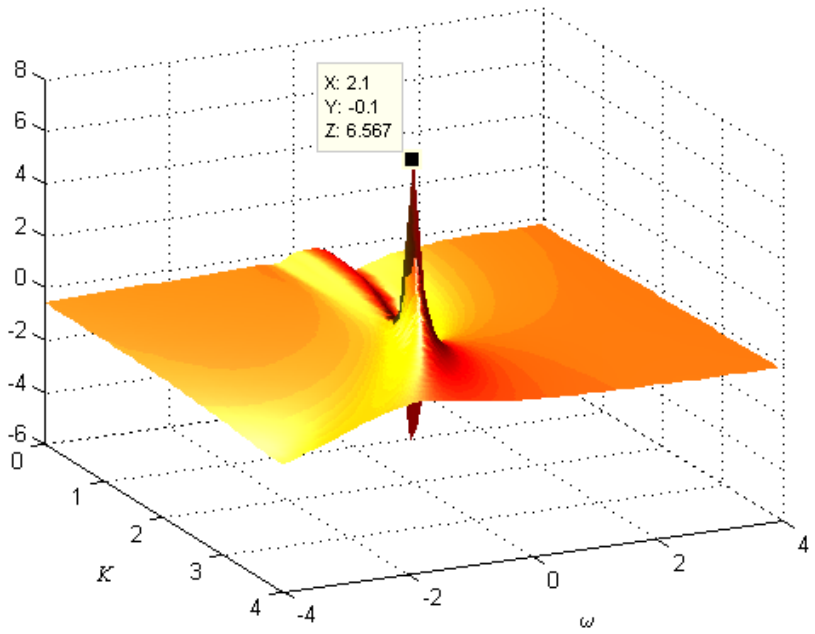

Figure 14(m): Spectral function; $\Pi = \mathrm{Im}[A(\omega,K)/B(\omega,K)]$, Q=3, Z=3/2, T=0.0597

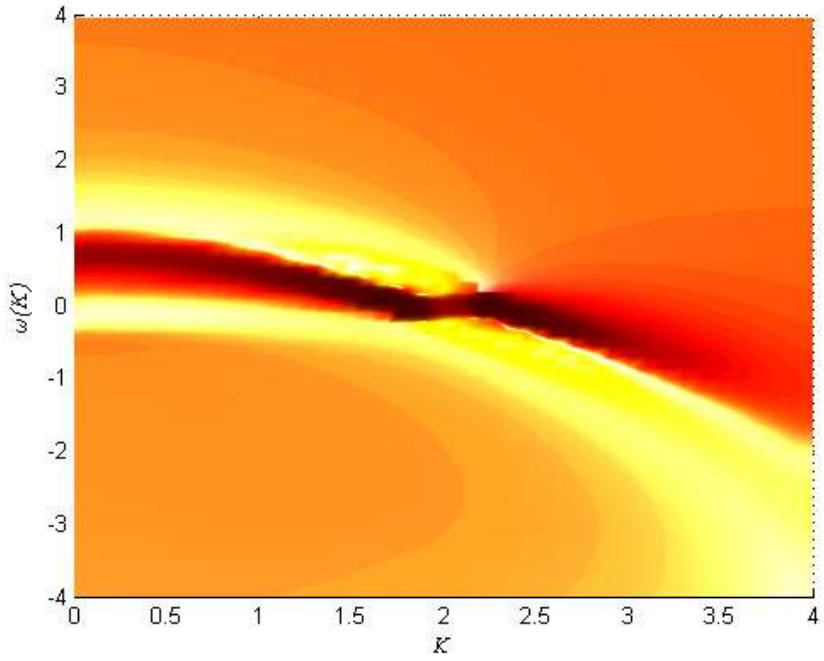

Figure 14(n): Contour of Fig 14(m),showing Dispersion Relations

The dispersion relations for the scalar at the AdS boundary can be seen easily from the contour plots in figures 13 and 14 above. They are merely the peak values on the large ridges, and are clearly marked in figure 13(b) as an example. At high temperatures, figures 13(b) and (d) for example, there is a definite symmetry between the upper and lower dispersion relations. As the temperature of the black hole is lowered, the upper branch disappears and this symmetry is lost. The interesting physics lies in the dispersion relations for which $\omega(0) \neq 0$. An example of such is the branch marked with the upper arrow in Figure 13(b). The zero momentum value of this branch represents the pseudo-particles mass, where the upper branch in each of the contour plots corresponds to the particles in the field, and the lower branch corresponds to their anti-particles. The gap between $\omega(0)=0$ and the point where each branch hits zero momentum gives the difference in the energy of the field between its vacuum energy and the next lowest energy state. More precisely it is the lowest possible bound for any energy state which is orthogonal to the vacuum, and it represents the lightest particle in the field. In the figures above, this "mass" gap increases as one lowers the temperature of the black hole. This only holds true for the upper branch until one reaches the critical temperature associated with the vev $\mathcal{y}(0)$, which was worked out in §2.3 to be $T_c=0.165$. At this point it becomes impossible to see a pseudo-particle mass. I provide a list of these pseudo-particle mass values below, denoting the value of the upper branch (particle) by Ω_+ and the lower branch (anti-particle) by Ω_-, which are both in units of $1/r_+L^2$. Recall that the Anti de-Sitter radius L and the outer horizon radius r_+ have now been set to unity and we are working in the case where the curvature constant $k = 0$. This means the temperature of the black hole is solely determined by the choice of the coupled scalar-black hole charge Q. The values chosen here for Q, cover essentially its entire range.

(1) Pseudo-particle mass for particle $\Omega_+ = |\Omega_+|$

$$
\begin{array}{lcll}
Q = 0.01; & \rightarrow & T = 0.239, & \rightarrow \quad \Omega_+ = 0.50 \\
Q = 0.1; & \rightarrow & T = 0.239, & \rightarrow \quad \Omega_+ = 0.65 \\
Q = 0.185; & \rightarrow & T = 0.238, & \rightarrow \quad \Omega_+ = 0.65 \\
Q = 0.2; & \rightarrow & T = 0.238, & \rightarrow \quad \Omega_+ = 0.65 \\
Q = 0.3; & \rightarrow & T = 0.237, & \rightarrow \quad \Omega_+ = 0.80 \\
Q = 0.4; & \rightarrow & T = 0.236, & \rightarrow \quad \Omega_+ = 0.80 \\
Q = 0.5; & \rightarrow & T = 0.234, & \rightarrow \quad \Omega_+ = 0.95 \\
Q = 0.6; & \rightarrow & T = 0.232, & \rightarrow \quad \Omega_+ = 0.95 \\
Q = 0.7; & \rightarrow & T = 0.229, & \rightarrow \quad \Omega_+ = 1.10 \\
Q = 0.8; & \rightarrow & T = 0.226, & \rightarrow \quad \Omega_+ = 1.25 \\
Q = 0.9; & \rightarrow & T = 0.223, & \rightarrow \quad \Omega_+ = 1.40 \\
Q = 1; & \rightarrow & T = 0.219, & \rightarrow \quad \Omega_+ = 1.55 \\
Q = 1.1; & \rightarrow & T = 0.215, & \rightarrow \quad \Omega_+ = 1.70 \\
Q = 1.2; & \rightarrow & T = 0.210, & \rightarrow \quad \Omega_+ = 1.85 \\
Q = 1.3; & \rightarrow & T = 0.205, & \rightarrow \quad \Omega_+ = 2.00 \\
Q = 1.4; & \rightarrow & T = 0.199, & \rightarrow \quad \Omega_+ = 2.30 \\
Q = 1.5; & \rightarrow & T = 0.194, & \rightarrow \quad \Omega_+ = 2.45 \\
Q = 1.6; & \rightarrow & T = 0.188, & \rightarrow \quad \Omega_+ = 2.75 \\
Q = 1.7; & \rightarrow & T = 0.181, & \rightarrow \quad \Omega_+ = 3.05 \\
Q = 1.8; & \rightarrow & T = 0.174, & \rightarrow \quad \Omega_+ = 3.35 \\
Q = 1.9; & \rightarrow & T = 0.167, & \rightarrow \quad \Omega_+ = 3.65 \\
Q = 1.93; & \rightarrow & T = 0.165, & \rightarrow \quad \Omega_+ = 3.80
\end{array}
$$

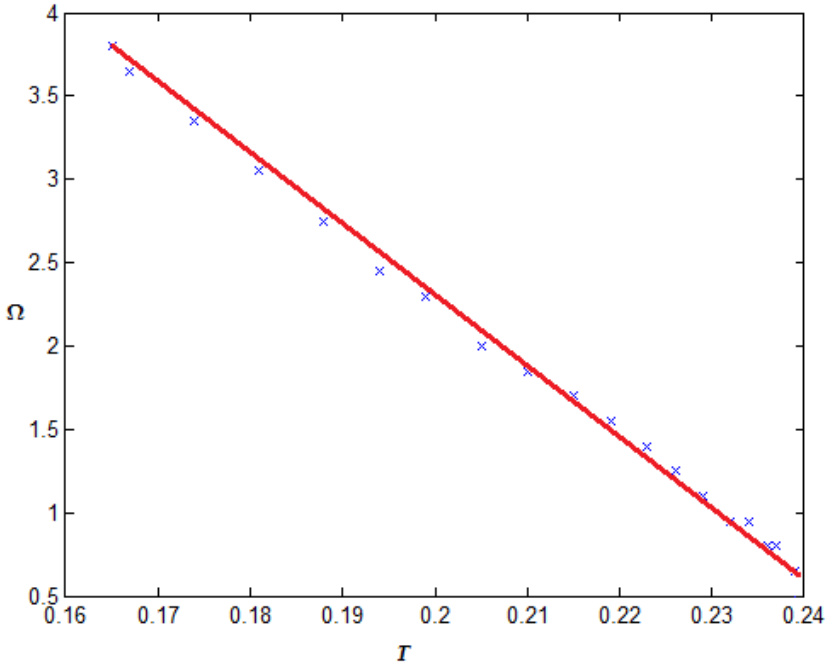

Figure 15: Best fit plot of pseudo-particle mass Ω_+ versus Temperature T for $\Omega_+ = |\Omega_+|$

(2) Pseudo-particle mass for Anti-particle Ω_- (The first plot below doesn't take absolute values of Ω_- while the second does.)

$$
\begin{array}{lcll}
Q = 0.01; & \rightarrow & T = 0.239, & \rightarrow \quad \Omega_- = -1.45 \\
Q = 0.1; & \rightarrow & T = 0.239, & \rightarrow \quad \Omega_- = -1.15 \\
Q = 0.185; & \rightarrow & T = 0.238, & \rightarrow \quad \Omega_- = -1.00 \\
Q = 0.2; & \rightarrow & T = 0.238, & \rightarrow \quad \Omega_- = -1.00 \\
Q = 0.3; & \rightarrow & T = 0.237, & \rightarrow \quad \Omega_- = -0.85 \\
Q = 0.4; & \rightarrow & T = 0.236, & \rightarrow \quad \Omega_- = -0.70 \\
Q = 0.5; & \rightarrow & T = 0.234, & \rightarrow \quad \Omega_- = -0.55 \\
Q = 0.6; & \rightarrow & T = 0.232, & \rightarrow \quad \Omega_- = -0.55 \\
Q = 0.7; & \rightarrow & T = 0.229, & \rightarrow \quad \Omega_- = -0.40 \\
Q = 0.8; & \rightarrow & T = 0.226, & \rightarrow \quad \Omega_- = -0.25 \\
Q = 0.9; & \rightarrow & T = 0.223, & \rightarrow \quad \Omega_- = -0.25 \\
Q = 1; & \rightarrow & T = 0.219, & \rightarrow \quad \Omega_- = -0.10 \\
Q = 1.1; & \rightarrow & T = 0.215, & \rightarrow \quad \Omega_- = -0.10 \\
Q = 1.1502; & \rightarrow & T = 0.212, & \rightarrow \quad \Omega_- = -0.10 \\
Q = 1.1503; & \rightarrow & T = 0.212, & \rightarrow \quad \Omega_- = 0.05 \\
Q = 1.2; & \rightarrow & T = 0.210, & \rightarrow \quad \Omega_- = 0.05 \\
Q = 1.3; & \rightarrow & T = 0.205, & \rightarrow \quad \Omega_- = 0.05 \\
Q = 1.4; & \rightarrow & T = 0.199, & \rightarrow \quad \Omega_- = 0.20 \\
Q = 1.5; & \rightarrow & T = 0.194, & \rightarrow \quad \Omega_- = 0.20 \\
Q = 1.6; & \rightarrow & T = 0.188, & \rightarrow \quad \Omega_- = 0.20 \\
Q = 1.7; & \rightarrow & T = 0.181, & \rightarrow \quad \Omega_- = 0.35 \\
Q = 1.8; & \rightarrow & T = 0.174, & \rightarrow \quad \Omega_- = 0.35 \\
Q = 1.9; & \rightarrow & T = 0.167, & \rightarrow \quad \Omega_- = 0.35 \\
Q = 1.93; & \rightarrow & T = 0.165, & \rightarrow \quad \Omega_- = 0.50 \\
Q = 1.95; & \rightarrow & T = 0.163, & \rightarrow \quad \Omega_- = 0.50 \\
Q = 2; & \rightarrow & T = 0.159, & \rightarrow \quad \Omega_- = 0.50 \\
Q = 2.1; & \rightarrow & T = 0.151, & \rightarrow \quad \Omega_- = 0.50 \\
Q = 2.2; & \rightarrow & T = 0.142, & \rightarrow \quad \Omega_- = 0.65 \\
Q = 2.3; & \rightarrow & T = 0.134, & \rightarrow \quad \Omega_- = 0.65 \\
Q = 2.4; & \rightarrow & T = 0.124, & \rightarrow \quad \Omega_- = 0.65 \\
Q = 2.5; & \rightarrow & T = 0.114, & \rightarrow \quad \Omega_- = 0.65 \\
Q = 2.6; & \rightarrow & T = 0.104, & \rightarrow \quad \Omega_- = 0.65 \\
Q = 2.7; & \rightarrow & T = 0.094, & \rightarrow \quad \Omega_- = 0.65 \\
Q = 2.8; & \rightarrow & T = 0.083, & \rightarrow \quad \Omega_- = 0.65 \\
Q = 2.9; & \rightarrow & T = 0.071, & \rightarrow \quad \Omega_- = 0.65 \\
Q = 3; & \rightarrow & T = 0.060, & \rightarrow \quad \Omega_- = 0.65 \\
Q = 3.1; & \rightarrow & T = 0.048, & \rightarrow \quad \Omega_- = 0.65 \\
Q = 3.2; & \rightarrow & T = 0.035, & \rightarrow \quad \Omega_- = 0.65
\end{array}
$$

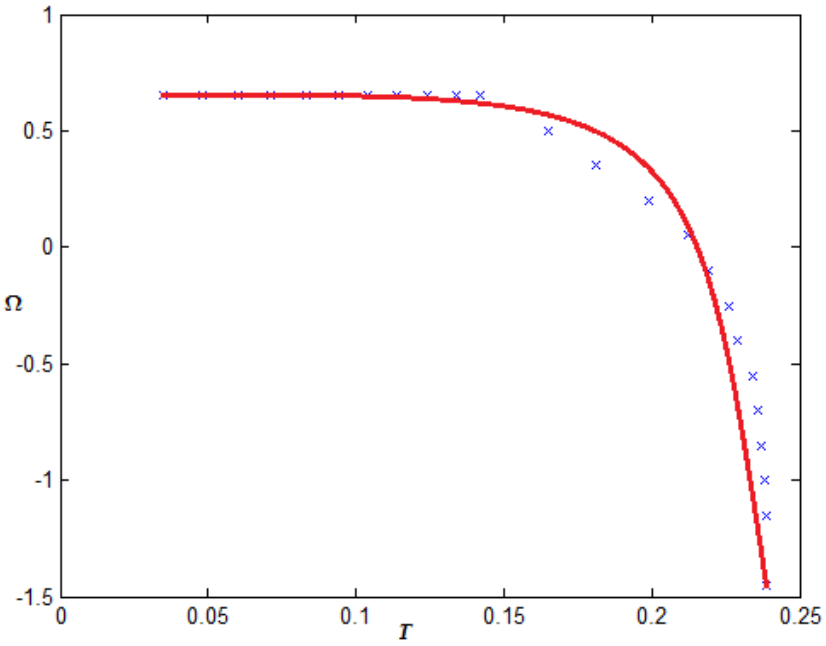

Figure 16(a): Best fit plot of pseudo-particle mass Ω_- vs T, for $\Omega_- \neq |\Omega_-|$

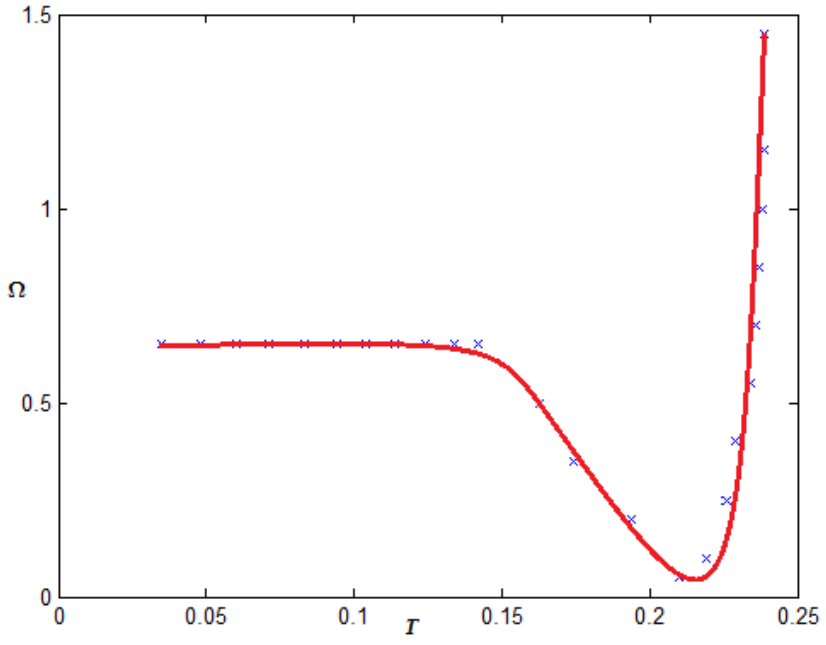

Figure 16(b): Best fit plot of pseudo-particle mass Ω_- vs T, for $\Omega_- = |\Omega_-|$

The curves in figures 15 and 16 where fitted as accurately as possible by eye over the values calculated above, which are shown in the figures as blue x's. For case (1) above, the results are completely consistent with a straight line. One can see the pseudo-particle mass increase linearly as the black hole grows colder until it reaches the critical temperature associated with the vev $y(0)$, which was found in §2.3 to be T_c=0.165. Beyond this point the pseudo-particles associated with Ω_+ are seen to disappear. There is no structure at the critical point for the coupling strength $y'(0)$, ie, at T_c=0.217.

There is slightly more to report from case (2). One can see that Ω_- passes through zero at $T_c = 0.212$ which is extremely close to the critical temperature of the coupling strength $y'(0)$. The slight difference in the third decimal place here can be put down to the numerics of the programme which generated it. A fine tuning, that is to say, a larger number of grid points would indeed produce a vanishing of Ω_- at exactly T_c=0.217. This tells us that the pseudo-particles associated with Ω_- become massless at exactly this critical temperature. The pseudo-particle mass Ω_-, effectively "switches on" at temperatures either side of this critical temperature. One can also readily see that Ω_- levels off and becomes flat immediately after the critical temperature, T_c=0.165 is reached. This is precisely the temperature that the Ω_+ branch disappears. At this critical temperature, Ω_- takes on a constant value of 0.5, and increases only slightly to 0.65 as the temperature of the black hole is lowered where it perhaps remains until the black hole becomes extremal (a more rigorous analysis in the lowest temperature regime would be required to see if Ω_- remains constant at 0.65, or decreases, etc). At this critical temperature, the particle and Anti-particle pseudo-masses can be very roughly related as, $\Omega_+ \approx (15/2)\Omega_-$. It should be noted that temperatures any lower than the ones considered here, could not really have been trusted to give accurate values for Ω_-. One needs only look back at figures 10(g) and (h) to see that temperatures below $T \approx 0.035$ produce highly unstable results.

It should also be recalled that the only difference between the parameters in the pseudo-particle mass analysis here, and that of the vevs in §2.3 is that L is now taken to be unity, so the critical temperature for the vev $y(0)$ corresponds to a charge of Q =1.93. In fact the temperature here is completely determined by the charge of the

system. On the other hand, in §2.3, the black hole charge was taken to be unity, and the critical temperature for the vev $y(0)$ was found at L =1.93. In that case, the temperature was completely determined by the Anti de-Sitter radius L.

Discussion

In this work I have examined the behaviour of the energy of a massive scalar field in an Anti de-Sitter - Reissner Nordström black hole space-time. The scalar field which was considered during these calculations was conformally coupled. We therefore took the curvature constant k=0, and assigned the field a negative mass. Following a detailed derivation of the equations of motion governing the system, I show that the boundary operator of the field corresponding to the trace of the energy momentum tensor in the bulk gravity theory begins to condense at a critical temperature which was calculated for two separate values of the scalar fields charge. This then suggests that the current related to this charged operator will superconduct. The vacuum expectation value of this operator was then found numerically, and it is seen to vanish periodically from the instance that the critical temperature is reached. It develops more and more zero nodes as the temperature of the black hole is decreased, ie, the energy of the field approaches an instability as the black hole approaches extremality. The operator and its coupling were plotted together in a parametric plot and a spiral-like behaviour is observed around the origin. This sort of behaviour has been observed in other works concerning Fermions, unlike the present paper concerning bosons, and references are given to this end for the interested reader. The vev's for operators with both mass dimensions of equation (1.78) both plotted back to back in what followed. The two curves are out of phase with each other however the behaviour of one mirrors that of the other exactly.

I then added a time dependent part to the field in order to extract the dispersion relations for the conformal field at the boundary. After providing a succession of graphs of the vevs of the operator and its coupling in momentum space, I provide plots of the relevant Greens and Spectral functions for the system. From these we can see the dispersion relations for the field at the AdS boundary. There is an obvious symmetry between the dispersion relations of the fields particles and Anti-particles at high temperatures. This symmetry is lost as the black hole gets colder.

The dispersion relations then allowed us to calculate pseudo-particle masses at zero momentum. This was done for both particles and Anti-particles at temperatures ranging from well above critical temperature down to temperatures in which the black hole was almost extremal. The absolute value of the pseudo-particle masses calculated, represent the lowest energy level that a particle in this field can take above its vacuum energy, and it was shown that as one lowers the temperature of the black hole, the value of the pseudo-particle masses increased. The boundary field also exhibits several resonant frequencies which can be clearly seen in the Greens and spectral function figures. At resonance, the field seems to manifest itself in the form of sharp quasiparticle like peaks, however there does not seem to be any symmetry in the emergence of these peaks.

Acknowledgements

I would like to extend my gratitude to my supervisor Dr Brian Dolan for many insightful conversations on this subject matter throughout the year, and for possessing a large amount of patience as the work proceeded. I am also indebted to my family and friends for the support they have shown, and in particular to my father, who is a constant source of inspiration for me, and without whose financial assistance I would not have been able to pursue this work. I would also like to extend my thanks to the many department members at NUI Maynooth who answered many questions for me.

Appendix: Matlab code used

Code 1

```
% This routine produces figures 4


function adscft
global k L Z Q Q1 q

L=1.31;
k=0;
Q1=1;
Z=Q1/2;
q=3/L;
Q=q*Q1;    % In case one wishes to change the intrinsic charge of the scalar

f1=(Z^2*L^2-k*L^2-3);
g0=f1;
g1=6*(Z^2*L^2-1)-4*k*L^2;
h0=(Z^2*L^2-k*L^2-1);
h1=3*(Z^2*L^2) - k*L^2 - (((Q*L^2)^2)/(3+k*L^2-Z^2*L^2)) - 1;
x1=-(h0/g0);
x2=(((h0/g0)*(g1+h0) - h1)/(f1+g0));

eps=0.000001;
dy1= x1 - eps*x2;
y1=1-eps*x1;


[u,y]=ode45(@renosol,[1-eps,0],[y1,dy1]);
plot(u,y(:,1))
xlabel('u')


function dy=renosol(u,Y)

dy=zeros(2,1);
dy(1) = Y(2);

global k L Z Q

f=(1-u)*(1+u+u^2 +k*L^2*u^2-u^3*Z^2*L^2);
g=u*(4*u^2*(Z*L)^2-3*u*(1+(k+Z^2)*L^2) +2*k*L^2);
h=((((Q*L^2)^2)*(1-u))/(1+u+u^2+k*L^2*u^2-u^3*Z^2*L^2)) -u*(1+L^2*(k+Z^2))+
2*u^2*Z^2*L^2;

dy(2) = -(h/f)*Y(1)-(g/f)*Y(2);
```

Code 2

```
% A slight modification to code 1 above solves for the scalar field at the
% AdS boundary. This code produces figures 6 -> 9. As mentioned, to obtain
% the VEV's of the field, a central difference formula was used on the
% solutions A and B below in accordance with eq (2.72) and (2.73)


function adscft2
global k L Z Q Q1 q

for L=(0:0.002:3.4641)

k=0;
Q1=1;
Z=Q1/2;
q=3/L;
Q=q*Q1;    % In case one wishes to change the intrinsic charge of the scalar

f1=(Z^2*L^2-3);
g0=f1;
g1=6*(Z^2*L^2-1);
h0=(Z^2*L^2-1);
h1=-((Q^2*L^4)/(3-Z^2*L^2))+3*Z^2*L^2-1;

eps=0.00001;
dy1= -(h0/g0)-eps*(((g1+h0)*(h0/g0)-h1)/(f1+g0));
y1=1+eps*(h0/g0);

[u,y]=ode45(@renosol,[1-eps,0],[y1,dy1]);
x=[u,y];
x2=size(x);
b=x2(1,1);
A=x(b,2);       % y(0)
B=x(b,3);       % y'(0)
disp(A)         % displays y(0)...
C=B.*A;    % Perturbation away from fixed action at the boundary
plot(L,A,'b')
hold on
xlabel('L')
end

function dy=renosol(u,Y)

dy=zeros(2,1);
dy(1) = Y(2);

global k L Z Q

f=(1-u)*(1+u+u^2 +k*L^2*u^2-u^3*Z^2*L^2);
g=u*(4*u^2*(Z*L)^2-3*u*(1+(k+Z^2)*L^2) +2*k*L^2);
h=((((Q*L^2)^2)*(1-u))/(1+u+u^2+k*L^2*u^2-u^3*Z^2*L^2)) -u*(1+L^2*(k+Z^2))+
2*u^2*Z^2*L^2;

dy(2) = -(h/f)*Y(1)-(g/f)*Y(2);     % Equations of motion
```

Code 3

```
% Code that solves for the scalar phi(r) in Gubser's paper [25]; figures 5

function gubser
global k q Q1 Q L Z m

k=0;
Q1=1;
Z=Q1/2;
L=3.23;
q=3/L;
Q=1;
m=sqrt(-2/L^2);


epsilon=0.000001;
y1=1;
dy1= (m^2*L^2)/(3+k*L^2-Z^2*L^2);     % boundary conditions


[r,y]=ode45(@gupsolution,[1+epsilon,10],[y1,dy1]);    % Integrator

plot(r,y(:,1),'g')
hold on
xlabel('r')
ylabel('phi(r)')
title('k=0, m^2*L^2=-2, qL=3')

function dr=gupsolution(r,Y)

dr=zeros(2,1);
dr(1) = Y(2);

global k L m Q Z q

f = (1/(r^2*L^2))*((r-1)*(r^3 + r^2 + (k*L^2 + 1)*r - Z^2*L^2));
fp = (1/(r^2*L^2))*(2*r^3 - 2*Z^2*L^2/r + Z^2*L^2 + k*L^2 + 1);
g = (2*f/r + fp);
h=(((((q*Q)^2)*(((1/r) - 1)^2))/f) - m^2);

dr(2) = -(h/f)*Y(1)-(g/f)*Y(2);
```

Code 4

```
% Code that solves for the Greens functions
% and Spectral functions at the AdS Boundary


function adscft3
global Z L Q Q1 q v k w

for k=(0: 0.1 :4)
for w=(-4 : 0.15 : 4)

Q1=1;
Z=Q1/2;
L=1;
q=1;
Q=q*Q1;
v=-(1i*w*L^2)/(3-Z^2*L^2);

f2=(Z^2*L^2-3);
g0=f2*(1+2*v);
g1=-6*(1-Z^2*L^2)*(1+v);
h0=(1-Z^2*L^2)*(((6*w^2*L^4)/((3-Z^2*L^2)^2))-3*v-1)-((2*Q*w*L^4)/(3-Z^2*L^
2))-k^2*L^2;
h1=-(1-3*Z^2*L^2)*(2*v+1)-(((w^2*L^4)*(3*Z^4*L^4+2*Z^2*L^2+3))/((3-Z^2*L^2)
^3)) +(((6*Q*w*L^4)*(1-Z^2*L^2))/((3-Z^2*L^2)^2)) -((Q^2*L^4)/(3-Z^2*L^2));
eps=0.000001;

dx1=-(h0/g0)-eps*((((g1+h0)*(h0/g0))-h1)/(f2+g0));
x1=1-eps*(-h0/g0);                                  % Bounary conditions

[u,x]=ode45(@renosol,[1-eps,0],[x1,dx1]);
y=[u,x];
y1=size(y);
b=y1(1,1);

A=(y(b,2));
B=(y(b,3));
A1=real(A);     % vevs...
B1=real(B);
A2=imag(A);
```

```
B2=imag(B);

C=A./B;

D=real(C);      % Greens function
E=imag(C);      % Spectral function

plot3(k,w,D)
hold on
xlabel('K')
ylabel('w')
end
end

function dx=renosol(u,X)

dx=zeros(2,1);
dx(1) = X(2);

global Z L Q k w v

v=-(1i*w*L^2)/(3-Z^2*L^2);
f=(1-u)*(1+u+u^2-u^3*Z^2*L^2);
f1=(1+u+u^2-u^3*Z^2*L^2);
g=-2*v*f1+4*u^3*Z^2*L^2-3*u^2*(1+Z^2*L^2);
h=((w^2*L^4)*(4-Z^2*L^2+u+u^2-Z^2*L^2*u^3)*(2+u-Z^2*L^2*(1+u+u^2)))/(((3-Z^
2*L^2)^2)*f1) +(((Q^2*L^4)*(1-u)-2*Q*w*L^4)/f1) + v*(3*Z^2*L^2*u^2-2*u-1)+2
*Z^2*L^2*u^2-u*(1+Z^2*L^2)-k^2*L^2;

dx(2) = -(h/f)*X(1)-(g/f)*X(2);        % Equations of motion

% To obtain the surface and contour plots, the solutions where reshaped
% into appropriatly sized matrices according to the size of the vectors ω
% and K, and plotted against them.
```

References

[1] J. M. Maldacena, Adv. Theor. Math. Phys. **2**, 231 (1998) [Int. J. Theor. Phys.**38**, 1113 (1999)] [hep-th/9711200].

[2] E. Witten, "Anti-de Sitter space and holography", Adv. Theor. Math. Phys.2: 253, 1998, arXiv:hep-th/9802150v2

[3] S. A. Hartnoll, "Lectures on holographic methods for condensed matter physics," [arXiv:hep-th/0903.3246].

[4] L. Susskind and E. Witten, "The Holographic Bound in Anti-de Sitter Space", hepth/9805114

[5] O. Aharony, S. S. Gubser, J. M. Maldacena, H. Ooguri and Y. Oz, *Large N FieldTheories, String Theory and Gravity,* Phys. Rept. 323, 183 (2000), hep-th/9905111.

[6] M. R. Douglas and S. Randjbar-Daemi, hep-th/9902022.

[7] J. L. Petersen, Int. J. Mod. Phys. A **14**, 3597 (1999) [hep-th/9902131].

[8] E. D'Hoker, D. Z. Freedman, "Supersymmetric Gauge Theories and the AdS/CFT Correspondence", (2002) [arXiv:hep-th/0201253v2]

[9] C. P. Herzog, P. Kovtun, S. Sachdev and D. T. Son, "Quantum critical transport, duality, and M-Theory", Phys. Rev. D75 (2007) 085020 [arXiv:hep-th/0701.036].

[10] S. A. Hartnoll, C. P. Herzog and G. T. Horowitz, "Holographic superconductors," JHEP 0812 92008) 015 [arXiv:hep-th/0810.1563].

[11] S. A. Hartnoll, P. K. Kovtun, M. Muller and S. Sachdev, "Theory of the Nerst effect near quantum phase transitions in condensed matter, and in dyonic black holes", Phys. Rev. B76 (2007) 144502 [arXiv:cond-mat/0706.3215].

[12] T. Faulkner, H. Liu. J. McGreevy, and D. Vegh, "Emergent quantum criticality, Fermi surface, and AdS2", [arXiv:hep-th/0907.2694].

[13] S. Sachdev and M. Muller, "Quantum criticality and Black holes", arXiv:cond-mat.str-el/0810.3005.

[14] S. Sachdev, "Finite temperature dissipation and transport near quantum critical points",

arXiv:cond-mat.str-el/0910.1139.

[15] S I. Muslih, Dumitru Baleanu, E M. Rabei, "SOLUTIONS OF MASSLESS CONFORMAL SCALAR FIELD IN AN n-DIMENSIONAL EINSTEIN SPACE", (2008) PACS numbers: 11.25.Hf

[16] Deser, S, & Waldron, A. (2004). Conformal invariance of partially massless higher spins. Physics Letters B, 603(1-2), 30-34. Multi-Campus: Retrieved from: http://escholarship.org/uc/item/068725c5

[17] Y C.Kim, Sugawa, T. A conformal invariant for nonvanishing analytic functions and its applications, Michigan Math. J. 54 (2006).

[18] I. Bengtsson, "Anti-De Sitter Space," Available at http://www.physto.se/~ingemar/.

[19] U. Moschella, "The de Sitter and Anti-de Sitter sightseeing tour," in *Einstein,1905-2005* (T. Damour, O. Darrigol, B. DuplAntier, and V. Rivesseau, eds.), Progress in MathematicalPhysics, Vol. 47, Basel: Birkhauser, 2006.

[20] Balasubramanian. V, Kraus. P, "A Stress Tensor For Anti-de Sitter Gravity", HUTP-99/A002, EFI-99-6NSFITP-98-132, hepth/9902121

[21] V. Balasubramanian, P. Kraus, A. Lawrence and S. P. Trivedi, "Holographic probes of Anti-de Sitter space-times," Phys. Rev. D59 , 104021 (1999), hepth/9808017.

[22] Mammadov. G, "Reissner-Nordstrom metric", (2009), Available at http://www.gmammado.mysite.syr.edu/notes/RN_Metric.pdf

[23] Ortín. T , Gravity and Strings, Cambridge University Press, 2004.

[24] M. P. Hobson, G. P. Efstathiou and A. N. Lasenby, General Relativity An Introduction for Physicists, 2006.

[25] S. S. Gubser, "Breaking an Abelian gauge symmetry near a black hole horizon," arXiv:0801.2977 [hep-th].

[26] Veselin G. Filev, Clifford V. Johnson, R. C. Rashkov, K. S. Viswanathan, , "Flavoured Large N Gauge Theory in an External Magnetic Field", [arXiv:hep-th/0701001v2]

[27] T. Albash, V. Filev, C. V. Johnson and A. Kundu, "Global currents, phase transitions,and chiral symmetry breaking in large [arXiv:hep-th/0605175].